Functional Characterization of Non-Coding RNAs in the Mammalian Retina

Thesis

UNRESTRICTED

Doctor of Philosophy, PhD

Nicola Meola

Functional Characterization of Non-Coding RNAs in The Mammalian Retina

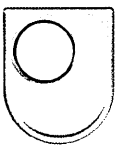

The Open University

Discipline: Life and Biomolecular Sciences

Affiliated Research Center: Telethon Institute of Genetics and Medicine

Thesis submitted in accordance with the requirements of the Open University for the degree of "Doctor of Philosophy"

August 2011

Date of Submission: 16 August 2011
Date of Award: 15 December 2011

to LINA

" I have had my results for a long time:
but I do not yet know how I am to arrive at them"

Karl Friedrich Gauss

TABLE OF CONTENTS

I. LIST OF FIGURES AND TABLES

II. ABBREVIATIONS

ONL, outer nuclear layer;

INL, inner nuclear layer;

GCL, ganglion cell layer;

RPE, retinal pigmented epithilium;

OPL, outer plexiform layer;

IPL, inner plexiform layer;

OLM, outer limiting membrane;

ILM , inner limiting membrane;

OS, photoreceptor outer segments;

IS, photoreceptor inner segments;

IFT, Intraflagellar transport;

Sw Mw and Lw, short medium and long wavelength;

IRDs, inherited retinal degenerations;

RP, retinitis pigmentosa;

LCA, leber congenital amaurosis;

AMD, age-related macular degeneration;

SHH, Sonic Hedgehog Homolog;

VEGF, Vascular endothelial growth factor;

ERK, extracellular signal-regulated kinase;

RNAP, RNA polymerase;

Dpf, day post fertilization;

RPC, retinal progenitor cell;

RGC, retinal ganglion cells;

CMZ, ciliary marginal zone;

CB, ciliary body;

PSCs, pigmented sphere colonies;

PN, postnatal day;

Fwk, fetal week;

CTRL, control;

WT, wild type;

AAV, adeno-associated virus;

LncRNA, long non-coding RNA;

LincRNAs, long intergenic non-coding RNAs;

OS transcript, opposite strand transcript;

cis-NATs, cis-natural antisense transcripts;

Kb, kilobase;

UTR, untranslated region;

eRNA, enhancer RNA;

PRC2, polycomb repressive complex;

RIP, RNA immunoprecipitation;

iPSCs, induced pluripotent stem cells;

CMV, cytomegalovirus;

CBA, CMV early enhancer/chicken β actin.

III. ABSTRACT

Long non-coding RNAs (lncRNAs) are emerging as regulators of a number of basic cellular pathways. Several lncRNAs are selectively expressed in the developing retina, although little is known about their functional role in this tissue. During my PhD thesis I characterized the expression pattern of three retinal-lncRNAs, namely *Six3os*, *Otx2os* and *Vax2os* in the developing mouse retina. Opposite Strand (OS) transcripts are transcribed in the opposite direction of protein-coding genes, in this case *Six3*, *Otx2* and *Vax2*, respectively. Furthermore, I performed a comprehensive functional study for *Vax2os1*, the most abundant transcript from the *Vax2os* cluster, whose expression is restricted to the mouse ventral retina. I demonstrated that misexpression of *Vax2os1,* both *in vitro* and *in vivo,* determines cell cycle alterations in photoreceptor progenitor cells. In particular, the overexpression of *Vax2os1* in the developing postnatal mouse retina caused an impaired cell cycle progression of photoreceptor progenitors toward their final committed fate and a consequent delay of their differentiation processes. At later developmental stages, this perturbation was accompanied by an increase of apoptotic events in the photoreceptor cell layer, in comparison with control retinas, without affecting the proper cell layering in the adult retina. Similar results were observed in mouse photoreceptor-derived 661W cells in which *Vax2os1* overexpression resulted in an impairment of the cell cycle progression rate and cell differentiation. Based on these results, I conclude that *Vax2os1* seems to ensure proper control of the cell cycle progression of photoreceptor progenitor cells in the ventral retina. Therefore, I propose *Vax2os1* as the first example of lncRNA that acts as a cell cycle regulator in the mammalian retina during development.

1 INTRODUCTION

1.1. THE RETINA

1.1.1 Anatomy of the retina

Vision is probably the most indispensable of our senses. The eye is the sensory organ for vision and its structure can be divided into three main layers or tunics whose names reflect their basic functions: the fibrous tunic, the vascular tunic, and the nervous tunic (Figure 1). Although all parts within the eye are important in order to obtain good images, the retina is the most fundamental organ for vision. The retina is considered part of the central nervous system (CNS), as it originates from the developing brain (see section

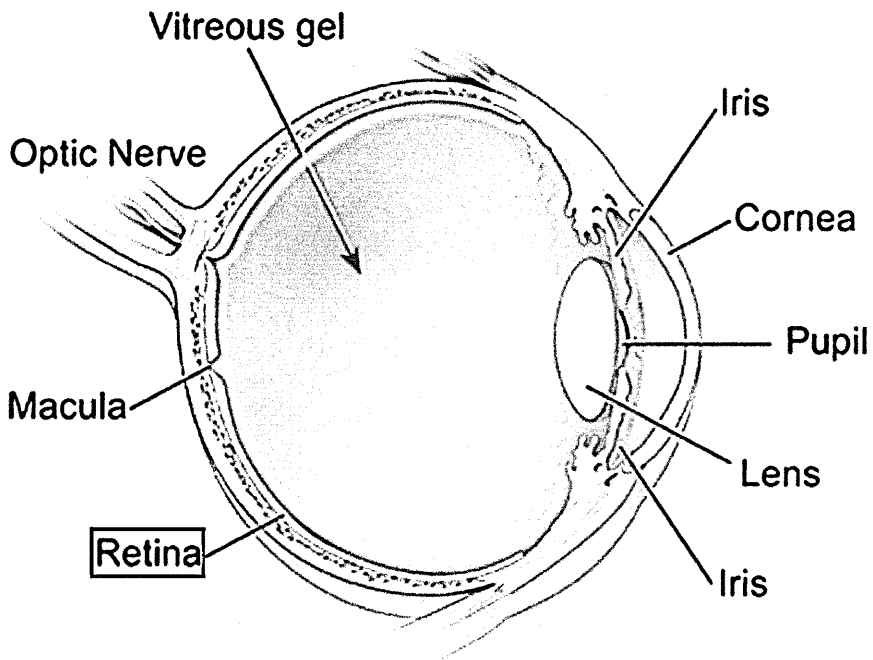

Figure 1. Schematic view of the human eye anatomy.

The retina, a nervous tissue, lines the back of the eye and represents the first station of the visual system. Modified image from http://www.nei.nih.gov/health/ maculardegen/armd_facts.asp.

1.1.3). The retina of all vertebrates, including humans, is composed of three layers of nerve cell bodies (or nuclei) and three layers of neural connections (Figure 2).

The outer nuclear layer (ONL) contains cell bodies of rods and cones (the photoreceptors), the inner nuclear layer (INL) contains cell bodies of bipolar, horizontal, Müller and amacrine cells and the ganglion cell layer (GCL) contains cell bodies of ganglion cells and displaced amacrine cells. Neuronal interconnections (synapses) are, instead, arranged in distinct histological layers: i) the outer plexiform layer (OPL), containing synapses linking the photoreceptor axons to the bipolar and horizontal cell dendrites; ii) the inner plexiform layer (IPL) where the bipolar and amacrine cells connect to the ganglion cells and iii) the nerve fiber layer, in which the axons of the ganglion cells converge and exit the eye as the optic nerve. The retinal pigment epithelium (RPE), which is a specialized pigmented monolayer, is situated above the photoreceptors. The Müller cells are the radial glial cells of the retina. They form the outer limiting membrane (OLM)

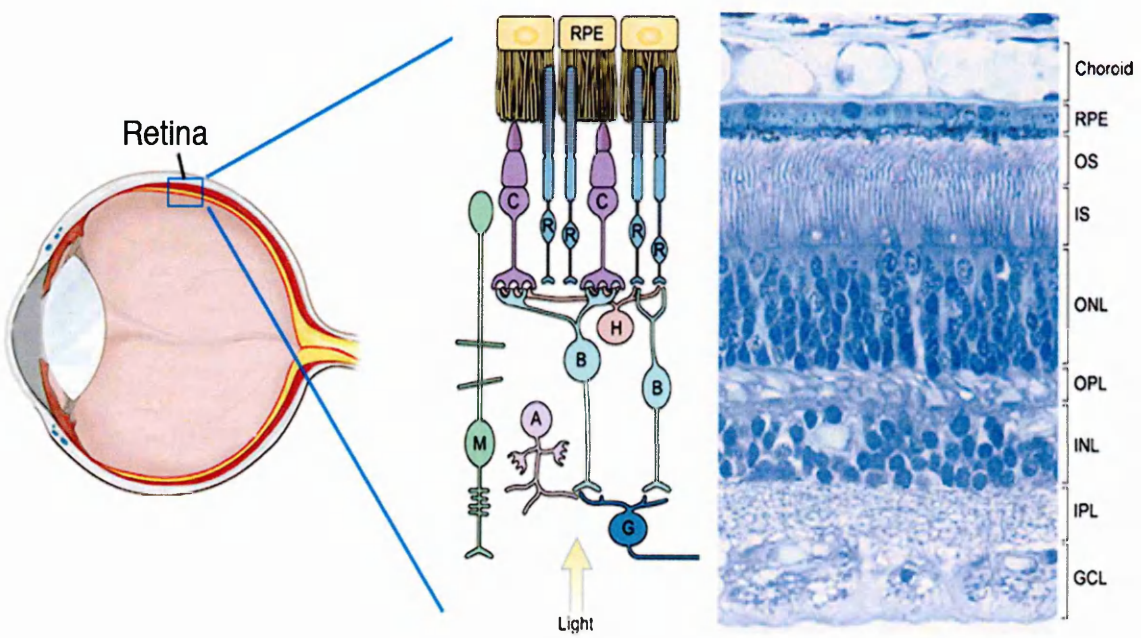

Figure 2. Organization of retina.

G, ganglion cells; M, Müller cells; A, amacrine cells; B, bipolar cells; H, horizontal cells; C, cones and R, rods. Modified image from (Sung and Chuang, 2010).

and the inner limiting membrane (ILM), which border the retina from the RPE and vitreous humor, respectively.

A radial section of the retina reveals that the ganglion cells are innermost in the retina while the photoreceptors lie outermost in the retina close to the RPE (Figure 2). Therefore, light must pass through the thickness of the retina before activating the rods and cones. Subsequently, the absorption of photons by the photoreceptors is translated into a first biochemical message. Next, it is transformed into an electrical message, elaborated in the INL, and eventually reaches the ganglion cells. Here the retinal message arising from the photic input is transmitted to the brain through the ganglion cell axons. The optic nerve, originating near the center of the retina, contains the ganglion cell axons that reach the brain and, additionally, blood vessels that vascularize the retinal layers and neurons (particularly the GCL and INL). Choroidal blood vessels are, instead, vital for the maintainance of the outer retina (particularly the ONL) (Kolb et al., 2011).

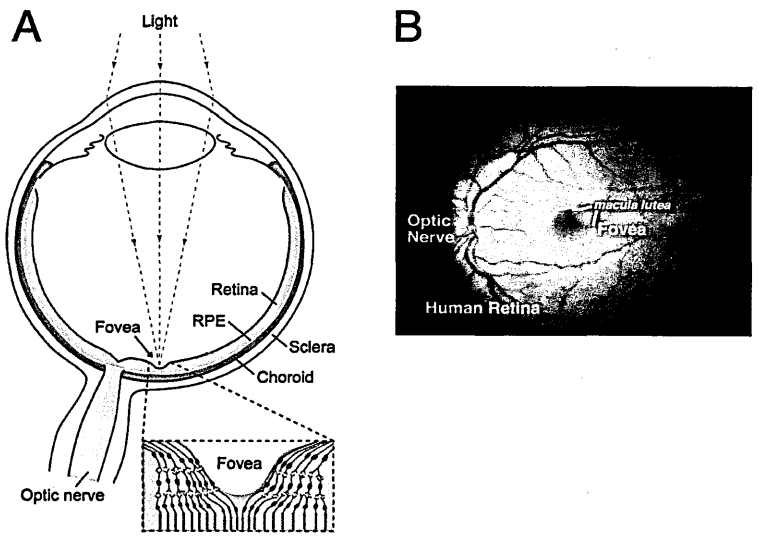

Figure 3. Enlarged diagram of the fovea and visualization of the macula lutea.

(A) The retina lines the posterior part of the eye; the RPE underlies the retina and separates it from the choroid (Sung and Chuang, 2010). (B) The macula lutea is the yellow oval spot at the center of the retina (back of the eye). From http://www.lookfordiagnosis.com /images.php?term=Macula+Lutea&lang=5.

Another structure of the central retina is the fovea, the oval-shaped and blood vessel-free spot that, among mammals, is only present in simian primates, including humans (Figure 3A-B). The fovea is a highly specialized region of the retina where the cone photoreceptors are highly concentrated to the exclusion of the rods; in fact the central retina is cone-dominated whereas the peripheral retina is rod-dominated. The fovea is responsible for the sharp central vision that is of primary importance for many activities in humans. A macular area, known as the macula lutea, is located in the fovea (Figure 3B). The macula lutea is thought to act as a short wavelength filter, additional to that provided by the lens (Kolb et al., 2011).

1.1.2 The photoreceptors

The rod and cone photoreceptors are highly specialized neurons able to "catch" light stimuli (electromagnetic radiation / photons) and to convert them into electrochemical signals through a complex biochemical pathway (see section 1.2.2). The photoreceptor function is strictly linked to that of the underlying RPE; indeed, cooperation between the photoreceptors and the RPE is essential for vision. Both the rods and cones can be structurally divided into four major functional segments: the inner segment (IS), the outer segment (OS), the nucleus, and the synaptic body (Figure 4A). The IS contains the cytoplasm and organelles of the cell and is linked to the OS through the connecting cilium. The non-motile connecting cilium plays an important role in the organization and function of the photoreceptors, and is responsible for the intracellular transport and turnover of proteins from and to the OSs (Figure 4B). The synaptic body is the portion that connects the photoreceptors to the horizontal and bipolar cells that represent the next stages of the visual circuit. The OS is a modified cilium and it is composed of an elaborate system of stacked membranous discs (1000/photoreceptor) that form as invaginations of the cell

plasma membrane (Swaroop et al., 2010) (Figure 4C).

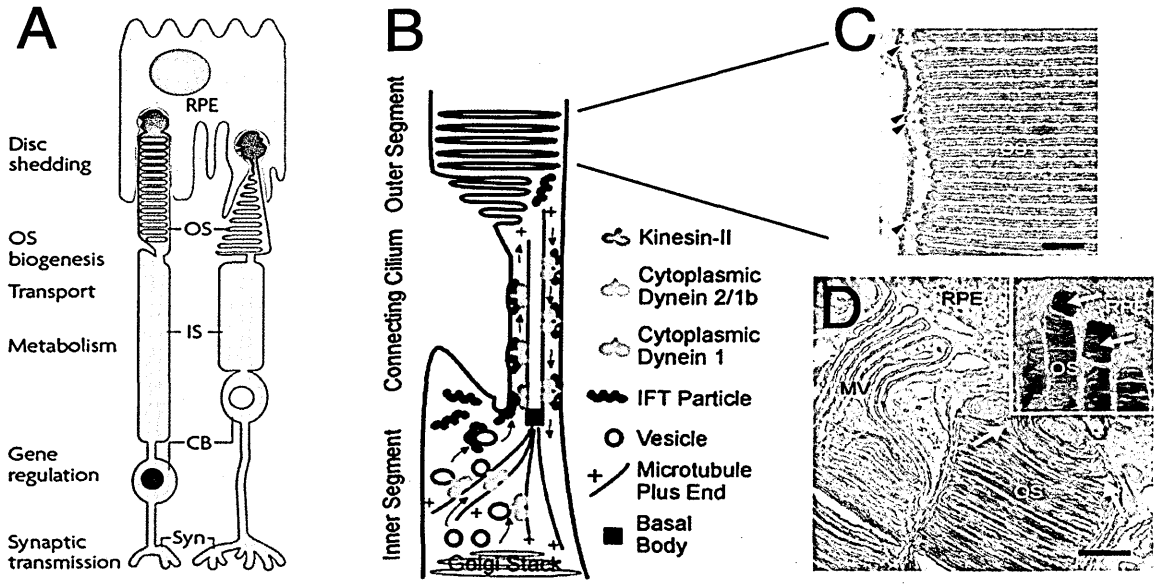

Figure 4. Schematic representation of rod and cone photoreceptors and photoreceptor intraflagellar transport (IFT) at the connecting cilium.

The electron microscopy of murine rod discs OS (C) and junction between the rod OS and RPE (D). (A) OS, outer segments; IS, inner segments; CB, cell body; Syn, synaptic body (Swaroop et al., 2010). (B) Cytoplasmic Dynein-1 transports vesicles from the Golgi stack to the base of the connecting cilium. The IFT particles with attached cargo are transported through the connecting cilium by Kinesin-II. At the distal end of the connecting cilium, the IFT particles dissociate from their cargo, the membrane is organized into disks, and then particles are picked up by cytoplasmic Dynein 1b/2 to be returned to the cell body (Pazour et al., 2002). (C) Rod discs (arrowheads) are highly impacted. Modified image from (Townes-Anderson et al., 1988). (D) RPE microvillar processes (MV) enwrapped the distal OS (Chuang et al., 2010).

In the rods, most of these sacs eventually become separated from the outer membrane, while the cone discs remain connected to the surface membrane (Figure 4A). The membranous sacs disintegrate near the apical surface of the cell, and their cellular debris is removed through phagocytosis by the adjacent RPE (Figure 4D). Newly formed discs, which originate from the OS base, gradually replace the "old" discs.

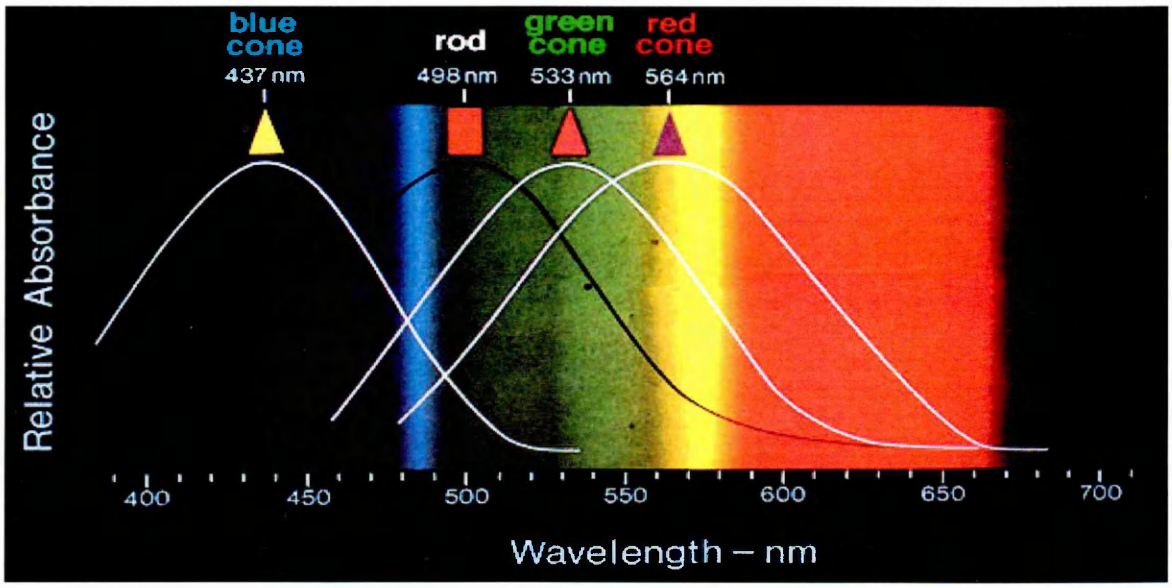

Figure 5. Spectral sensitivity of human photoreceptors.

Adapted image from (Dowling, 1987).

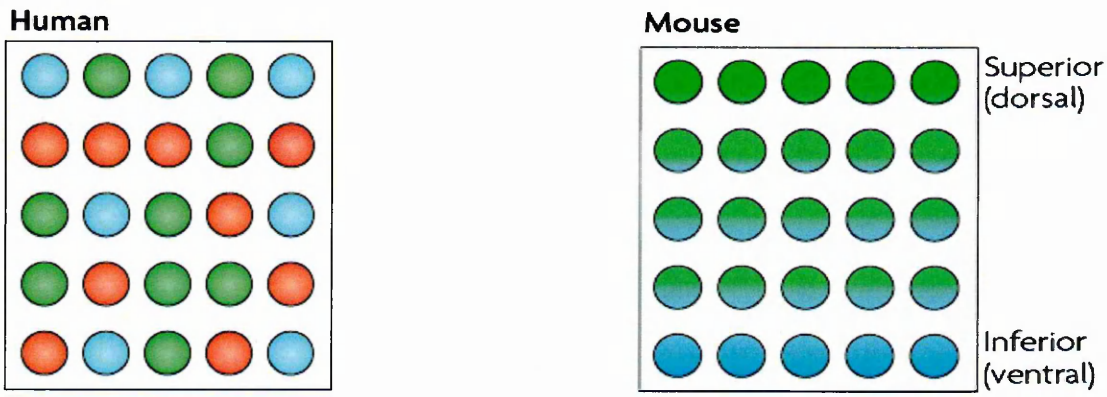

Figure 6. Schematic surface-view representation of the cone distribution across the human and mouse retina.

Human cones express sw (blue), lw (red) or mw (green) Opsins in a mosaic like pattern. Murine cones express sw-Opsin and mw-Opsin in opposing distribution gradients along the dorsal to ventral axis (Swaroop et al., 2010).

The visual pigments and other components of the phototransduction pathway, which are key players for proper photoreceptor function, localize to the OS discs. In mice and

humans, the photoreceptors represent over 70% of the retinal cells, but the rods are more numerous than the cones by 30:1 in mice and 20:1 in humans. The cones respond to bright light (photopic vision), mediate colour vision and allow the high resolution of images. In the central portion of the fovea the blood vessels, GCL, INL and plexiform layers are displaced allowing light to reach the cones with a minimal distortion, thus guaranteeing acute and detailed vision. The rods function mainly under low light conditions and are responsible for peripheral and night vision (scotopic vision) being a hundred-fold more sensitive to light stimuli than the cones. Photoreceptor light-sensitivity results from the expression of visual pigments defined as "opsins". Opsins are light-sensitive membrane-bound G protein-coupled receptors of the retinylidene protein family that covalently bind to a vitamin A-based retinaldehyde chromophore which undergoes photoisomerisation following the absorption of a photon of light. The mammalian retina has only one type of rod visual pigment, rhodopsin, which has a peak spectral sensitivity at about 500 nm and represents 95% of the total amount of the rod disc proteins. Most mammals (including the mouse) have two types of cone opsin that confer dichromatic colour vision: i) sw-Opsin, which has a peak sensitivity in the short wavelength (415-450 nm, blue) region of the spectrum; and ii) mw-Opsin, which has a peak sensitivity in the medium-long wavelength (530-555 nm, green) region of the spectrum. Duplication of an ancestral mw-Opsin-like gene on the X chromosome has provided humans and diurnal primates with an additional opsin, lw-Opsin, which is sensitive to longer wavelength (555-590 nm, red) light and, together with the sw- and mw-Opsins, confers trichromatic colour vision (Kolb, 1991) (Figure 5). In humans, the sw, mw and lw cones are distributed in a mosaic-like pattern while, in mice, the cones express sw-Opsins and mw-Opsins in opposing distribution gradients along the superior (mw-Opsin-high) to inferior (sw-Opsin-high) axis (Swaroop et al., 2010) (Figure 6). Another opsin of the mammalian retina, melanopsin, is expressed in a

subpopulation of the ganglion cells (intrinsically-photosensitive GCs); it is involved in circadian rhythm regulation but does not contribute to the image-forming processes (Mustafi and Palczewski, 2009).

1.1.2.1 Formation of the photoreceptor outer segments

The photoreceptors have evolved a unique structure for the outer segments (OS) to detect and process light and therefore their formation is worth mentioning. More is known about the process of rod outer segment (ROS) morphogenesis than about cone outer segment (COS) morphogenesis. Rod differentiation in rodents starts postnatally and it takes two-three weeks for the OS to fully mature. ROS morphogenesis begins with the extension of a primitive cilium from the basal body anchored on the plasma membrane (ciliary stalk) (Figure 7A), followed by the filling of the primitive cilium with a variety of membranous vesicles, tubules, and sacs. At postnatal days 8-10, disc-like vesicles begin to fill the primitive OS (Sung and Chuang, 2010). These discs, however, are still long and highly disorganized (Figure 7B). Many of them are aligned parallel to the ciliary stalk. While differentiation proceeds, a major remodeling reorganizes the discs in order for them to become aligned perpendicularly to the ciliary stalk. The terminal phase of rod differentiation is the elongation of the OS. The lengths of the OS containing the disc stacks increase rapidly during this period, with a gradient central to the peripheral retina, until the OS reach their mature size. Intraflagellar transport (IFT) is essential for the assembly of the cilia (Sung and Chuang, 2010). IFT is a bidirectional movement of multiprotein particles along the microtubules of the ciliary axonemes. Many retinal disease-genes are involved in photoreceptor IFT (see section 1.1.6). Two additional macromolecular complexes (i.e., NPHP complex and BBSome) associated with the IFT complex are also important for early

OS development. Mutations of each component in either of these complexes are linked to syndromic retinitis pigmentosa diseases, referred to as ciliopathies. Retinal degeneration is a hallmark of many of the ciliopathies (Sung and Chuang, 2010).

Rhodopsin has an indispensable role in disc formation in addition to its well-known role in signal transduction since Rhodopsin-null mice form primitive cilia without disc-containing OSs (Lee et al., 2006). Knockout mice for Peripherin-2, or Rds, (a photoreceptor-specific tetraspan membrane protein), like Rhodopsin-null mice, form a bare cilium without OS (Connell et al., 1991). As mentioned above, the outer and inner segments of a vertebrate photoreceptor are connected by a canonical cilium that contains nine outer microtubule doublets (Figure 7C) (Arikawa and Williams, 1993).

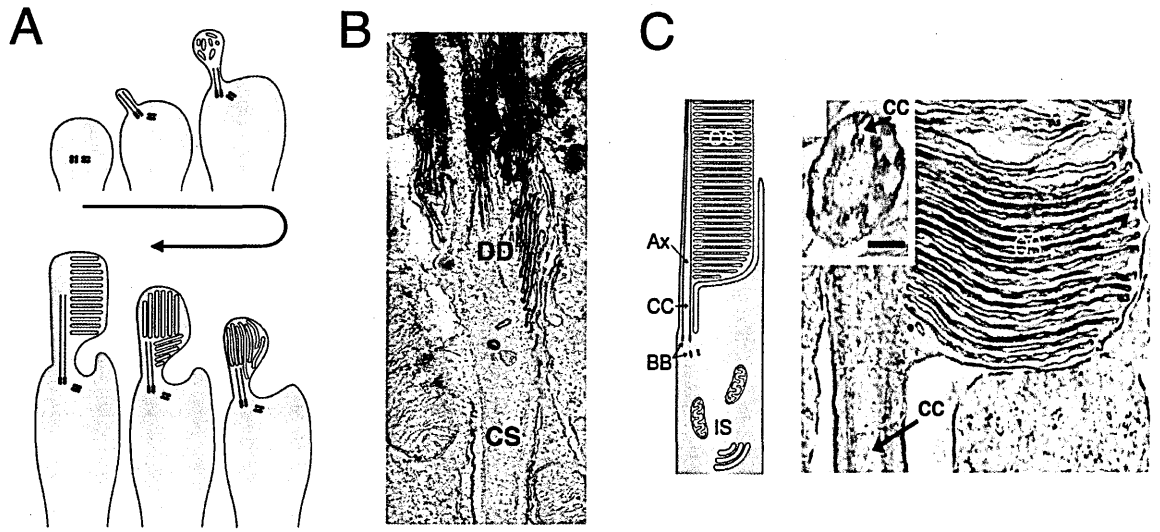

Figure 7. OS morphology during rod development. The electron microscopy of rodent rod OS at the connecting cilium.

(A), A drawing depicting the transformation of developing rods during their OS morphogenesis. (B), Representative electron micrograph of postnatal day 10 rat rods. This morphological appearance may represent a stage in OS morphogenesis. Many discs are longer than the matured discs. (C), A schematic drawing of a mammalian mature rod depicting its ciliary stalk and microtubule organizations. Electron micrograph shows the longitudinal sectioning view of IS–OS junction of a rat rod. CS, ciliary stalk; DD, disorganized discs; BB, basal body; CC, connecting cilium; Ax, axoneme. Adapted images from (Sung and Chuang, 2010).

In a mature photoreceptor, the connecting cilium is important in order to maintain the separation of the outer and inner segment compartments. It is also the site of the morphogenesis of new membrane discs, which are added to replace those shed from the distal end of the outer segment. The microtubules of the developing connecting cilia are labeled by acetylated α-tubulin from the early developmental stages. Moreover, acetylated α-tubulin in the photoreceptors is found only in the microtubules of the ciliary axoneme of the outer segments at later stages of development and in the mature photoreceptors (Arikawa and Williams, 1993).

1.1.2.2 Phototransduction and the visual cycle

The process by which the absorbed photons are converted into electrochemical responses occurs in the photoreceptor OSs and represents the first stage of visual processing defined as "phototransduction". Photoreceptor phototransduction has been comprehensively studied in the rods (Fu and Yau, 2007). Briefly, in the dark Rhodopsin is bound to 11-*cis*-retinal forming inactive Rhodopsin (R), and the basal activity of the Guanynyl-cyclase (Gc) keeps the cGMP levels high (Figure 8). Both Na^+ and Ca^{2+} enter the membrane channels leading to high Ca^{2+} levels and to the activation of the Guanylate-cyclase-activating protein (Gcap). The Ca^{2+}-bound Calmodulin (CaM) confers a high cGMP affinity to the cGMP-gated channels in the OS plasma membrane that remain open (Figure 8). Light (hv) photoisomerizes the 11-*cis*-retinal to all-*trans*-retinal and activates Rhodopsin (R*) that releases all-*trans*-retinal and activates the G-protein Transducin (αβγ) by catalyzing the GDP to GTP exchange. Next, the dissociated α-subunit of Transducin activates cGMP-Phosphodiesterase 6 (Pde-6), which rapidly hydrolyzes the cytoplasmic cGMP. The decreased cGMP concentration causes the closure of the cGMP-gated cation

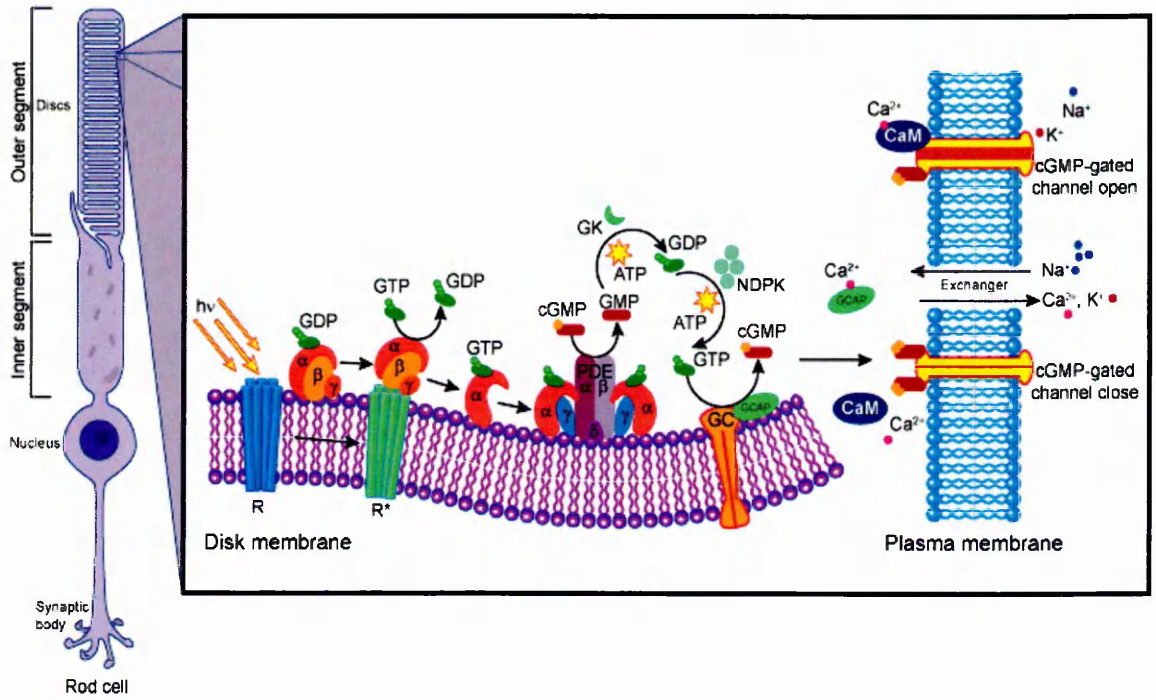

Figure 8. Scheme of phototransduction in rods.

Rhodopsin (R), photoactivated Rhodopsin (R), Transducin (αβγ), Guanynyl cyclase (Gc), Phoshodiesterase 6 (Pde-6), Guanylate-cyclase-activating protein (Gcap), Guanylate kinase (Gk), Calmodulin (CaM), Nucleoside diphosphate kinase (Ndpk). Modified picture from http://mutagenetix.scripps.edu/phenotypic/phenotypic_rec.cfm?pk=282).*

channels on the plasma membrane, thus reducing the Ca^{2+} influx (Figure 8). As a result, the rods are hyperpolarized and release fewer glutamate transmitters to the bipolar cells. In the recovery phase, a desensitization of the photoactivated Rhodopsin (R*) is achieved by G protein receptor kinase-1 (Grk-1) phosphorylation at the Rhodopsin C-terminus and subsequent Arrestin binding. Retinal Gc and Gcap replenish the cGMP levels in a Ca^{2+}-dependent manner while the Na/Ca-K exchanger, which resides on the plasma membrane, regulates the Ca^{2+} homeostasis. All the components of the phototransduction cascade are arranged in close proximity to the disc membranes and/or to the plasma membrane of the photoreceptors (Fu and Yau, 2007) (Figure 8). The photransduction cascade is closely

associated to the visual cycle, an enzymatic pathway in which the retinoids that are isomerized by light are "recycled" and provided back to the PRs (Figure 9).

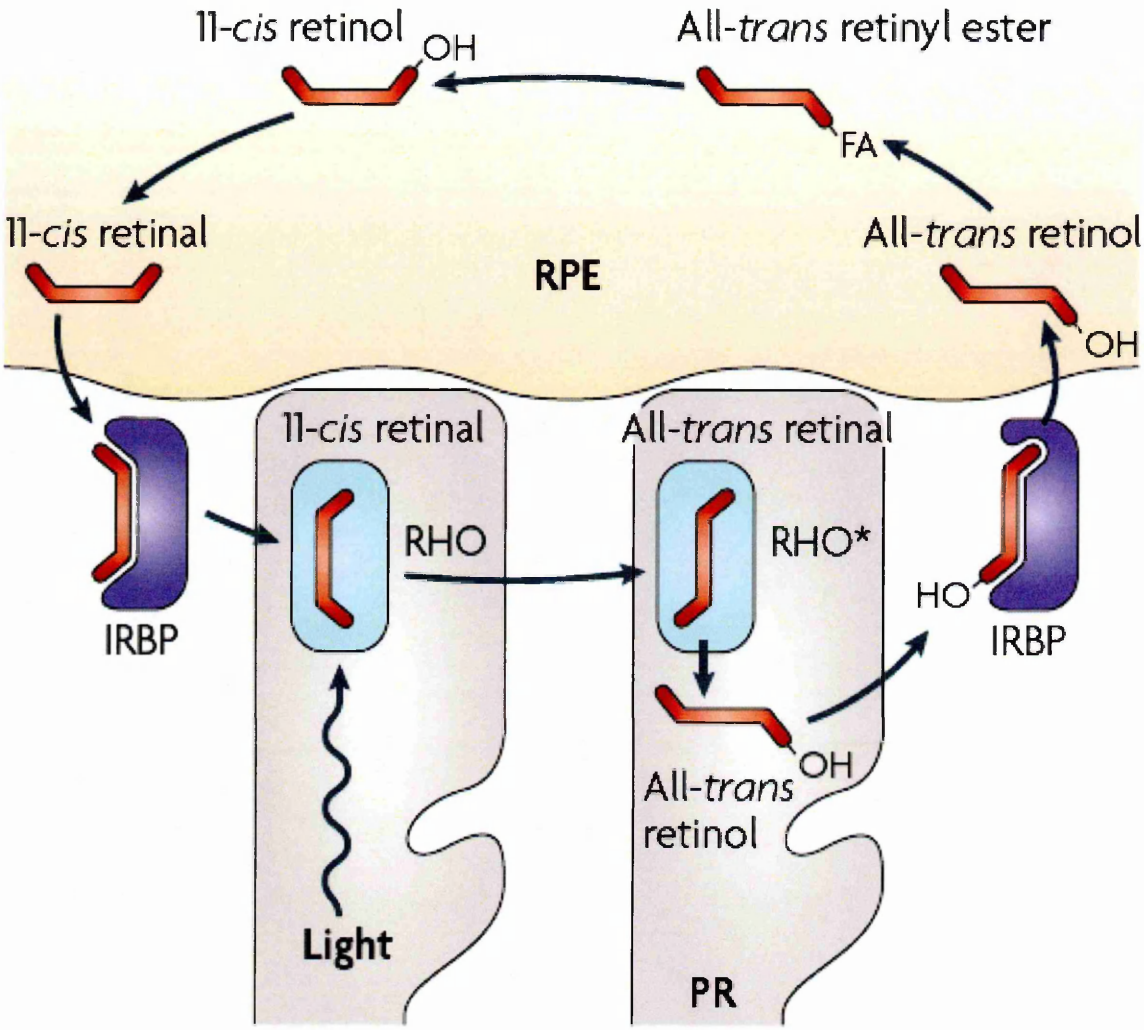

Figure 9. The visual cycle.

Rhodopsin (Rho), activated Rhodopsin (R), hydroxyl group (OH), Interphotoreceptor retinol-binding protein (IRBP), fatty acyl group (FA). Modified image from (Wright et al., 2010).*

In the rods, photoisomerization converts the 11-*cis*-retinal to all-*trans*-retinal that is released from the Rhodopsin, conjugated with the membrane lipid phosphatidyl-ethanolamine and transported to the OS cytoplasm by the ATP-binding cassette, subfamily

A, member 4 (Abca-4) and converted to all-*trans* retinol by a Retinol dehydrogenase. Retinoid-binding proteins, such as Interphotoreceptor retinol-binding protein (Irbp) are involved in the transport of the hydrophobic retinoids in an aqueous environment from the photoreceptor OS to the RPE (Wright et al., 2010) (Figure 9).

In the RPE, the all-*trans*-retinol undergoes a series of enzymatic reactions to be converted back into 11-*cis*-retinal: it is esterified to a fatty acyl group by Lecithin retinol acyltransferase (Lrat) to form all-*trans* retinyl ester which is in turn subjected to *trans* isomerization to 11-*cis*- retinal through the actions of two enzymes (Rpe-65 and 11-*cis* Retinol dehydrogenase). Finally, 11-*cis*-retinal molecule returns to the OS where it regenerates rhodopsin and completes the visual cycle (Figure 9).

1.1.3 Retinal development

As previously mentioned (section 1.1.1), the retina develops from dividing neural cells in the neural plate that are specified to form the eye field. This field is split into two lateral domains, each of which evaginates into an optic vesicle. This optic vesicle then invaginates to form the structure of the retina, with an outer epithelial layer of cells forming the retinal pigmented epithelium (RPE) and an inner neuroepithelial layer (neural retina) (Figure 10).

At the earlier stages of development, progenitors of the neural retina proliferate and expand the number of cells. At a specific point in the development of each species, the RPCs (retinal progenitor cells) start to exit from the cell cycle and begin to differentiate (Fuhrmann, 2010). The RPCs undergo a variable number of divisions to give rise to clones of different sizes and cell type compositions. Almost all combinations of cell fates are possible within a single clone (Holt et al., 1988; Turner et al., 1990; Wetts and Fraser, 1988).

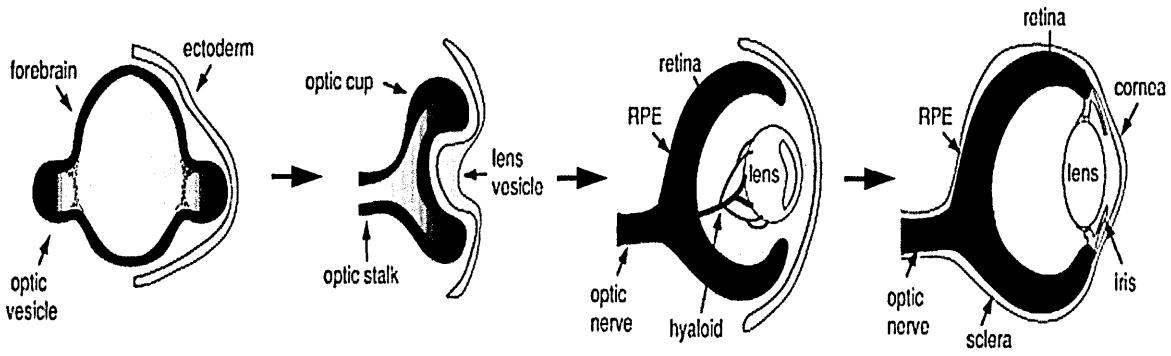

Figure 10. Development of the eye and retina.

Optic vesicles give rise to the two eyes. Lens vesicle invaginates and forms the optic cup. Later in the development, the outer surface of the optic cup becomes the RPE and the inner surface becomes the retina until reaching the final localization with the mature eye. Adapted image from (Sernagor, 2006).

Cell fate production follows a histogenetic sequence in all retinas studied, with the ganglion cells born first and the Müller glial and bipolar cells born last (Figure 11A-B). Moreover, differentiation follows a central to peripheral spatio-temporal gradient. Single-cell labeling studies, in fact, show a higher clonal size for the peripheral compared to the central cells in the mouse (Turner et al., 1990), consistent with birth-dating studies (Holt et al., 1988) (Figure 11C).

Birth dating, by continuous administration of the nucleotide analog BrdU, or by ^{3}H-thymidine injections (^{3}H-TdR), has suggested that there is an overlap in birth dates between cell types, in that the retinal ganglion cells (RGCs) are on average born earliest, but some RGCs are born after other cells, especially in animals that develop quickly such as frogs and chickens (Belecky-Adams et al., 1996).

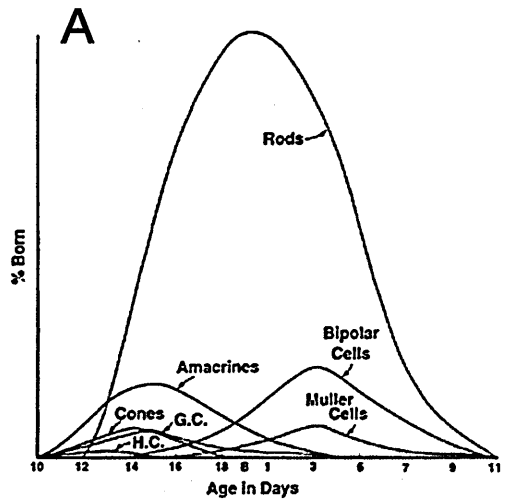

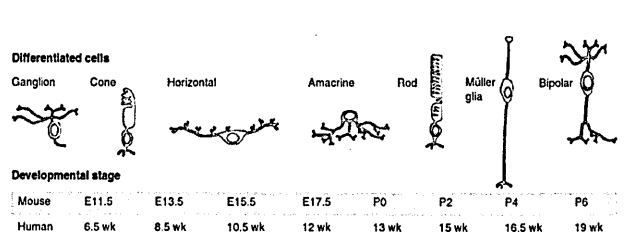

C

	Center			Periphery		
Type of cell	1 day	3 days	5 days	1 day	3 days	5 days
Ganglion cells	0	0	0	2.0	1.0	0
Amacrine cells	1.0	0	0	1.1	1.4	0
Müller cells	2.7	1.8	1.8	2.4	2.3	1.2
Bipolar cells	3.1	1.5	1.2	5.5	2.3	1.7
Rods, inner	2.1	1.8	0	2.1	2.2	1.4
Rods, outer	5.4	1.9	1.8	20.5	3.6	1.9

Figure 11. Retinal cell birth.

(A), Summary of retinogenesis in the mouse retina (Young, 1985). (B), Comparison between retinal cell birth in human and mouse. Adapted from (Reynolds and Olitsky, 2011). (C), Ratio of ^{3}H-TdR-positive nuclei to all nuclei in the center and periphery of the mouse retina after a single injection at post-natal day 1, 3 and 5 (Young, 1985).

As the retinal development progresses, the progenitors take longer to divide (Alexiades and Cepko, 1996) and produce postmitotic cells with increasing frequency (Livesey and Cepko, 2001). Regarding the photoreceptors, in mammals their genesis occurs over a long temporal window (Rapaport et al., 2004; Young, 1985). The functional maturation of a committed photoreceptor precursor (rod or cone) in fact can take weeks to months depending on the species (Figure 12).

The development of the photoreceptor cells can be divided into five steps: first, the proliferation of the multipotent RPCs; second, the restriction of the competence of the RPCs; third, the cell fate specification and commitment to photoreceptor precursor during or after final mitosis; fourth, the expression of the photoreceptor genes, such as those for phototransduction and morphogenesis; and fifth, the axonal growth, synapse formation and

outer segment biogenesis.

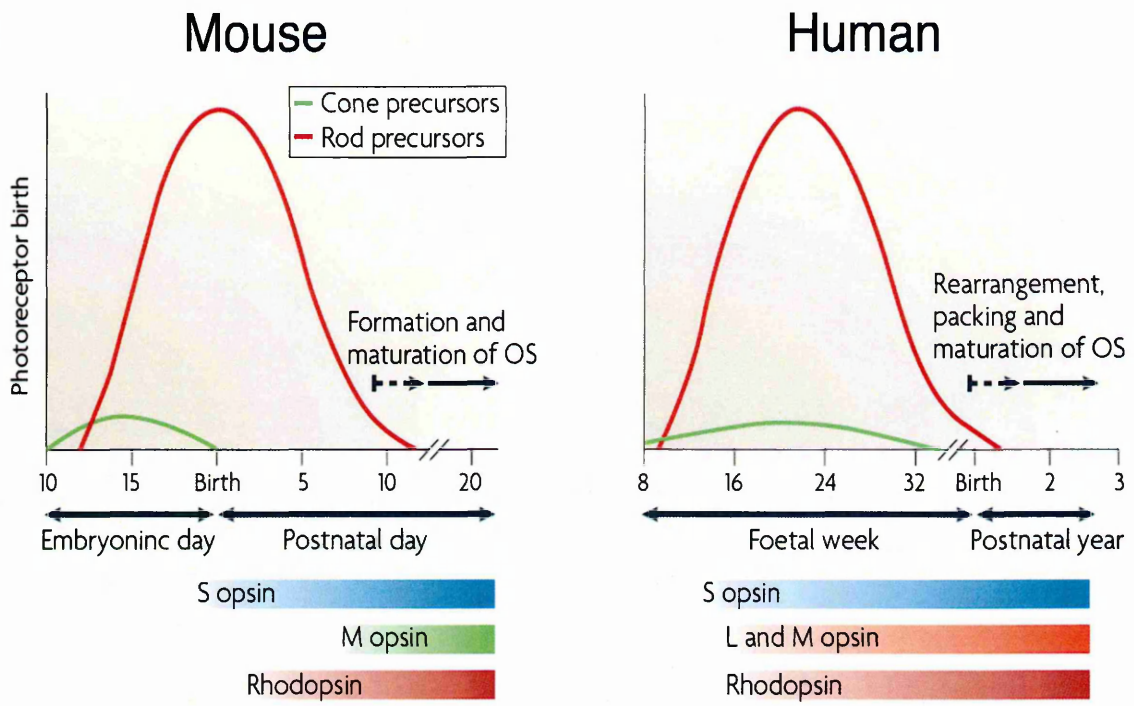

Figure 12. Photoreceptor genesis and maturation in mice and humans.

The relative numbers of cone and rod precursor cells that are born over time are shown for mouse and human retinogenesis. Modified image from (Swaroop et al., 2010).

In humans, all photoreceptors are generated prenatally. The first cones and rods are born around fetal weeks (Fwk) 8 and 10, respectively (Cornish et al., 2004). Cone *sw-Opsin* (short-wavelength) mRNA is produced as early as Fwk 12, followed by rod *Rhodopsin*, cone *mw-Opsin* (medium-wavelength) and cone *lw-Opsin* (long-wavelength) transcripts at Fwk 15 (Hendrickson et al., 2008).

At birth, the opsin expression patterns are reasonably well established, but the photoreceptors are still immature. In the mouse, the photoreceptor development is less advanced than in humans at birth, and the eyes of the newborn pup remain closed for

almost 2 weeks. Cone genesis is essentially complete at birth (having started at embryonic day (E) 11), and *sw-Opsin* is expressed at the late embryonic stages. In mice, the rods are born both pre and postnatally. The peak of rod genesis occurs in the first few postnatal days, accompanied, soon after, by the expression of *Rhodopsin* (Carter-Dawson and LaVail, 1979) (Figure 12). The expression of *mw-Opsin* by the cones begins around postnatal day 6 and lags behind that of other opsins. As the photoreceptors mature, the Opsin levels increase substantially, the outer segments elaborate towards the RPE and the synapses form with horizontal and bipolar neurons.

1.1.3.1 Programmed cell death in the developing retina

In the retina two phases of cell death have been reported to occur during development. An early phase takes place concomitant with the processes of neurogenesis, cell migration and cell differentiation. A later phase, affecting mainly the neurons, occurs when the connections are established and the synapses are formed, resulting in the selective elimination of inappropriate connections (Vecino et al., 2004). This pattern of cell death in the developing retina is common among different vertebrates and the timing of both processes has been analyzed in different vertebrate species (Figure 13).

Apoptotic processes in the zebrafish retina are detected in the GCL and INL at days 3-4 post-fertilization (dpf), followed by a second but clearly smaller wave at 6-7 dpf. Apoptosis in the ONL starts at 5 dpf and peaks at 7 dpf (Biehlmaier et al., 2001). This peak of photoreceptor apoptosis is lower than that observed in other fish (Hoke and Fernald, 1998).

Studies of cell death in the developing frog retina show that the physiological degeneration of retinal cells in these vertebrates takes place in three successive waves.

TIMING OF RETINAL CELL APOPTOSIS

Hatching/Birth	Zebrafish 2-3 dpf	Xenopus 2dpf+2hpf	Chicken 21 d	Rat 22 d	Mouse 19 d	Human 36 wg
ONL	5-7 dpf			P12-P72	P5-P11	23-24 wg
INL			E8- E14	P3-P26 (AC) P4-P48 (BC)	P3-P8 (AC) P8-P11 (BC,MC)	15-20 wg
GCL	3-4 dpf 6-7 dpf	1d 16h-12dpf 26 dpf	E4-E7 E10-E14	P1-P6	P2-P11	14-30 wg

Figure 13. Timing of retinal cell apoptosis in the different layers of vertebrate retina.

AC, amacrine cells; d, days; dpf, days post-fertilization; E, embryonic day; hpf, hours post fertilization; MC, Müller cells; P, postnatal; wg, weeks of gestation. Modified image from (Vecino et al., 2004).

In the first wave, the mitotic cells in the center of the retina become pyknotic and degenerate prior to the onset of cell differentiation. Next, after the formation of the ganglion cell layer and the inner plexiform layer, many cells degenerate in the region of the newly formed inner nuclear layer. Finally, a third wave of cell death is observed in the outer and inner nuclear layers in the periphery of the retina. Apoptosis has also been analyzed during the development of the chicken retina (Frade et al., 1996; Mayordomo et al., 2003). Two waves of programmed cellular death occur in the developing chicken retina. The first wave takes place between E4 and E7 (Cuadros and Rios, 1988; Garcia-Porrero and Ojeda, 1979) while a later wave occurs between E10 and E14 (Hughes and La Velle, 1975; Hughes and McLoon, 1979). In the INL, the pyknotic cells appear during embryonic day 8. However, the highest levels of apoptosis are observed in this layer at E11. The degenerating cells are initially located in the central retina. However, in subsequent days, they are also found in the peripheral zones. It has been postulated that cell death occurs

because of competition for adequate arborization space. If the number of retinal afferent fibers which arrives is higher than the number of available tectal termination sites, the supernumerary fibers may degenerate. Cell death in the mouse retina occurs primarily during the first 2 weeks after birth and is essentially completed by the end of the third week. The pattern of death of the different retinal cell types has been described also in mice. RGC degeneration is prominent during the first 11 days after birth, peaking on postnatal days 2 to 5 (Young, 1984). The amacrine cells die within the inner plexiform and inner nuclear layer, particularly between postnatal days 3 and 8, whereas the bipolar and Müller cell degeneration reaches a peak at postnatal days 8-11. Degeneration among the rods occurs rapidly from post-natal days 5 to 11. Nevertheless, the sporadic death of rods continues during the following two weeks (Young, 1984) (Figure 13).

1.1.3.2 Retinal cell determination

Once the retinal differentiation has been initiated, regulatory mechanisms guarantee that the progenitor cells preserve their capacity to undergo several divisions, in parallel with the production of the differentiated cells, and that the progenitors stop dividing at variable times. Both extrinsic and intrinsic factors are involved in the regulation of these events (Agathocleous and Harris, 2009). For example, Sonic hedgehog homolog (Shh) production from the RGCs influences both the speed of proliferation and the onset of differentiation. Vascular endothelial growth factor (VEGF) produced by differentiated RGCs enhances the proliferation of the progenitors through ERK (extracellular signal-regulated kinase) and prevents them from becoming RGC, illustrating a local control by a negative feedback (Hashimoto et al., 2006). Another example of local control is the Notch-Delta signaling pathway (Perron and Harris, 2000). Delta is a ligand for Notch that is under the control of

the proneural genes, which are themselves inhibited by Notch activity. Initially the cells have random fluctuations in their levels of Delta/Notch activity. When a cell has slightly more Delta activity, Notch signalling is enhanced in its neighboring cell, which means a lower proneural activity. The cells with high levels of Delta protein and high proneural activity in the retina differentiate as neurons, whereas the cells that have a high Notch activity remain neuroepithelial or become Müller cells (Dorsky et al., 1995; Furukawa et al., 2000). This mechanism ensures an heterogeneity in the population; in its absence, all progenitors would exit at the same time and adopt similar fates.

Regarding the photoreceptors, taurine, an unusual amino acid, is an extrinsic factor produced from P0 rat retinal cultures and its addition to retinal explants promotes rod differentiation (Altshuler et al., 1993). Retinoic acid and FGF signalling also promote the differentiation of the progenitors in the rods and indeed the inhibitors of both retinoic acid and FGF reduce rod differentiation (Hyatt et al., 1996; McFarlane et al., 1998).

In addition to these extrinsic signaling systems, the RPCs display intrinsic changes in order to generate different retinal cell types (Cepko, 1999). The processes of retinal proliferation and cell determination are mostly regulated by bHLH transcription factors. At early stages, bHLH genes such as *Hairy and enhancer of split 1* and *5* (*Hes1* and *Hes5*) maintain the retinal progenitors in an undifferentiated state and produce progenitor pools. Then, the proneural bHLH genes start to be expressed, and the retinal progenitors undergo neuronal differentiation. This process requires also the activity of homeobox-containing domain genes. Without proper combinations of homeobox and the bHLH genes, the retinal progenitors would fail to acquire the proper cell fate (Cepko, 1999) (Figure 14).

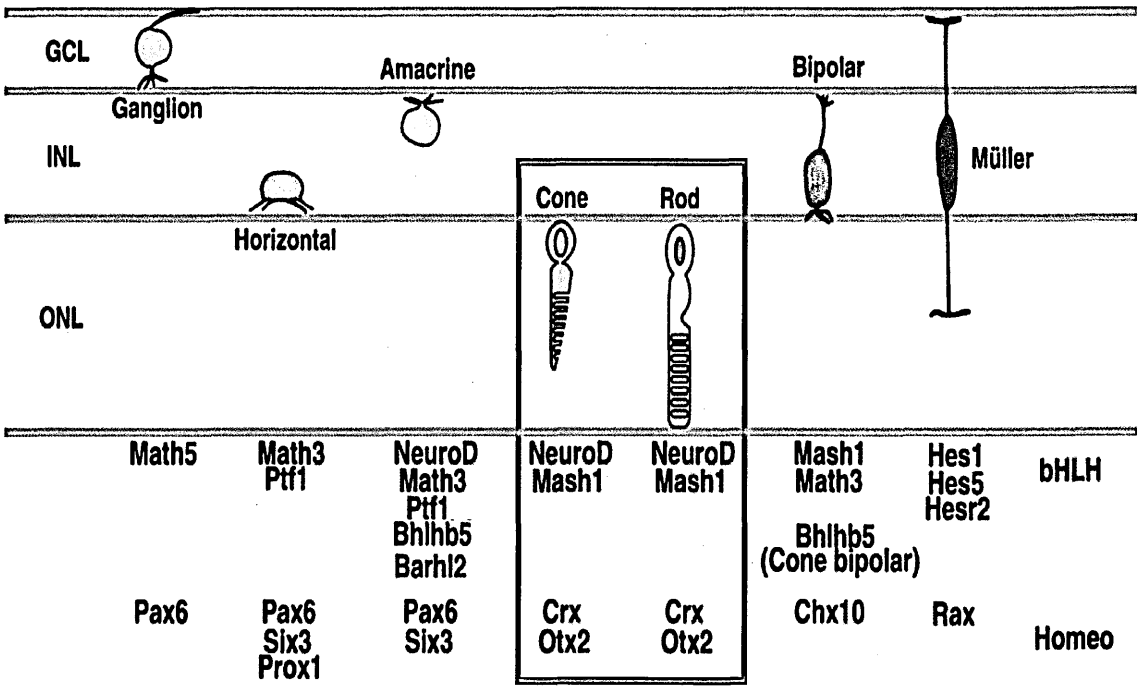

Figure 14. Regulation of retinal cell fate specification by transcription factors.

Combinations of multiple transcription factors, such as bHLH-type and homeobox-type factors, are required for proper specification of retinal cell types (red box highlights photoreceptor transcription factors). Modified image from (Ohsawa and Kageyama, 2008).

Photoreceptor cell development is regulated by two homeobox genes: *Crx* and *Otx2*. *Otx2* transactivates *Crx* and is required for photoreceptor cell fate determination, because deletion of *Otx2* results in the conversion from photoreceptor cells to amacrine-like cells (Chen et al., 1997; Nishida et al., 2003). Likewise, Crx-mutant retinas display defects in photoreceptor cell genesis (Furukawa et al., 1999). The transcription factors from the bHLH gene family involved in photoreceptor cell genesis are still poorly understood. *NeuroD* is a bHLH gene with the ability to drive retinal progenitors toward a photoreceptor cell fate as is demonstrated by the misexpression of *NeuroD* which results in an enhanced rod cell genesis (Inoue et al., 2002) (Figure 14).

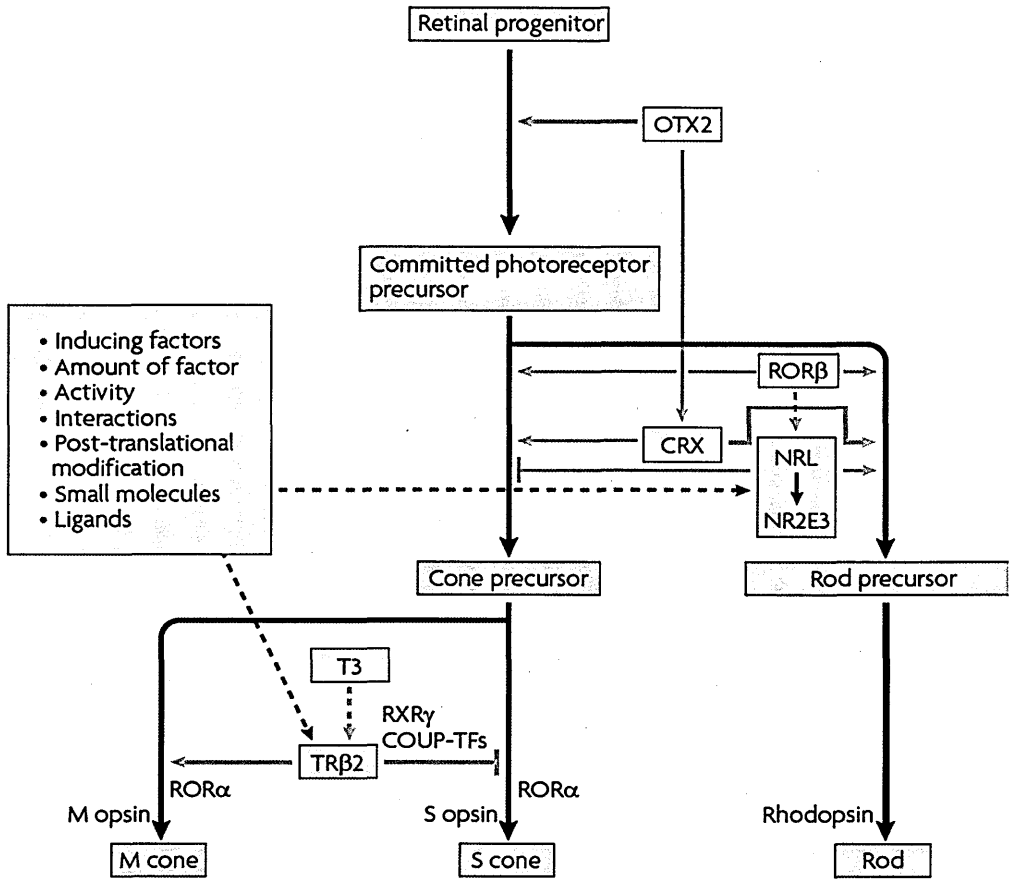

Figure 15. Transcriptional dominance model of photoreceptor cell fate determination.

Other factors involved in M opsin and S opsin patterning include Retinoid X receptor-γ (Rxrγ), Rorβ, Rorα, Thyroid hormone receptor β2 (Trβ2) and COUP transcription factors (Coup-TFs). Modified image from (Swaroop et al., 2010).

Recent studies have elucidated the molecular mechanism regulating cone and rod subtype decision. *Nrl* is a basic leucine zipper transcription factor, preferentially expressed in the rod photoreceptors. Targeted disruption of *Nrl* leads to the loss of rod cells (Mears et al., 2001). In the *Nrl* mutant retina, expression of *Nr2e3*, an orphan nuclear receptor, is lost (Mears et al., 2001). *Nr2e3* activates rod-specific genes and represses cone-specific genes in concert with *Crx* (Cheng et al., 2004; Peng et al., 2005). Therefore, *Nrl* regulates fate decisions, either rod or cone, through the activation of *Nr2e3*.

Although a unified mechanism cannot be proposed for all vertebrates, some experimental evidence suggests that the cones may differentiate into a common default form before diversifying into distinct cone subtypes (Figure 15). This model of photoreceptor cell fate determination includes three fundamental features: i) all terminally differentiated photoreceptors originate from a common postmitotic photoreceptor precursor; ii) a photoreceptor precursor cell differentiates by a default pathway into an S cone (cone cells expressing *sw-Opsin* gene) unless additional regulatory signals direct the precursor to acquire a rod or M cone (cone cells expressing *mw-Opsin* gene) identity; and iii) the acquisition of a specific fate by a photoreceptor precursor is established by a particular set of transcription-regulatory factors. The model predicts in addition that these transcription factors exert their function at two key decision points: i) the decision to form either a rod or a cone; and ii) the decision for a cone to differentiate with an S cone or M cone identity (Swaroop et al., 2010).

1.1.4 Stem cells and transdifferentiation in the retina

Depending on the species, whether it is fish, amphibian, bird or mammal, retinas can regenerate from two major cell sources, the RPE and Müller cells, and might also have an active stem cell zone, the ciliary marginal zone (CMZ) (Figure 16A). Progenitor cells from the CMZ of amphibian and fish generate most of the mature retina (Lamba et al., 2008). Birds have a retinal area that resembles the CMZs of fish and amphibians, and cells comprising this zone contribute to the growth of the retina that occurs postnatally, even though cells of the CMZ in birds can generate only a small part of the mature retina (Fischer and Reh, 2000).

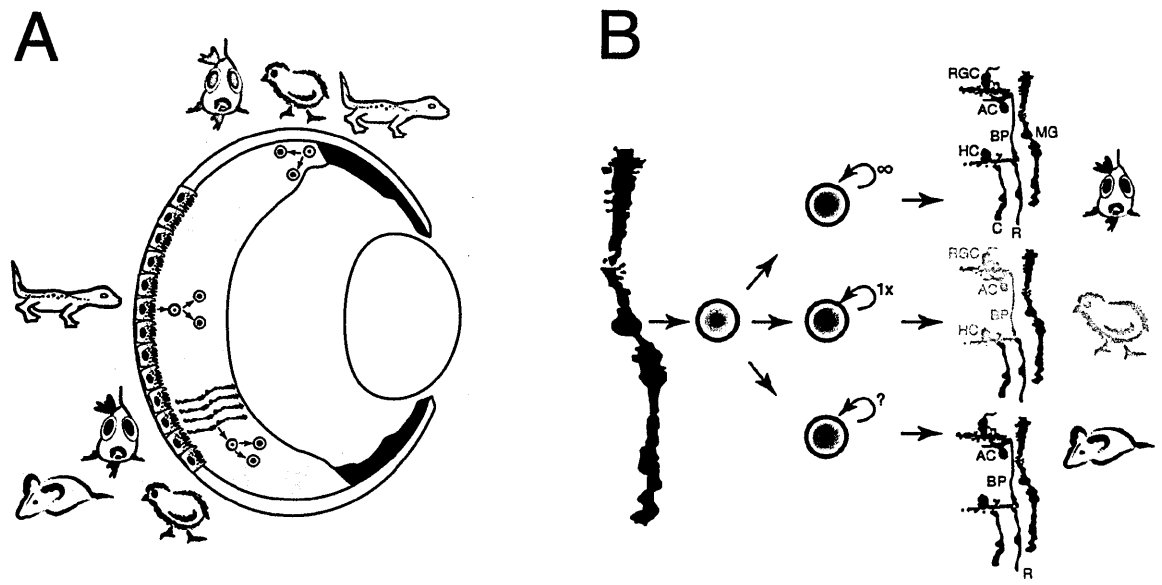

Figure 16. Sources of retinal regeneration in vertebrates.

(A), Progenitor cells (blue) in amphibian and fish CMZs generate most of the mature retina, but only a small part in birds. Upon damage of the central retina in amphibians, the RPE cells (brown) dedifferentiate, proliferate and regenerate neurons; retinal damage causes Müller cells (magenta) to dedifferentiate, proliferate and regenerate neurons. (B), In comparison with fish and chicks, retinal regeneration in mice is limited because of a restricted number of Müller cells re-entering the cell cycle and the limited number and types of neurons regenerated (colored/labeled cells are regenerated in the respective species; RGC, retinal ganglion cell; AC, amacrine neuron; BP, bipolar neuron; HC, horizontal neuron; R, rod and C, cone photoreceptor; MG, Müller cells). Adapted image from (Karl and Reh, 2010).

In a study that searched for a comparable region in the mammalian retina it was discovered that there is no CMZ in the mouse retina (Kubota et al., 2002) and it seems that the CMZ has progressively decreased in size during vertebrate evolution (Kubota et al., 2002). However, another retinal region in the adult mammalian eye, the ciliary body, CB, contains a quiescent population of cells that can be expanded *in vitro* (Tropepe et al., 2000). When the CB from adult mouse retinas was dissociated into single cells, these cells proliferated to form pigmented sphere colonies (PSCs) without any dependence on growth

factor conditions (Tropepe et al., 2000). In addition, it has been demonstrated that cells comprising PSCs possess the potential to differentiate into different retinal cell types *in vitro* (Tropepe et al., 2000).

After damage to the central retina in amphibians, the RPE cells de-differentiate, proliferate and regenerate neurons (Lamba et al., 2008). If the retina of a salamander is removed surgically, the pigmented epithelial cells re-enter the mitotic cell cycle and form a new layer (Lamba et al., 2008). The cells of this new layer continue to proliferate and ultimately generate a complete new retina, with normal lamination, and can even reconnect with the central visual nuclei to restore visual function (Reh et al., 1987). The process starts with the de-differentiation of the pigmented cells and continues with the production of de-differentiated cells that re-express neural retinal progenitor genes, and recapitulate the sequence of normal histogenesis. In contrast to amphibians, the RPE of the fish retina does not regenerate if all retinal tissue is removed (Reh et al., 1987). Retinal regeneration can occur also from intrinsic retinal cell sources. After a variety of different types of retinal lesions, including neurotoxic, genetic or light-induced, the Müller cells in the fish retina have a strong proliferative response and regenerate all the different classes of retinal neurons (Karl and Reh, 2010) (Figure 16B).

Also in birds, re-entry into the mitotic cell cycle by Müller cells after damage has been reported (Fischer and Reh, 2001), although with a limited regenerative response compared to fish. In the mammalian retina, the regenerative response of the Müller cells to injury is even more limited than in the bird. In response to injury in the mouse or rat retina, the Müller cells become hypertrophic and only a few of them re-enter the mitotic cell cycle (Bringmann et al., 2009). Mouse Müller cells can be stimulated to proliferate when neurotoxic damage is coupled with growth factor injections (Karl et al., 2008). To determine if there is a set of transcription factors involved in the cell cycle re-entering

process of these Müller cycling cells, several groups have found that markers of progenitor cells are expressed in the Müller cells after damage, for example like Pax6 and components of the Notch pathway, such as Dll-1, Notch-1 and Nestin (Das et al., 2006; Dyer and Cepko, 2000; Wan et al., 2007). Studies in the human retina have indicated that at least some part of the progenitor gene expression profile can also be upregulated (e.g. Sox-2 and Pax-6) in human Müller cells (Bhatia et al., 2009). Despite the evidence that many progenitor genes are reactivated in mammalian Müller cells after damage, many fundamental progenitor cell genes do not seem to be re-expressed. This partial de-differentiation in mammalian Müller cells is in contrast to the more complete regeneration phenomenon observed in non-mammalian vertebrates, and could partly explain the very limited regeneration observed in mammals (Karl and Reh, 2010).

1.1.5 Immortalized retinal cell lines

The culture of retinal cells is a widely used system. As with all *in vitro* tools, there are both advantages and limitations. The advantages include controllable conditions, time-course flexibility and a reduction in the number of animals used for research. The limitations include selective loss of specific cell phenotypes and functions, changes in tissue structure and the potential inconsistency of the *in vitro* results (Seigel, 1999). For many applications, the advantages of *in vitro* studies outweigh the potential limitations. Indeed, in conjunction with animal studies, *in vitro* studies can provide important basic information about normal retinal functions. Retinal cells exist in three basic forms: primary cultures, retinoblastoma cultures, and genetically-engineered cultures (Figure 17). The major drawbacks of primary retinal cell cultures are their limited supply and finite lifespan. Conversely, retinoblastoma cells are proliferative retinal cell cultures with a virtually infinite lifespan. The first retinoblastoma cell line described was the Y79 cell line, derived

from the intraocular tumor of a 2.5 year old human (Reid et al., 1974).

A COMPARISON OF RETINAL CULTURE SYSTEMS: CHARACTERISTICS OF RETINAL CELL CULTURES

	Primary Cultures	Retinoblastoma Cultures	Engineered Cell Lines
Examples	Explants, Reaggregates Monolayers	Y79, WERI-Rb1,	661W
Lifespan	Finite (2-4 weeks)	Indefinite	Indefinite
Freezer storage	No	Yes	Yes
Phenotypic Marker Expression	Excellent	Immature	Variable
Growth Characteristics	Post-mitotic or slow-growing	Highly proliferative	Mitotic
Tumor-forming ability	None	High	Range: none to high

Figure 17. Summary of the major differences between the basic types of retinal cultures.

Adapted from (Seigel, 1999).

The WERI-Rb1 (McFall et al., 1977), WERI-Rb24 and WERI-Rb27 (Sery et al., 1990) cell lines were also established from human intraocular tumors. These human retinoblastoma tumor cell cultures have several characteristics in common, such as growth in suspension as "grape-like" clusters, immunoreactivity to glial and/or neuronal markers (Kyritsis et al., 1984), and the ability to form tumors *in vivo* (del Cerro et al., 1993). Retinoblastoma cells were found to exhibit alterations in the expression of the retinoblastoma susceptibility gene, *Rb* (Lee et al., 1987). The undifferentiated nature of the Y79 retinoblastoma cells makes them very useful in the testing of putative retinal

differentiating agents. Differentiating agents, such as cAMP, retinoids, and sodium butyrate were found to affect the morphology, growth rate, and biochemistry of Y79 cells *in vitro* (Kyritsis et al., 1985; Tsokos et al., 1986). In addition to the human retinoblastoma cell lines, mouse (Bernstein et al., 1994) and rat (Nishida et al., 1982) cell lines are useful in studies of retinal cell differentiation and anti-cancer treatment.

More commonly, cell-cycle-related genes that induce cell proliferation, such as the simian virus (SV)40 large T antigen, *E1A* gene of adenovirus or *Src* are introduced by investigators to promote an immortalized, growth stimulated culture. These "genetically-engineered" retinal cultures often lack the potential to form tumors and retain more differentiated features (Seigel, 1999). Like the retinoblastoma cell lines, the genetically-engineered cells are also immortal. A mouse photoreceptor-derived cell line (661W) was immortalized by the expression of the SV40 T antigen under the control of the human promoter of interphotoreceptor retinol-binding protein (IRBP) (al-Ubaidi et al., 1992). 661W cells have been reported to express photoreceptor markers of both rod cells (Roque et al., 1999) and cone cells (Tan et al., 2004). Interestingly, 661W cells express high levels of retinal progenitor markers such as *Nestin* and *Pax-6*, but not *Rhodopsin* (Sheedlo et al., 2007). The variability in the characteristics of the 661W cells suggests that the cells may initially arise as undifferentiated cells but gradually acquire a rod or cone photoreceptor phenotype, a fact which could be explained by the culture conditions established in the different laboratories. The transformed 661W photoreceptor cell line is currently used in the *in vitro* investigations of therapies designed to promote photoreceptor cell survival in both cone dystrophies and rod degenerative diseases, such as age-related macular degeneration (AMD) and Retinitis Pigmentosa (RP), respectively (Sheedlo et al., 2007).

1.1.6 *Inherited photoreceptor degenerative diseases*

Vision loss leading to blindness is the consequence of many genetic and/or acquired disorders whose etiology is highly heterogeneous. Indeed, the retinal cells are among the most specialized cells in the human body and depend on a huge number of specific genes; in addition, due to the close interdependence between the photoreceptors, the RPE and the choroid that nourishes them, dysfunctions in any of these components can cause secondary dysfunctions to the others (Inglehearn, 1998). The most severe and common blinding pathologies affecting the retina are mainly characterized by photoreceptor dysfunction/degeneration. Progressive photoreceptor degeneration is the principal feature of many inherited retinal degenerations (IRDs), affecting the photoreceptors and/or the retinal pigment epithelium. IRDs include conditions such as Retinitis Pigmentosa (RP) (Hims et al., 2003), Leber Congenital Amaurosis (LCA) (den Hollander et al., 2008) and Cone-Rod Dystrophies (Hamel, 2007), mostly inherited as mendelian traits and characterized by a high clinical and genetic heterogeneity.

RP is the most widespread form of IRD, in which most patients lose night vision in adolescence, side vision in young adulthood and central vision in later life because of a progressive loss of rod and cone photoreceptors. The worldwide prevalence of RP is about 1 in 4000 resulting in more than 1 million affected individuals. RP is genetically very heterogeneous; so far, more than 45 disease causing genes have been identified that account for about 60% of all cases (Hartong et al., 2006) (Figure 18).

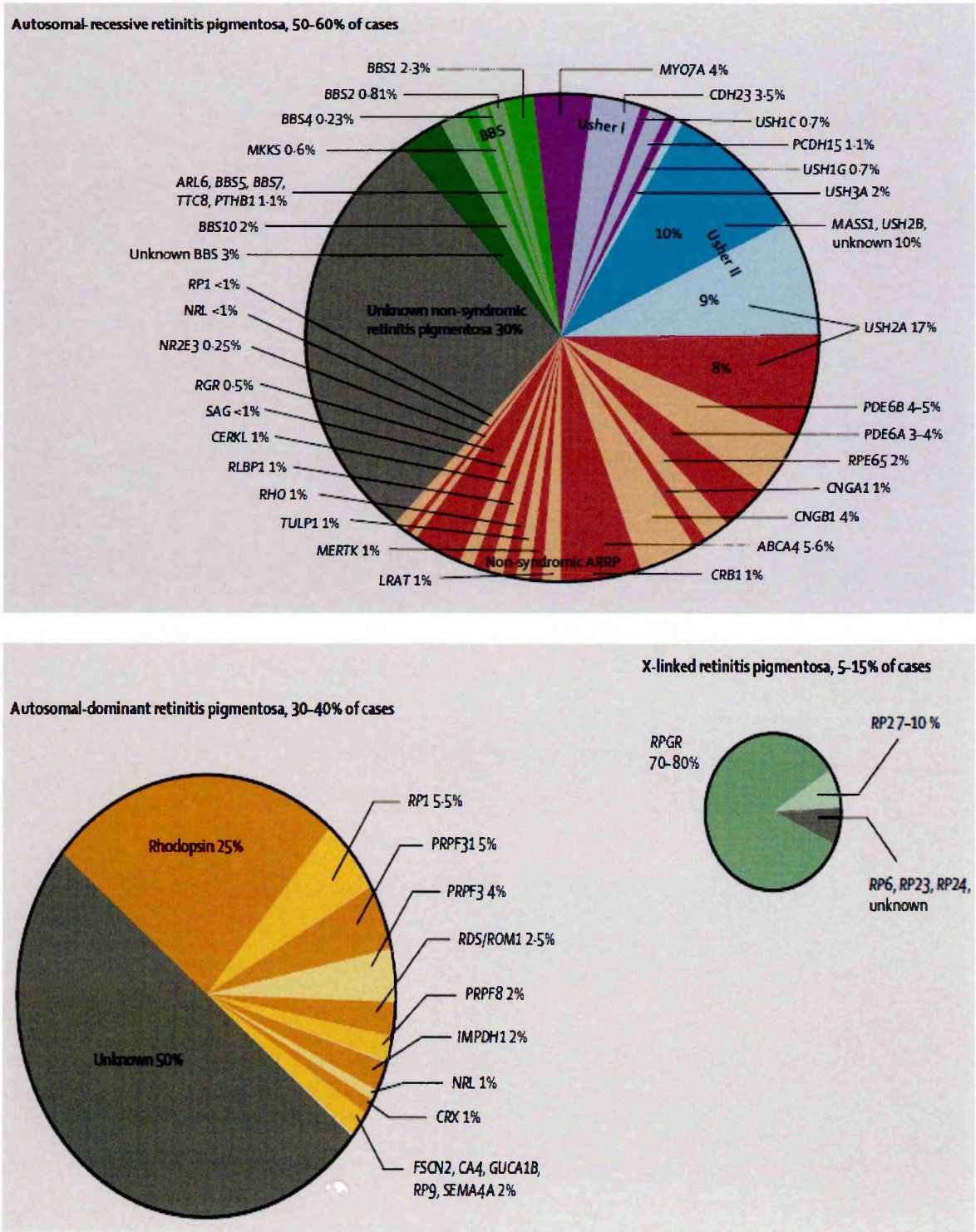

Figure 18. Causal genes and their relative contribution to RP.

Top panel, autosomal-dominant (left panel) and X-linked (right panel) RP forms. Bottom panel, autosomal-recessive RP forms (ARRP), including USH and Bardet-Biedl (BBS) syndromes. About 40% of RP cases are due to still unknown mutations. Modified image from (Hartong et al., 2006).

Considering all IRD forms, causative mutations have so far been identified in 208 genes encoding mainly eye-specific products (the Retinal Information Network, RetNet: www.sph.uth.tmc.edu/retnet/) that show a huge variety of functions (Figure 19). Interestingly, independently of the primary causative gene, the IRDs share a common degenerative process in which photoreceptor cell death represents the final outcome.

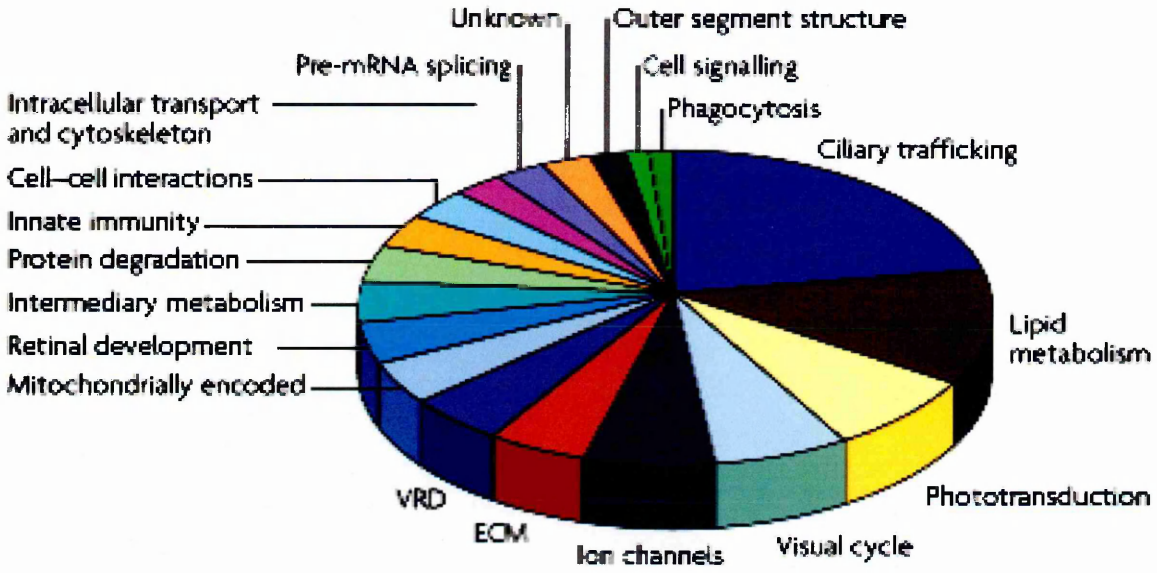

Figure 19. The functional categorization of the IRD causative genes.

Pie chart showing the functional categorization of 146 genes implicated in PR degeneration. IRD-causative mutations fall in genes involved in PR physiology, biochemistry and structure. Most mutations affect genes involved in the PR ciliary trafficking. The data are from the Retinal Information Network (RetNet). ECM: extracellular matrix; pre-mRNA: precursor mRNA; unknown: function undetermined; VRD: vitreoretinal degeneration; EM: extra-cellular matrix. Modified image from (Wright et al., 2010).

Photoreceptor cell death has been extensively studied in animal models of IRD and in most cases apoptosis has been found to be activated in the dying photoreceptors (Travis, 1998). However, during the past decade many studies have shown that photoreceptor degeneration is a very complex process in which multiple pathways act at different stages

of the disease or even simultaneously with significant cross-talk (Wright et al., 2010). These pathways include: Caspase-dependent and -independent apoptosis, Calpain-mediated cell death, autophagy, proteasome activity and complement-mediated lysis (Wright et al., 2010). In many systems, apoptotic cell death invariably involves the activation of Caspases that cleave over 100 known substrate proteins on the carboxyl side of the aspartate residues.

Two major pathways have been described for Caspase activation: the first is initiated by extracellular ligands that bind to death receptors like Fas/CD95 or the Tumor necrosis factor alpha (Tnfα)–receptor, while the second pathway (also known as the intrinsic pathway) induces the release of Cytochrome c and other polypeptides from the mitochondria without the involvement of death receptors. Non-Caspase proteases linked to the apoptotic cell death include the Cathepsins, Calpains, Granzymes A and B, Poly (ADP-ribose) polymerase-1, serine proteases and the proteasome (Wright et al., 2010). Most of the enzymes can act together with, or independent of, the Caspases as executioners of apoptosis. In addition, mitochondrial membrane permeabilization may be induced in a Caspase-independent manner with the release of Caspase-independent effectors such as Aif (Apoptosis-inducing factor) (Wright et al., 2010).

1.1.6.1 Gene therapy approaches: retinal AAV vectors

Recently, effective treatments for IRDs have produced important results for the cure of the Leber congenital amaurosis (LCA). LCA is an inherited retinal disease that causes severe visual impairment in infancy or early childhood. Gene transfer therapy has offered hope to people with a form of this disease (Colella and Auricchio, 2010).

During the past decade, thanks to the identification and cloning of many IRDs causative genes, gene therapy strategies have rapidly evolved and showed promising results

in several animal models of retinal degeneration (Allocca et al., 2006; Colella et al., 2009). Gene therapy is defined as the treatment/cure of human diseases based on the transfer of nucleic acids (DNA or RNA) to target somatic cells. Nucleic acid delivery to different eye structures can be performed both by viral and non viral-based methods. Even though non viral gene transfer efficiency has been consistently improved by complexing nucleic acids with lipids or cationic polymers and using electroporation, the resulting transfection rate is low and the expression of the transgene is short lived (Naik et al., 2009). Thus, viral gene transfer represents the preferred method for gene delivery to the eye given the availability of different viral vectors that are able to efficiently transduce the ocular tissues. Viral vectors commonly used for ocular gene transfer are derived from adenoviral, lentiviral and adeno-associated (AAV) viruses (Colella et al., 2009; Kumar-Singh, 2008). Improvements in vector design, and modifications to surface proteins (for adenoviral vectors), envelopes (for lentiviral vectors) or capsids (for AAV vectors) have expanded the vector toolkit in order to achieve the desired transduction parameters.

Vectors derived from the small adeno-associated virus (AAV) are the most widely used and promising tools for retinal gene transfer given their favourable safety profile and the long-term gene expression that is observed after a single AAV administration (Surace and Auricchio, 2008). AAV is a small (25-nm), non-enveloped virus that packages a linear single-stranded DNA genome of about 4.7kb. AAVs can replicate in the nucleus of target cells only in the presence of helper viruses such as adeno, herpes or papillomaviruses. The AAV genome is flanked by two palyndromic inverted terminal repeats (ITR, 145 bp), that are the only viral sequences required for the production of AAVs carrying the exogenous DNA of choice.

Dozens of different AAV serotypes have so far been identified (Allocca et al., 2007). The availability of a different capsid from each serotype and the versatility of the

AAV production system allow an easy exchange of capsids among various AAVs thus creating hybrid vectors containing a genome with the same AAV ITRs (i.e. from AAV2) and the capsid from a different serotype (Allocca et al., 2007). The ability of the various AAV serotypes to transduce the retina has been extensively documented with vectors encoding marker proteins (Figure 20). AAV2/8 is the most efficient for photoreceptor transduction after subretinal injection (Allocca et al., 2007). Moreover, retinal progenitor cells can also be transduced by AAV serotypes (Surace et al., 2003).

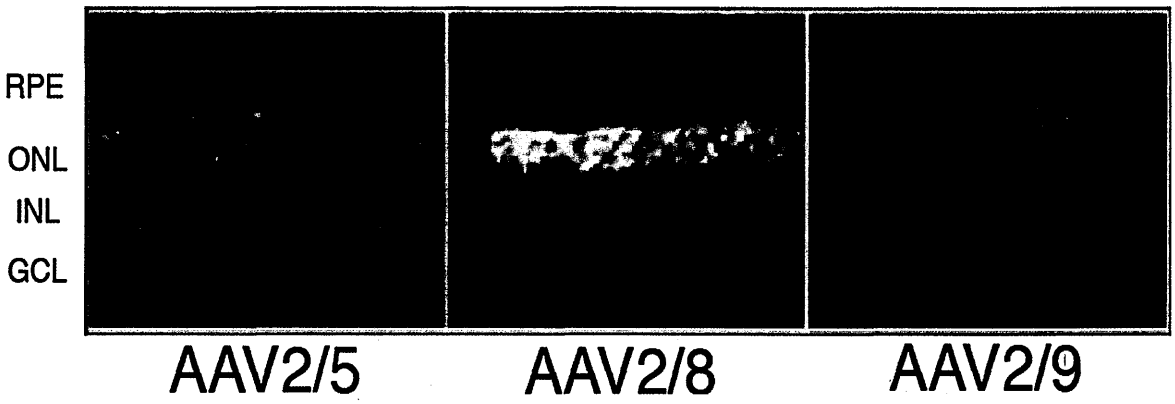

Figure 20. The transduction of murine photoreceptor by various AAV serotypes.

The pictures show the histological analysis of the eGFP expression at 4 weeks following subretinal injection of AAV2/5, 2/8 or 2/9. The AAV vector genome encodes eGFP under the control of the Rhodopsin promoter that drives transgene expression in photoreceptors only. Adapted image from (Allocca et al., 2007).

Due to their low toxicity and immunogenicity and their efficiency in transducing photoreceptors, AAV vectors derived from various serotypes have been widely used to treat IRDs in animal models (Colella and Auricchio, 2010).

1.2 LONG NON-CODING RNAS: NEW FUNCTIONAL PLAYERS

1.2.1 "RNA World"

The "RNA world" theory suggests that life was initially based on RNA, which subsequently transferred this amount of information into more stable DNA and its catalytic functions to proteins. Consequently, in the past, RNA has been relegated to an intermediate stage between gene and protein, as shown in the central dogma formula 'DNA-RNA-protein'. However, the finding that most of the genome in complex organisms is transcribed (Carninci et al., 2005; Denoeud et al., 2007) and the discovery of new classes of regulatory non-coding RNAs (ncRNAs) (Kapranov et al., 2007), challenges this assumption and suggests that RNA has evolved and expanded in coexistence with proteins and DNA.

Non-coding RNAs comprise a diverse group of transcripts including 'housekeeping' ncRNAs (ribosomal RNA, transfer RNA, small nuclear RNA and small nucleolar RNA) and regulatory ncRNAs (Jacquier, 2009). Regulatory ncRNAs can be classified according to their size as small ncRNAs (<200 bp) (for example, miRNAs, endogenous small interfering RNAs (endo-siRNAs) and PIWI-interacting RNAs (piRNAs)) and long ncRNAs (lncRNAs). Members of both classes are known for their ability to regulate gene expression by a wide range of mechanisms. For example, miRNAs can act at the RNA level by destabilizing and degrading their target RNAs or at the protein level by downregulating translations of their targets (Bartel, 2009).

LncRNAs can also act at multiple levels. LncRNAs regulate gene expression by a range of mechanisms, including transcriptional interference by antisense transcription and modulation of chromatin modifications (see section 2.4).

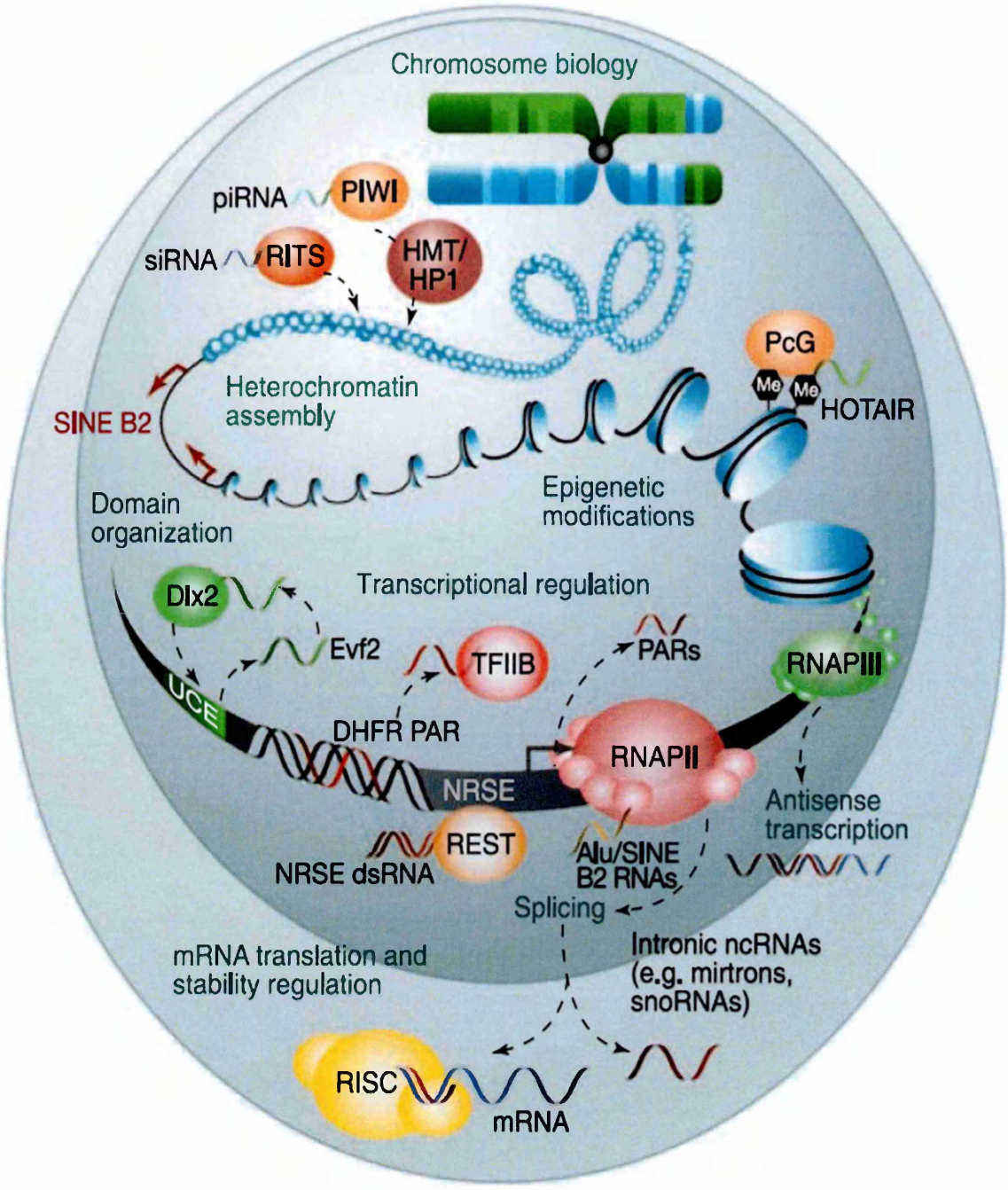

Figure 21. Recent examples of the various levels of regulation of eukaryotic gene expression and cell biology by ncRNAs.

DsRNA, double-stranded RNA; HMT, histone methyltransferases; HP1, heterochromatin protein 1; PARs, promoter-associated RNAs; PcG, Polycomb group proteins; RISC, RNA-induced silencing complex; RITS, RNA-induced initiation of transcriptional gene silencing; siRNA, small interfering RNA; TFIIB, transcription factor IIB; and UCE, ultraconserved element. Modified image from (Amaral and Mattick, 2008).

Moreover, ncRNAs are an integral component of the chromosomes and contribute to their structural organization (Rodriguez-Campos and Azorin, 2007). It is now becoming apparent that chromatin architecture and epigenetic memory are regulated by RNA-directed processes that, although the exact mechanisms are yet to be understood, involve the recruitment of histone-modifying complexes and DNA methyltransferases to specific loci (Mattick, 2007). In addition, lncRNAs have been implicated in the regulation of dosage compensation and genomic imprinting in animals (for details about lncRNA functions see section 2.4) (Figure 21).

1.2.2 Long non-coding RNAs (lncRNAs)

Long non-coding RNAs (lncRNAs) were first described during the large-scale sequencing of full-length cDNA libraries in the mouse (Okazaki et al., 2002). Although distinguishing lncRNAs from other protein-coding mRNAs is not a simple process it has become apparent that a consistent part of the transcriptome has little protein-coding capacity. Genome tiling array experiments have revealed, in fact, that the extent of the non-coding sequence transcription is at least four times greater than that of the coding sequence (Kapranov et al., 2007). These studies have also shown that the transcriptome is surprisingly complex, with lncRNAs often overlapping with or interspersed between coding transcripts (Kapranov et al., 2005). This complexity has modified the common understanding of gene organization from a linear to a more complex model, in which it is possible for a gene sequence to be transcribed into sense and antisense, coding and non-coding transcripts (see section 2.3).

Defining lncRNAs simply on the basis of size reflects a current imperfect understanding of their functions and is far from satisfactory. However, there is some sense

in defining non-coding transcripts according to the absence of a protein-coding capacity given that the ability to identify protein-coding transcripts has improved immeasurably in recent years (Dinger et al., 2008). Many long, previously wrongly annotated as protein-coding genes, instead, represent non-protein coding transcripts (Ponting, 2008).

Before considering their potential for functionality, it is important to consider whether a large proportion of the proposed lncRNAs are the results of "transcriptional leakage" or of artefactual computational prediction. However, there are several pieces of evidence against the above hypothesis. Among mouse transcripts annotated as non-coding RNAs, from different high-throughput studies, very few have both long open reading frames and a suppression of nucleotide substitutions at putative non-synonymous sites, attributes that would indicate a coding capability (Ravasi et al., 2006). The majority of these non-coding RNAs, in fact, appear to represent *bona fide* transcripts, a view that is also corroborated by the regulation of their expression levels (Cawley et al., 2004). A large number of lncRNAs are expressed in specific regions of the brain, exhibiting precise cellular locations (Mercer et al., 2008). Some mark new domains within the cell (Sone et al., 2007), which means that lncRNAs are also set to have a major impact in cell biology. Comparative analyses indicate that lncRNA promoters are, on average, more conserved than those of protein-coding genes (Carninci et al., 2005) and that lncRNA sequences, secondary structures, and splice site motifs have been subject to purifying selection (Torarinsson et al., 2008). Moreover, many lncRNAs are evolving quickly, and some have undergone recent positive selection, as exemplified by HAR1 RNA expressed in the human brain, which contains the sequence conserved in mammals that most rapidly diverged after the human-chimpanzee separation (Pollard et al., 2006). Given the functional versatility of the RNAs, it is plausible that the lncRNAs represent a rich substrate for evolutionary innovations in the eukaryotes.

Finally, a database providing expression and other information on mammalian lncRNAs has recently become available (Dinger et al., 2009).

1.2.3 Genomic organization of lncRNAs

A lncRNA can be assigned to one of five broad categories: (1) sense, or (2) antisense, when overlapping one or more exons of another transcript on the same, or opposite, strand, respectively; (3) bidirectional, when its transcription and that of a neighboring coding transcript on the opposite strand are initiated in close genomic proximity, (4) intronic, when it is derived wholly from within an intron of a second transcript or (5) intergenic, when it lies within the genomic interval between two genes (Figure 22).

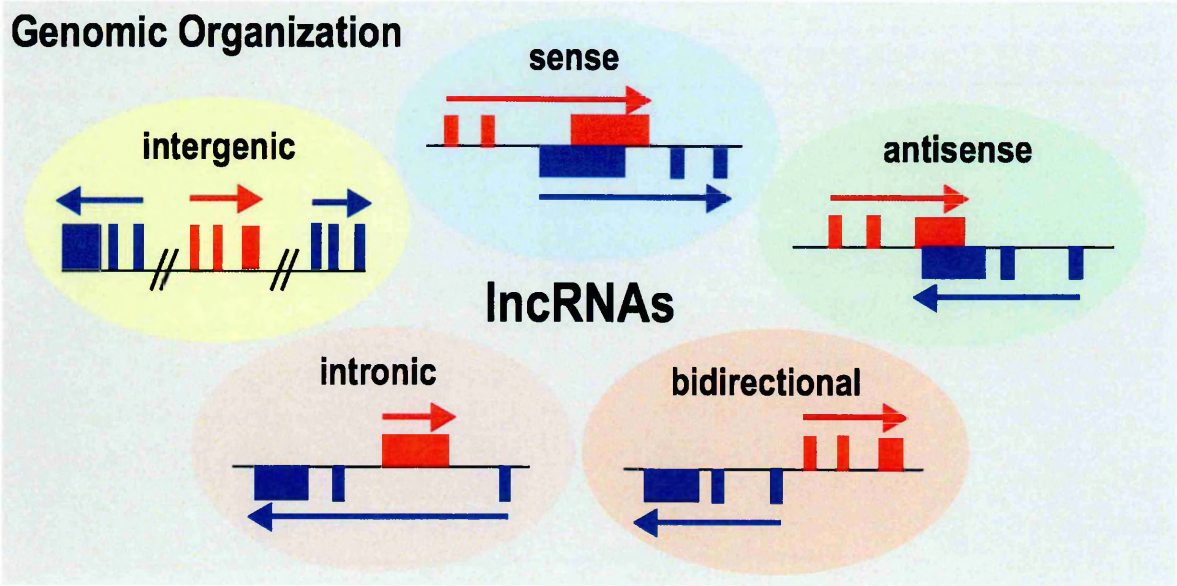

Figure 22. Genomic organization of long non-coding RNAs (lncRNAs).

A significant fraction of long non-coding RNAs are spliced and polyadenylated, like cytosolic messenger RNAs, however some mature lncRNAs can be unspliced and retained

in the nucleus (Seidl et al., 2006).

A relevant fraction of lncRNAs is constituted by natural antisense transcripts (NATs) that are RNAs displaying sequence complementarity to other transcripts (Carmichael, 2003). NATs can be divided in two main subgroups, namely *cis*-NATs and *trans*-NATs. In particular, *cis*-natural antisense transcripts are transcribed from the same genomic locus as their cognate genes but from the opposite DNA strand and form perfect pairs. On the contrary, *trans*-NATs, e.g. microRNAs, are transcribed from a different location than their targets and usually have complementarity to multiple transcripts with some mismatches (Carmichael, 2003). A large proportion of genes (more than 30%) in diverse eukaryotes have been found to harbor cis-natural antisense transcripts (*cis*-NATs) (Lapidot and Pilpel, 2006). *Cis*-NATs have been implicated in many levels of eukaryotic gene regulation including translational regulation, genomic imprinting, RNAi, alternative splicing, XCI, RNA editing, and gene silencing (see section 2.4) (Lavorgna et al., 2004). Even though the eukaryotic genome contains a large number of NATs, our understanding of how antisense transcription regulates gene expression remains largely incomplete.

In human tissues, bidirectional transcripts tend to be coexpressed and/or inversely expressed more frequently than would be expected by chance, and this expression pattern tends to be evolutionarily conserved (Chen et al., 2005).

Of the large numbers of intronic lncRNAs that have been proposed, many may, instead, be pre-mRNA fragments (Louro et al., 2008). Nevertheless, some intronic non-coding RNAs whose expression profiles contrast with those of their host protein-coding gene have also been reported (Dinger et al., 2008).

Intergenic non-coding RNAs are beginning to reveal their mystery. Those that are transcribed well away from protein-coding loci appear to have little opportunity for *cis*-regulated transcription within such loci. They may, however, often act in *trans* within large

ribonucleoprotein complexes. Many intergenic non-coding RNAs are transcribed in close proximity to protein-coding genes (Bertone et al., 2004) and these are more likely to act *in cis*, perhaps through transcriptional interference (for details see section 2.4).

1.2.4 Functional examples of lncRNAs

Unlike the microRNAs or proteins, the function of the lncRNAs is not deduced from sequence or structure signatures. The functional repertoire of the lncRNAs includes roles in high-order chromosomal dynamics, telomere biology and subcellular structural organization (Amaral and Mattick, 2008). One major emergent theme is the involvement of lncRNAs in regulating the expression of neighboring protein-coding genes. The importance of this regulation was understood through the study of the phenomenon in which non-coding loci affect the expression of nearby protein-coding genes *in trans* (Mattick and Gagen, 2001). Additionally, the recent observation that human chromosome 21 largely recapitulates its native expression profile in mouse cells, despite interspecies differences in epigenetic machinery, cellular environment and transcription factors, suggests that most of the information required for gene regulation is embedded in the chromosome sequence (Wilson et al., 2008).

1.2.4.1 Transcriptional and post-transcriptional regulation

LncRNAs regulate transcription through a diversity of mechanisms. Proximal promoters can be transcribed into lncRNAs that recruit and integrate the functions of RNA binding proteins into the transcriptional program, as exemplified by the repression of *CcnD1* (Cyclin D1) transcription in human cell lines (Wang et al., 2008). DNA damage signals induce the expression of lncRNAs associated with the *CcnD1* gene promoter, where they

act cooperatively to modulate the activities of the RNA binding protein TLS. TLS subsequently inhibits the histone acetyltransferase activities of the CREB binding protein and P300 to silence *CcnD1* expression (Figure 23).

The ability of the ncRNAs to recruit RNA binding proteins, one of the largest protein classes in the mammalian proteome, to gene promoters hugely expands the regulatory repertoire available to the transcriptional program (Wang et al., 2008).

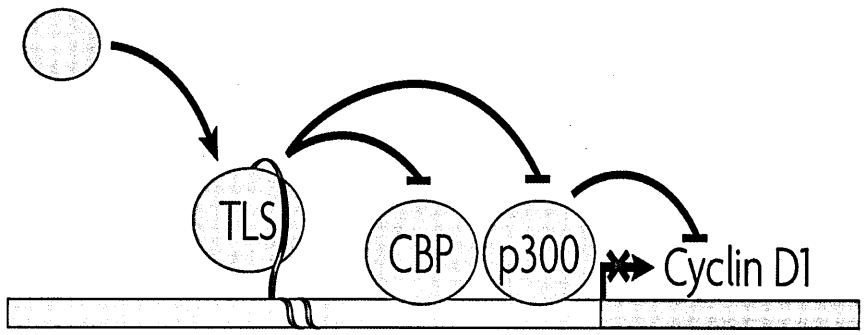

Figure 23. Transcription regulation of lncRNA by protein recruitment.

LncRNAs (in red) tethered to the CcnD1 gene recruit the RNA binding protein TLS to modulate the histone acetyltransferase activity of CREB binding protein (Cbp) and p300 to repress gene transcription. Modified image from (Mercer et al., 2009).

LncRNAs also act as co-factors to modulate transcription factor activity. For example, in mice, the lncRNA *Evf2* is transcribed from an ultraconserved distal enhancer and recruits the binding and action of the transcription factor *Dlx2* to this same enhancer to induce expression of adjacent protein-coding genes (Feng et al., 2006) (Figure 24).

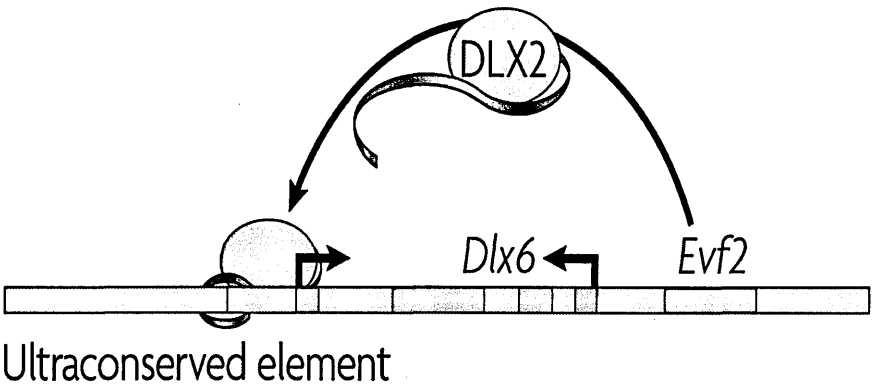

Figure 24. Transcription regulation of lncRNA by transcription factor co-activation.

An ultraconserved enhancer is transcribed as a lncRNA, Evf2, which subsequently acts as a co-activator to the transcription factor DLX2, to regulate the Dlx6 gene transcription. Modified image from (Mercer et al., 2009).

Many similar enhancers are transcribed in cells in which they are active. This could be a general strategy to regulate the expression of key developmental genes (Ashe et al., 1997). LncRNAs can regulate RNA polymerase (RNAP) II activity through other mechanisms, including the interaction with the initiation complex to influence promoter choice. For example, in humans, a lncRNA transcribed from an upstream region of the dihydrofolate reductase (*DHFR*) locus forms a triplex in the major promoter of *DHFR* to prevent the binding of the transcriptional co-factor TFIID31 (Figure 25).

This could be a widespread mechanism to control promoter usage as thousands of triplex structures exist in the eukaryotic chromosomes (Ohno et al., 2002). Long ncRNAs can also effect global changes by interacting with basal components of the RNAP II-dependent transcription machinery. LncRNAs that interact with the RNAP II machinery are typically transcribed by RNAP III, thereby decoupling their expression from the RNAP II-dependent transcription reaction they regulate (Mariner et al., 2008). For example, *Alu*

elements that are transcribed in response to heat shock bind tightly to RNAP II to preclude the formation of active preinitiation complexes (Mariner et al., 2008). *Alu* elements contain modular domains that can independently mediate polymerase binding and repression. In light of their abundance and distribution in the mammalian genome, these functional domains might have been co-opted into other lncRNAs during evolution; an observation supported by the finding that functional repeat sequence domains are a common characteristic of several known lncRNAs (Amaral and Mattick, 2008).

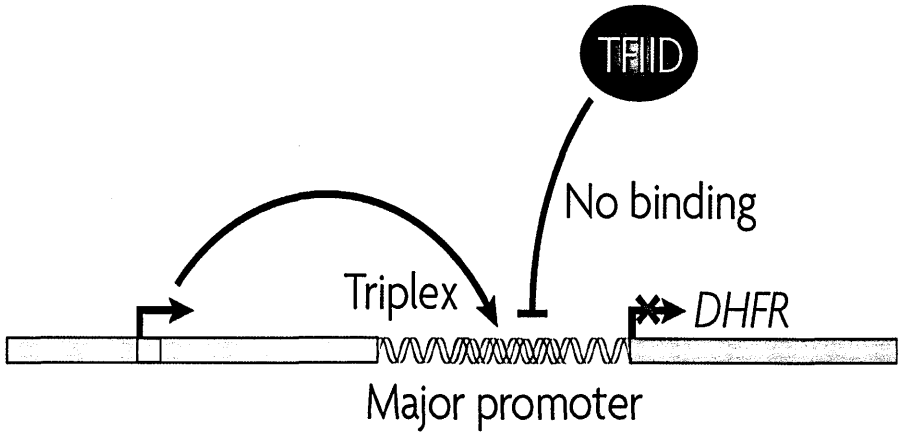

Figure 25. Transcription regulation of lncRNA by promoter blocking.

A lncRNA transcribed from the DHFR minor promoter in humans can form a triplex at the major promoter to occlude the binding of the general transcription factor TFIID, and thereby silence DHFR gene expression. Modified image from (Mercer et al., 2009).

A recent screening for lncRNAs regulated by *TP53* (tumor suppressor transcription factor p53) has revealed that *lincRNA-p21* targets silencing activity to multiple genes located throughout the genome in response to DNA damage (Huarte et al., 2010).

A search for the factors that interact with *lincRNA-p21* has identified heterogeneous nuclear ribonucleoprotein K (hnRNP-K), a component of a repressor complex that acts in the p53

pathway. hnRNP-K interacts with a 5' domain of *lincRNA-p21* that is necessary but not sufficient to induce apoptosis, suggesting that other regions of the RNA are required to recruit other factors or target the complex to chromatin or both. Thus, *lincRNA-p21* is a trans-acting downstream repressor of multiple genes in the p53 pathway, potentially explaining how p53 can activate many genes while simultaneously repressing many others (Figure 26).

The ability of the lncRNAs to recognize complementary sequences also allows highly specific interactions that are amenable to regulating various steps in the post-transcriptional processing of mRNAs, including their splicing, editing, transport, translation and degradation.

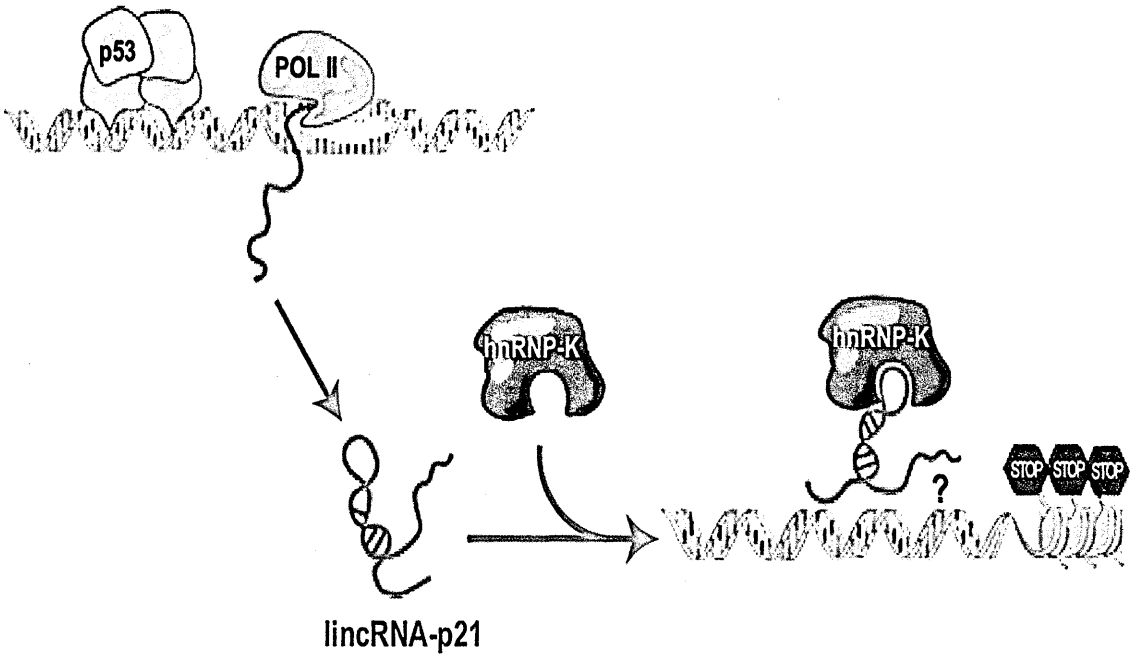

Figure 26. Function of lncRNA-p21 in the p53 transcriptional response.

Induction of p53 activates the transcription of lncRNA-p21 by binding to its promoter. LncRNA-p21 binds to hnRNP-K, and this interaction imparts specificity to genes repressed by p53 induction. LincRNA, long intergenic non-coding RNA. Modified image from (Baker, 2011).

Most mammalian genes express antisense transcripts, which might constitute a class

of lncRNA that is particularly proficient at regulating mRNA dynamics (He et al., 2008).

Antisense lncRNAs can mask key *cis* elements in mRNA by the formation of RNA duplexes, as in the case of the *Zeb2* (also called *Sip1*) antisense RNA, which complements the 5′ splice site of an intron in the 5′ UTR of the zinc finger Hox mRNA *Zeb2*. Expression of the lncRNA prevents the splicing of an intron that contains an internal ribosome entry site required for the efficient translation and expression of the ZeB2 protein (Figure 27).

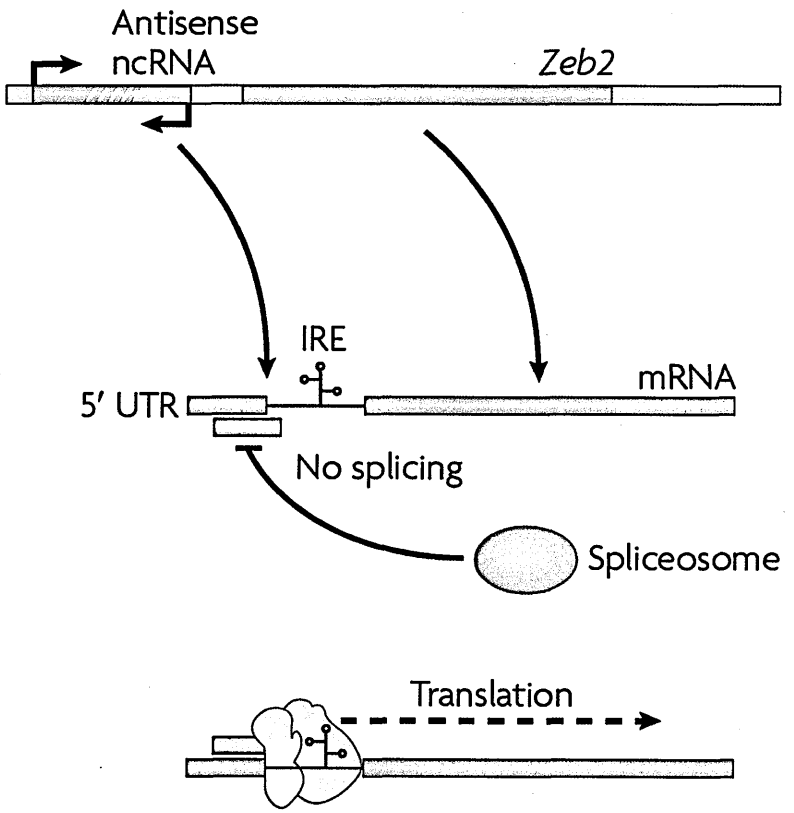

Figure 27. Example of post-transcriptional regulation by lncRNAs.

An antisense ncRNA can mask the 5′ splice site of the zinc finger homeobox mRNA Zeb2 from the spliceosome, resulting in intron retention. The translation machinery can then recognize and bind an internal ribosome entry site (IRE) in the retained intron, resulting in efficient Zeb2 translation and expression. Modified image from (Mercer et al., 2009).

This sets a precedent for the lncRNAs in directing the alternative splicing of mRNA

isoforms. Indeed, a number of studies have noted the prevalence of antisense lncRNAs to the introns, and they could similarly regulate splicing (He et al., 2008). Alternatively, the annealing of lncRNA can target protein effector complexes to the sense mRNA transcript in a manner analogous to the targeting of the RNA-induced silencing complex (RISC) to mRNAs by siRNAs.

RNA duplexes resulting from the annealing of complementary transcripts or even of long ncRNAs with extended internal hairpins can be processed into endogenous siRNAs to silence gene expression, raising the possibility that many long ncRNAs feed into RNA silencing pathways (Ogawa et al., 2008). There are probably many other functions of the long ncRNAs that still await discovery. For example, the lncRNA *NRON* has been shown to regulate the nuclear trafficking of the transcription factor NFAT36 (Willingham et al., 2005). The observation that many lncRNAs are located in the cytoplasm suggests that they might have undiscovered roles in cell biology.

1.2.4.2 Chromatin modification

Another important aspect is the ability of the lncRNAs to bind chromatin modification complexes. Numerous lncRNAs are pulled down by RNA immunoprecipitation (RIP) of PRC2 (polycomb repressive complex) and other chromatin-modifying factors. The PRC2 complex has histone methyltransferase activity and primarily trimethylates histone H3 on lysine 27 (i.e. H3K27me3), a mark of a transcriptionally silent chromatin. PRC2 has four subunits: Suz12 (zinc finger), Eed and Ezh2 (SET domain with histone methyltransferase activity) (Figure 28) (Khalil et al., 2009). *In vitro* evidence suggests that the PRC2 complex may bind directly to RNA stem-loop structures via EZH2 (Zhao et al., 2010).

Comparison of the PRC2 "transcriptome" to known PRC2-binding sites and bivalent domains (genomic regions with high H3K27me3 and H3K4me3) in ES cells has revealed that many (~20%) bivalent domains contain at least one RNA, suggesting that lncRNAs may also recruit PRC2 to their sites of synthesis as well as to distal sites. PRC2 is not the only histone-modifying complex found to bind to lncRNAs. The *HOTAIR* lncRNA is expressed from an intergenic region of the *HoxC* cluster and is necessary for PRC2 occupancy, H3K27me3, and silencing of the *HOXD* locus, located on a different chromosome (Rinn et al., 2007). Analysis of *HOTAIR* has revealed that a 5' end domain binds PRC2 and a 3' end domain binds an LSD1 (H3K4me2 demethylase) containing complex. Thus *HOTAIR* can act as a scaffold for these two distinct histone modification complexes and appears to target them to specific regions to remove the active histone modification H3K4me2, while methylating H3K27 toward a repressive mode (Figure 28).

What is not clear from many of these studies is the precise mechanism by which these lncRNAs affect multiple genes. It is possible that they act as mobile scaffolds that target key complexes to multiple gene loci wherever they happen to be. This model fits other chromatin modifying complexes, such as Mll, PcG, and G9a methyltransferase, which can be similarly directed by their associated lncRNAs (Mercer et al., 2009) (Figure 29).

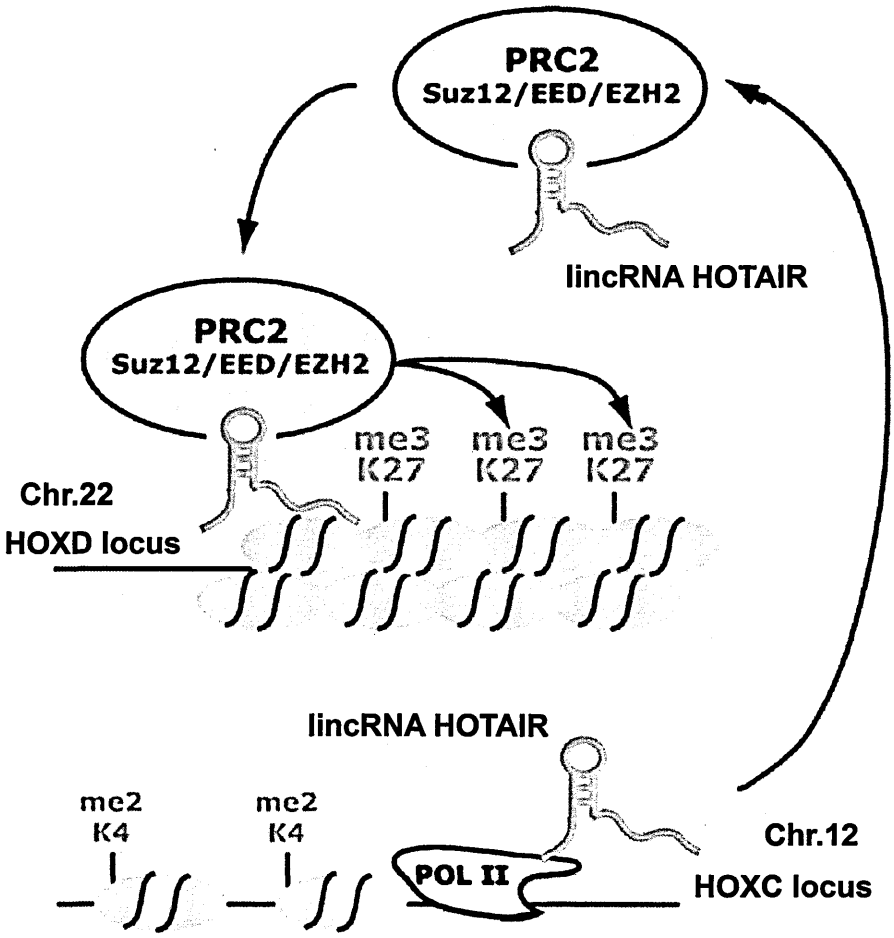

Figure 28. Model of lncRNA HOTAIR regulation of chromatin domains via histone-modification enzymes.

Recruitment of PRC2 is programmed by lncRNA HOTAIR produced in trans, which targets PRC2 activity to target loci. PRC2 recruitment leads to H3K27 methylation and transcriptional silencing of neighboring HOX genes. Modified image from (Rinn et al., 2007).

However, they may also function as organizing centers, performing the same functions by gathering multiple loci and factors into higher-order structures such as described for lncRNAs *Xist*, *Air* and *Kcnq1ot1*. LncRNA *Xist* mediates X chromosome inactivation. A small internal non-coding transcript from the *Xist* locus, *RepA*, recruits PRC2 to silence one X chromosome (Zhao et al., 2008), whereas PRC2 is titrated from the

remaining active X chromosome by the antisense transcript *Tsix*. However, another study describes an alternative mechanism whereby *Xist* and *Tsix* anneal to form an RNA duplex that is processed by Dicer to generate small interfering RNAs (siRNAs), which are required for the repressive chromatin modifications on the inactive X chromosome (Ogawa et al., 2008). The contribution of these two different pathways to coordinate long and small RNAs in chromatin remodeling implies the existence of a global, integrated regulatory network based in RNA.

Other lncRNAs such as *Air* and *Kcnq1ot1* also create repressive environments that may recruit and silence specific *cis*-linked gene loci by interacting with chromatin and targeting repressive histone modifiers (Nagano et al., 2008; Pandey et al., 2008) (Figure 29).

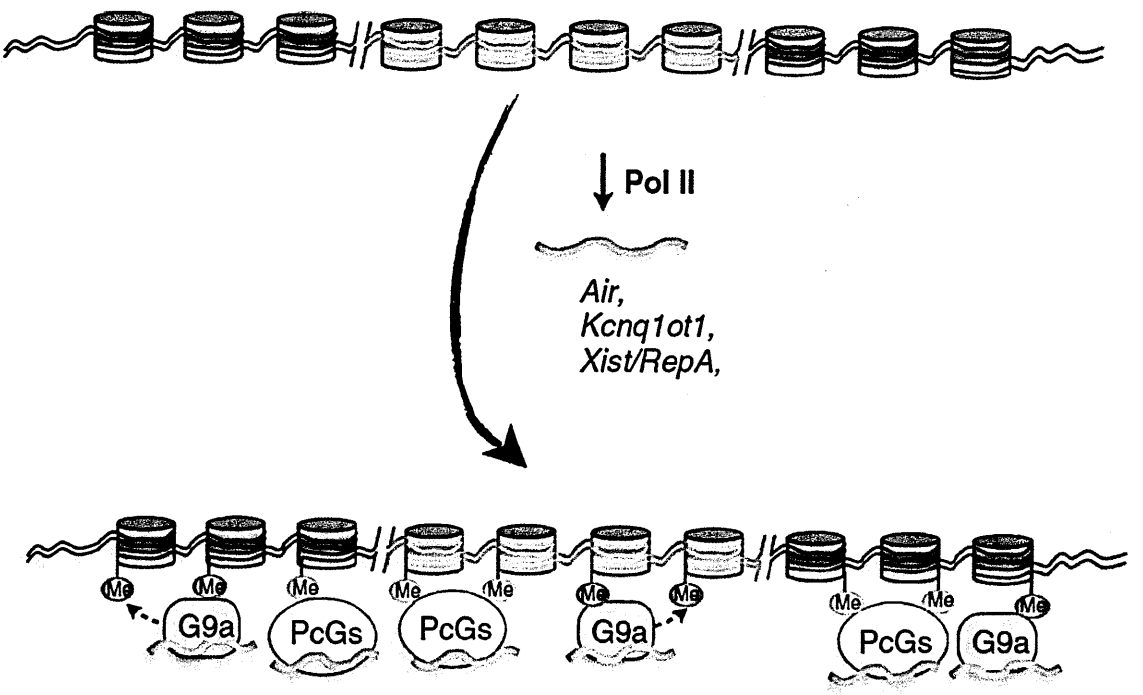

Figure 29. Long noncoding RNA-mediated heterochromatin silencing.

Examples shown here are Air, Kcnq1ot1, Xist /RepA. Modified image from (Chen and Carmichael, 2010).

The lncRNAs *Kcnq1ot1* and *Air* are all paternally expressed, and repressed on the maternal allele by promoter DNA methylation originating in the oocyte (Peters and Robson, 2008). There is very little splicing of these RNAs, which are therefore largely colinear with the DNA (Redrup et al., 2009). Perhaps, during their evolution, they may have lost the capacity to be spliced in order to evade the nonsense mediated decay pathway. For both *Air* and *Kcnq1ot1*, it has been found that the RNA appears to establish a nuclear domain, which is closely associated with the genes that are inactivated in *cis*, whereas the genes outside the cluster, which are not regulated by the lncRNAs, are found outside the nuclear RNA domain. The *Kcnq1ot1* RNA domain excludes Pol II and is enriched with PRC1 and PRC2 components (Terranova et al., 2008). The Kcnq1ot1 RNA also binds to the histone methyltransferase G9a (Pandey et al., 2008); the *Air* RNA also binds to G9a and appears to target this enzyme to a silenced gene in the cluster (Nagano et al., 2008).

1.2.4.3 Regulation of enhancer activity

Another large non-coding RNA group (potentially long non-coding RNAs) is represented by the enhancer-related RNAs. Many of the ~12,000 neuronal activity-regulated enhancers in the mouse genome are transcribed as bidirectional transcripts by RNAP to yield non-coding enhancer RNAs called eRNAs (Kaikkonen et al., 2011; Kim et al., 2010) (Figure 30). The expression level of the eRNAs generally correlates with that of the nearby protein-coding (target) genes, and in at least one example, eRNA expression requires an intact target gene promoter, suggesting a reciprocal interaction between enhancers and promoters during promoter activation. At the molecular level, RNAP-bound enhancers have been found to be enriched with a large number of eRNAs, suggesting that the transcription of enhancers may be a general feature (De Santa et al., 2010) (Figure 30).

However, the possibility that eRNAs are byproducts of target gene activation cannot be excluded, as it has not been confirmed that they play an essential role.

High-throughput siRNA screening on lncRNAs, located further than 1 kb from known protein-coding genes, has put forward evidence that the lncRNAs themselves may have an enhancer function (Orom et al., 2010). Importantly, these lncRNA loci have the chromatin signatures of transcribed protein-coding gene loci (H3K4me3 at the 5' end and histone H3 lysine 36 trimethylation downstream), suggesting that they are not enhancer elements, which are characterized by H3K4 monomethylation. Knockdown of these lncRNAs results in corresponding decreases in the expression of neighboring protein-coding genes.

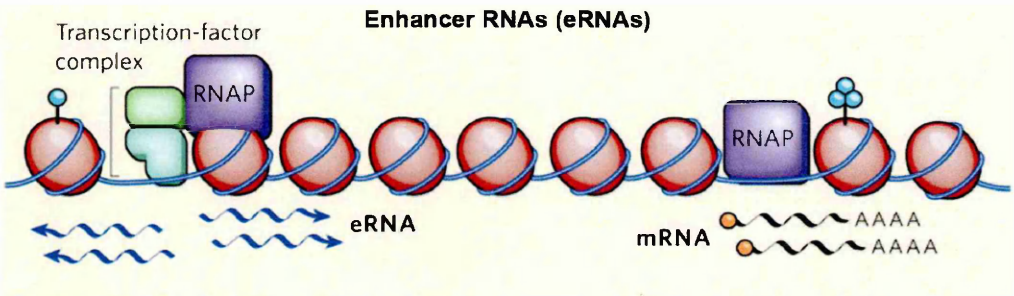

Name	Length (nt)	Characteristics	Function
Enhancer RNA (eRNA)	100–9000	ssRNA produced bidirectionally from enhancer regions enriched for H3K4me1, PolII and coactivators such as p300 Short half-life Evolutionarily conserved sequences Dynamically regulated upon signalling Expression correlates positively with nearby mRNA expression	Mostly unknown but plays a role in transcriptional gene activation

Figure 30. Enhancer RNAs (eRNAs).

RNA polymerase (RNAP) bind to enhancers and produce the transcription of enhancer RNAs (eRNAs). Simultaneously, RNAP and transcription machinery also bind to promoters and initiate mRNA transcription. Below, table describes the properties of eRNAs. Modified images from (Kaikkonen et al.,, 2011; Ren, 2010).

It is tempting to speculate that enhancer RNAs may function by physically positioning a putative partner factor with the promoter region of the target gene by long-range loop formation. Along this line, it has recently been described how DEAD-box RNA helicase p68 (DDX5) and its associated lncRNA, SRA (steroid receptor RNA activator), form a complex with CTCF (CCCTC binding factor) (Yao et al., 2010). CTCF binds to specific genomic binding sequences and plays an important role in transcriptional insulation and long-range physical interaction with other CTCF sites. These interactions are mediated by the ring-like cohesin complex that appears to use chromatin-bound CTCF as a binding platform (Figure 31). The insulator function of CTCF is dependent on p68 and

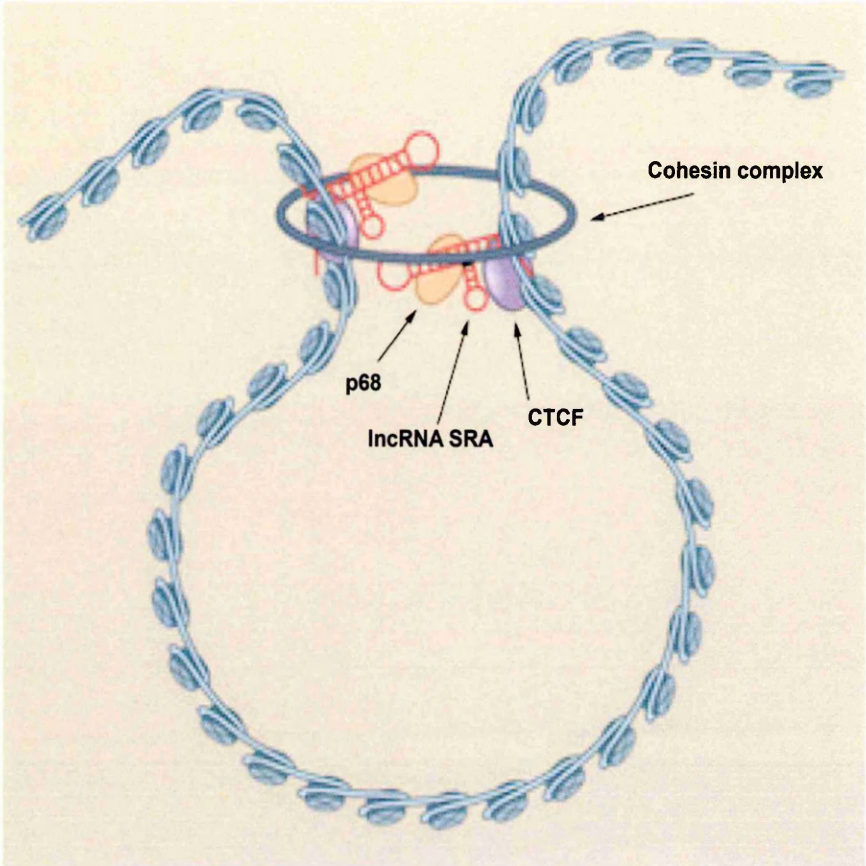

Figure 31. Higher-order chromatin loops such as those mediated by CTCF and cohesin appear to involve lncRNA.

Adapted image from (Nagano and Fraser, 2011).

SRA, as depletion of either mitigates CTCF-mediated insulation between IGF2 and its long-range enhancer at the IGF2/H19 locus. The protein p68 binds both SRA and CTCF, and SRA stabilizes binding between CTCF and cohesin. Depletion of either p68 or SRA does not affect CTCF binding to its genomic sites but reduces the presence of cohesin at these sites.

1.2.5 Genomic reprogramming and organization of nuclear structures.

LncRNAs have also been implicated in the global remodeling of the epigenome and gene expression during the reprogramming of somatic cells to the induced pluripotent stem cells (iPSCs). Recently, a subset of lncRNAs has been described to be specifically upregulated both in human iPSCs compared to the cell of origin and in iPSCs compared to the ES cells, suggesting that this increased expression of lncRNAs may promote reprogramming (Loewer et al., 2010). These lncRNA loci enriched with iPSCs are bound by the key pluripotency transcription factors *OCT4*, *SOX2*, and *NANOG*, and knockdown of *OCT4* leads to a downregulation of the lincRNAs, suggesting that their expression is directly regulated by the pluripotency factors. In particular, two of these lincRNAs, *lncRNA-RoR* and *lncRNA-SFMBT2*, have shown the strongest response to *OCT4* knockdown and therefore their potential role in reprogramming has been investigated by knocking them down in fibroblasts and assessing iPSC colony formation induced by infection with viruses expressing the pluripotency factors. Knockdown of *lncRNA-RoR* has resulted in a significant decrease in iPSC colony formation compared to control cells, indicating that it plays a role in iPSC derivation. This idea has subsequently been supported by the fact that cells stably overexpressing *lncRNA-RoR* were 2-fold more efficient in iPSC colony formation. By microarray analysis it has been found that knockdown of *lncRNA-RoR* leads to an upregulation of genes involved in the p53 response, the response to oxidative stress

and DNA-damage-inducing agents, and cell death pathways, suggesting that *lncRNA-RoR* plays a role in promoting iPSC survival (Loewer et al., 2010) (Figure 32).

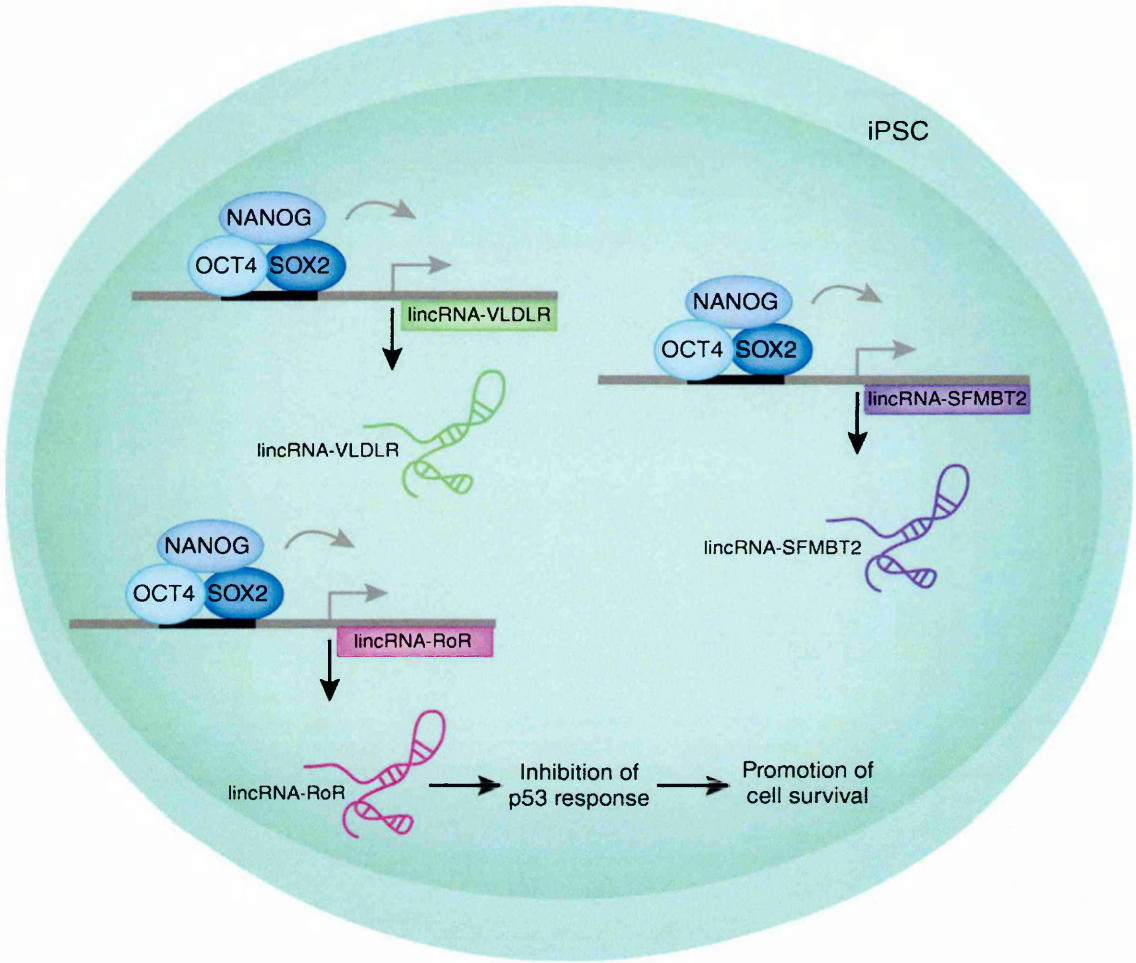

Figure 32. LncRNAs and genome reprogramming.

OCT4, SOX2 and NANOG activate the expression of genes coding for lncRNA-RoR, lncRNA-VLDLR and lncRNA-SFMBT2. LncRNA-RoR suppresses the p53 response and promotes iPSC survival. LincRNA, long intergenic non-coding RNA. Modified image from (Ng and Ng, 2010).

Recent live-cell results show that lncRNAs can also act as platforms for the assembly of dynamic nuclear structures such as paraspeckles. Paraspeckles are discrete ribonucleoprotein bodies found in mammalian cell nuclei, implicated in the nuclear retention of hyperedited mRNAs (Mao et al., 2011). *LncRNA-Men3/b* is the RNA

component of the paraspeckles. It has been demonstrated that paraspeckle-associated proteins are rapidly recruited and assembled on the *lncRNA-Men3/b* as they are being transcribed. These assembled structures persist near the nuclear site of transcription and the maintenance of paraspeckle structures is dependent on an active transcription of *lncRNA-Men3/b*. A temporary and reversible blocking of transcription leads to a disassembly of the paraspeckle components, whereas a reversal of the transcriptional block results in a reassembly of the paraspeckle proteins on nascent *lncRNA-Men3/b* only, not on mature *Men3/b* (Mao et al., 2011).

Furthermore, several types of nascent non-coding RNA can trigger the assembly of various nuclear bodies by serving as scaffolds for the accumulation of specific proteins, accentuating the capability of RNAs to act as modular scaffolds for the rapid assembly of multiple components (Shevtsov and Dundr, 2011).

1.2.6 Long non-coding RNAs in the retina

In the last few years, the expression of many retinal lncRNAs has been described. The first studied retinal-lncRNAs were the bidirectional transcripts or "opposite strand" transcripts (OS) whose transcription starts near (less than 1kb) and at the opposite direction to the protein-coding genes that play an important role in retinal development. In particular, a systematic investigation, performed in our laboratory, of OS transcripts associated with retinal homeodomain factors identified eight homeodomain-associated opposite-strand transcript partners (Alfano et al., 2005). These OS transcripts are named *Pax6os*, *Six3os*, *Six6os*, *Vax2os*, *Crxos*, *Otx2os*, *Pax2os*, and *Raxos* for their partnered transcription factors *Pax6*, *Six3*, *Six6*, *Vax2*, *Crx*, *Otx2*, *Pax2*, and *Rax*, respectively (Figure 33). The retinal expression of each OS transcript was confirmed by reverse transcriptase (RT)-PCR analysis. The majority of these OS transcripts lack any clear protein-coding potential and

have relatively little primary sequence homology among mammalian species, despite often being found in syntenic positions. Many, such as *Six3os*, undergo such extensive alternative splicing that little common sequence is found among the various isoforms. It is thus highly plausible that they represent genuine non-coding RNAs.

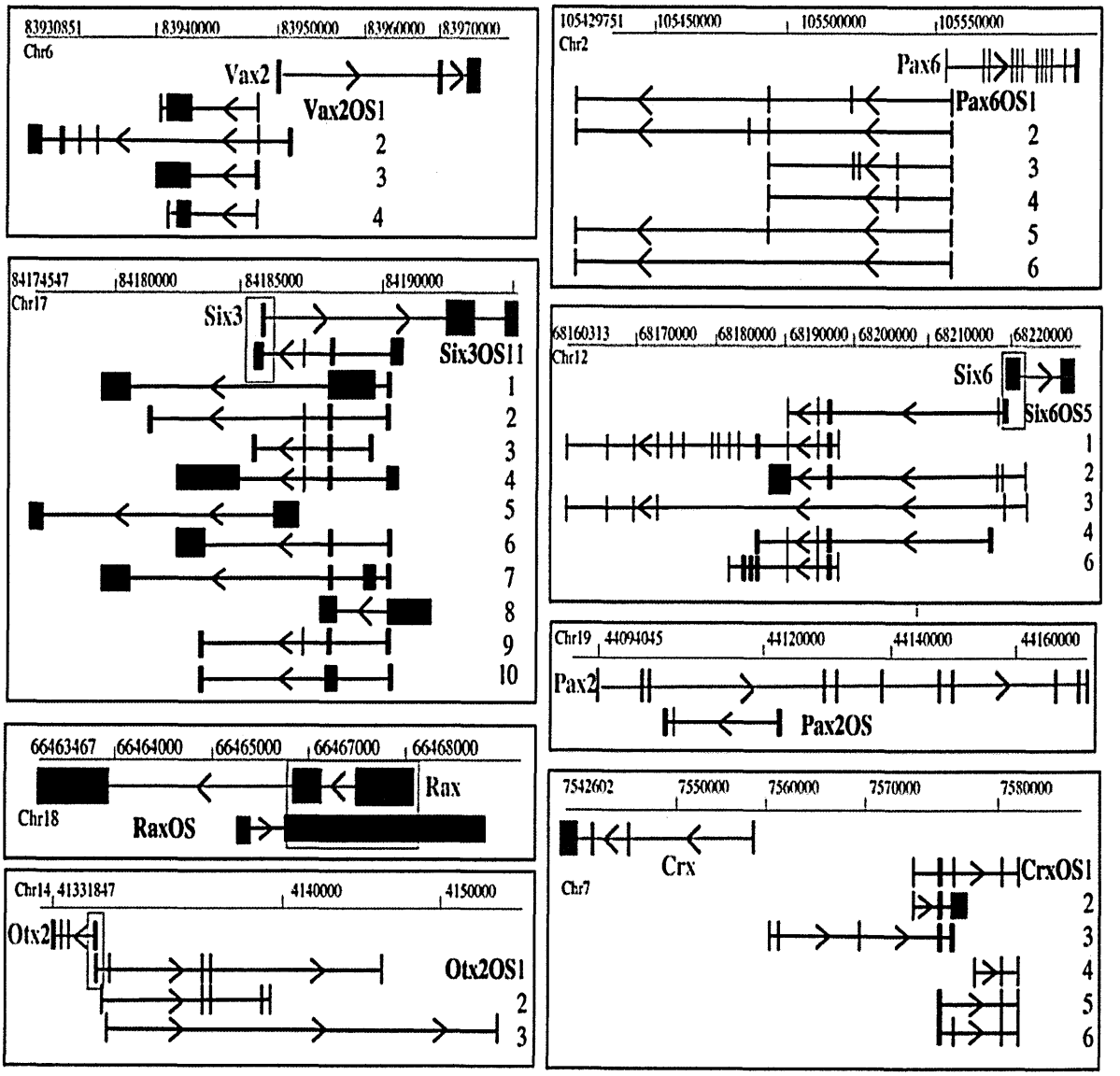

Figure 33. Genomic structure of murine natural antisense transcripts (NATs) associated with eye transcription factor genes.

Modified image from *(Alfano et al., 2005).*

Both the cellular expression pattern and the RNA expression level of a given OS RNA and its partnered homeodomain transcription factor can be either concordant or discordant in the retina. The RNA expression levels of both the OS transcript and its associated coding sequence can be practically identical, as is demonstrated by *Six3* and *Six3os*. The RNA levels of the OS transcript can also be far less abundant than the coding transcript, as is seen in *Six6* and *Six6os*. The cellular expression patterns of OS transcripts and coding sequences can likewise converge or diverge. *Six3os* is essentially coexpressed with *Six3* in retinal and diencephalic progenitor cells, while several other regions of the developing brain that express *Six3* do not express *Six3os* (Geng et al., 2007).

In the mature retina, different *Six3os* splice forms show differing expressions, with some isoforms coexpressed with *Six3* in the retinal ganglion cells while others are restricted to the Muller glia, which do not express *Six3* (Blackshaw et al., 2004).

Other OS transcripts are expressed in very different cellular patterns from their partnered homeodomain transcription factors. Both *Crxos* and *Otx2os* are expressed primarily in the amacrine and ganglion cells in the adult retina, while *Crx* and *Otx2* are expressed in the photoreceptor and bipolar cells, and thus show essentially complementary patterns of expression (Alfano et al., 2005). The only other OS transcript whose cellular expression pattern has been examined in the retina is *Vax2os*, which was independently identified as a transcriptional target of both *Crx* and *Nrl* in a recent microarray-based screening (Corbo et al., 2007; Hsiau et al., 2007). *Vax2os* is selectively expressed in the rod photoreceptors and, uniquely for rod-enriched transcripts, at higher levels in the ventral than in the dorsal retina. This is reminiscent of the embryonic expression pattern of *Vax2*, which is confined to the ventral retinal progenitors (Barbieri et al., 1999; Ohsaki et al., 1999). *Vax2* is weakly expressed in the outer nuclear layer of the adult retina, with RNA accumulating in the outer plexiform layer, and thus it is also likely to overlap with *Vax2os* in the adult retina. In some

cases, there appears to be either a mutually reinforcing or a reciprocal relationship between the expression levels of the OS transcripts and their partnered homeodomain transcription factors. Mutually reinforcing relationships are seen for *Vax2* and *Vax2os*, as mice bearing a targeted deletion of *Vax2* also showed a decrease in *Vax2os* RNA (Alfano et al., 2005). This same study, however, reported that reciprocal relationships are seen for *Crx* and *Crxos*, as an overexpression of *Crxos* by adenoviral transduction in the postnatal retina leads to a decrease in *Crx* mRNA levels. A caveat applies here though, because the isoform of *Crxos* selected contains an open reading frame and may be translated into protein, as discussed above, and these experiments did not directly determine whether these effects are mediated by the *Crxos*-encoded protein or by the *Crxos* RNA itself. In the case of *Six3* and *Six3os*, neither relationship was observed, as mice mutant for Six3 showed no change in *Six3os* expression (Geng et al., 2007).

Other lncRNAs have been discovered in the retina. *Taurine upregulated gene-1* (*Tug1*) was found in a screen to identify genes that are upregulated in response to taurine, which induces rod photoreceptor production (Young et al., 2005). When *Tug1* was knocked down, the developing rod photoreceptors showed a defect in migration into the outer nuclear layer, an ectopic expression of cone-specific markers, and an increased apoptosis in the transfected cells. Another lncRNA, termed *Rncr2* (*retinal non-coding RNA-2*), is evolutionarily conserved from amphibians to mammals and highly abundant in the developing retina (Blackshaw et al., 2004). Knockdown of *Rncr2* in the developing retina promotes the development of both the amacrine and Müller cells, suggesting a role for this lncRNA in selectively inhibiting the differentiation of specific retinal cell lineages (Rapicavoli et al., 2010).

1.3 AIMS OF THE THESIS

The main objectve of the research described in this thesis was to start elucidating the functional role of long non-coding RNA (lncRNA) in the mouse retina. Towards this goal, we took advantage of the studies previously carried out in my lab on a dataset of eight OS transcripts associated with retinal homeobox genes (Alfano et al., 2005). In particular, we proposed to achieve the following two aims during the course of my thesis project. First, we aimed at determining the expression patterns and levels of three retinal-specific lncRNAs, namely *Six3os*, *Otx2os* and *Vax2os*, in the developing mouse retina in order to select an interesting expression pattern for a particular isoform, useful for further functional experimental approaches (Part 1). Secondly, we performed a gain of function study both *in vitro* and *in vivo* for a selected one of the above mentioned lncRNAs in order to gain insight into the general function annotation of this class of transcripts in the mouse retina (Part 2). To achieve all these objectives, we selected the following main goals:

Section 3.1

1. To perform quantitative RT-PCR (qRT-PCR) in the developing and adult mouse retina for all the spliced isoforms of Six3os, Otx2os and *Vax2os;*

2. To determine the spatial expression of the most highly expressed isoforms of Six3os, Otx2os and *Vax2os in the developing and adult mouse retinas by RNA in situ hybridization (RNA-ISH).*

Section 3.2

3. To perform more detailed expression analysis by qRT-PCR and RNA-ISH for a selected lncRNA, which I will choose for further functional studies both in vitro and in vivo.

4. To carry out "gain of function" and "loss-of-function" experiments for a selected lncRNA in the mouse 661W cell line by means of transient transfection.

5. To perform "gain of function" and "loss-of-function" experiments for a selected lncRNA in the developing and adult mouse retinas by injecting at early postnatal stages Adeno Associate Vectors (AAVs) carrying appropriate expression cassettes.

SUMMARY OF THE RESULTS

The research performed in the first part of the thesis (Section 3.1) was driven by the evidence that many spliced isoforms of our selected retinal-lncRNAs exist. Therefore, there was a need to identify the most highly expressed isoforms for each lncRNA and also to understand their spatial expression patterns. I have obtained preliminary results in which the isoform 1 of *Vax2os* (*Vax2os1*) is the most highly expressed isoform during post natal retinal development. Moreover, I have detected, by RNA-ISH, that *Vax2os1* is expressed mostly in the ventral retinal areas at all the stages analyzed. Regarding *Six3os* and *Otx2os*, I have found that the isoform 9 of *Six3os* (*Six3os9*) and the isoform 3 of *Otx2os* (*Otx2os3*) are the most highly expressed isoforms and their cellular localizations are comparable with those of their near genes, *Six3* and *Otx2*, respectively. However, I have decided to focus my attention on *Vax2os1* not only because of its interesting spatial expression pattern (ventral high - dorsal low), but also due to the fact that the localization of *Vax2os1* in the retina differs from that observed for the near gene *Vax2*, as assessed by RNA-ISH. In particular, *Vax2os1* is expressed in the photoreceptor layer while *Vax2* is expressed in the remaining retinal cell types.

The second part of my PhD project (Section 3.2) has been focused on the determination of a functional annotation for *Vax2os1* in the mouse retina. First, I have performed *in vitro* gain of function experiments for *Vax2os1* in the mouse photoreceptor-like 661W cell line.

These experiments showed that *Vax2os1* might be implicated in the regulation of the cell cycle progression of the 661W cells. To gain a further insight into the role of *Vax2os1* in the regulation of photoreceptor cell cycle regulation I have injected post-natal retinas with AAVs overexpressing *Vax2os1*. I have carried out a systematic analysis of the expression patterns of some markers for proliferation that have showed that *Vax2os1* is able to regulate the cell cycle progression of the photoreceptor progenitor cells also *in vivo*. In particular, I have demonstrated that the overexpression of *Vax2os1* in the developing postnatal mouse retina determines an impaired cell cycle progression of the photoreceptor progenitors toward their final committed fate and a consequent delay of their differentiation processes.

Based on these results, I suggest that the role of *Vax2os1* is to ensure a proper control of the cell cycle progression of the photoreceptor progenitor cells in the ventral retina. Therefore, *Vax2os1* represents the first example of a lncRNA that acts as a cell cycle regulator in the mammalian retina during development. In conclusion, my study contributes to an increase in knowledge about the biological role *in vivo* of the emerging, although still poorly characterized, class of long non-coding RNAs.

2 MATERIALS AND METHODS

2.1 Generation of the plasmids for *Vax2os1* overexpression.

The *Vax2os1* full-length cDNA sequence was obtained from RNA samples of mouse adult retina retro-transcribed with SuperscriptIII kit (Invitrogen) using a mixture of oligo-dT and random primers. The PCR product for the *Vax2os1* full-length sequence was obtained with EcoRV tagged primers (*Vax2os1*-RV.F 5'-aaaagatatcGGACAGCCCCGTGGTACAGA-3', *Vax2os1*-RV.R 5'-aaaagatatcTTTATTCAAAAAGAAGGATGCG-3') and digested with EcoRV to obtain blunt ends. The digested PCR product was inserted in the pAAV2.1 CMV-BGH vector, CMV-citomegalovirus promoter, (Auricchio et al., 2001), provided by the TIGEM AAV Injection Core, previously linearized with PstI and BglII (NEB) and blunt ended with a T4 polymerase (Roche).

The cassette comprising the CMV promoter, the *Vax2os1* full-length and the BGH polyA sequence was amplified with the XbaI-tagged primers (cOS1b-XbaI.F 5'-gctctagagCTCCGCGTTACATAACTTACGG-3', cOS1b-XbaI.R 5'-gctctagagCCCTTAACTCGAGTCCCCAGC-3'), then digested with XbaI and inserted in the pAAV2.1 CBA-eGFP-BGH, overexpressing the GFP protein under the chicken beta-actin promoter (CBA), GFP-OE vector, (Allocca et al., 2007), previously linearized with NheI to obtain the final OS1-OE vector used for all the *in vitro* studies.

To generate the control vector overexpressing a mutagenized version of *Vax2os1*, the aforementioned plasmid was digested with ApaI enzyme and re-ligated to obtain the final delOS1-OE vector.

2.2 Expression studies.

The embryonic and the adult murine eye tissues were obtained from C57BL/6 wild-type mice. For postnatal and adult stages RNAs were extracted from whole mouse eye and retina, respectively. For the expression studies in mouse and in human, total RNA was extracted and digested with DNaseI using RNeasy extraction kit according to the manufacturer's instructions.

The cDNAs were generated by the Quantitect kit for the qRT-PCR analysis. As controls in the RT and qRT-PCR experiments we used RT-minus samples, i.e., samples to which we did not add the reverse transcriptase enzyme in the cDNA preparation. The cDNAs for the directional qRT-PCR in human Y79 cells were generated by SuperscriptIII kit using gene-specific primers.

The qRT-PCR reactions were performed with nested primers and carried out with the Roche Light Cycler 480 system. The PCR reaction was performed using cDNA (200-500 ng), 10 ul of the SYBR Green Master Mix and 400 nM primer, in a total volume of 20 ul. The PCR conditions for all the genes were as follows: preheating, 95°C for 5 min; cycling, 40 cycles of 95°C for 15 s, 60°C for 15 s and 72°C for 25 s. Quantification results were expressed in terms of cycle threshold (Ct). The Ct values were averaged for each triplicate. The *Hprt* gene was used as the endogenous control for the experiments in mouse (reference marker). For the experiments in the human Y79 cells, *HPRT1* was used as the endogenous control. Differences between the mean Ct values of the tested genes and those of the reference gene were calculated as $\Delta Ct_{gene} = Ct_{gene} - Ct_{reference}$. Relative expression was analysed as $2^{-\Delta Ct}$. Relative fold changes in expression levels were determined as $2^{-\Delta\Delta Ct}$ (Alfano et al., 2005).

The sequences of oligonucleotide primers are summarized in Table 1.

The genomic localization of the primers is shown in Figure 34.

Table 1. List of the sequences of the primers used in qRT-PCR experiments.

HUMAN			
Name	**Forward**	**Reverse**	**Bp**
VAX2OS	F 5'- TCCCTGACCTGCTTTTGAAC -3'	R 5'- GGGTCAGCGGGAATTAGC -3'	99
VAX2OS.2	F 5'- CTGACCTGCTTTTGAACCC-3'	R 5'- TCAGCGGGAATTAGCGCG-3'	91
nested VAX2	F 5'- AGCTGAACCTCTCCGAGACC -3'	R 5'- GCTTCTCCAGGTCTCTGCTC -3'	98
CRX	F 5'- AGGCACTGTTTGCCAAGACC -3'	R 5'- TTCTTGAACCAAACCTGAACC -3'	97
NRL	F 5'- CAGGGAGCCCAGAGGAGAC -3'	R 5'- GGTTTAGCTCCCGCACAGAC -3'	94
NR2E3	F 5'- CCTGCAGGAAACTATCTCTCG -3'	R 5'- CGCGTCTCTGGCTTGAAGA -3'	95
RHODOPSIN	F 5'- ATGCAATTTGGAGGGCTTCT -3'	R 5'-ATGGGCTTACACACCACCAC -3'	95
HPRT	F 5'- TGGCGTCGTGATTAGTGATG -3'	R 5'- AACACCCTTTCCAAATCCTCAG -3'	92
DNA	F 5'- TGGGGACCAATGAAAAACTG -3'	R 5'- TCACACACACTTTCGCCATC -3'	100
MOUSE			
Name	**Forward**	**Reverse**	
Vax2os1	F 5'-GAGTGGAGCGGGCGTTCT-3'	R 5'-GGGATACTTTCTTGCCGTCAG-3'	92
Vax2os2	F 5'-GGCGGTATCCAAGCGAGTG-3'	R 5'-AAGCGGAGCCAGACTGAAAG-3'	96
Vax2os3	F 5'-GCAAATAAGCTGCTCGGTTC-3'	R 5'-CCCGCCTAAAGAAGGAGAGAC-3'	97
Vax2os4	F 5'-CTGTGGAACCCCTGAGATC-3'	R 5'-GAAACTTCTCCCCTGCGTG-3'	103
Vax2os5	F 5'-GCTGTGAGTTTGAGTTCCAGAG-3'	R 5'-CGTTCTCAGCGTCCAGTTCC-3'	99
Vax2	F 5'-TCCTGGTACGAGATGCTAAGG-3'	R 5'-TCTGCTGTGAAGGAAGTACGG-3'	97
Six3os1	F 5'-TGCTAACCTCAAGACCCCATTC-3'	R 5'-CTCTACGCAGCCCCACTCTG-3'	96
Six3os3	F 5'-AACAGGTGGCTGGGTAGTGC-3'	R 5'-GGGGTGAGGTGAGGGGTAAG-3'	101
Six3os5	F 5'-AGGTGGCTGGTGATCAGAGG-3'	R 5'-AGCTTCTCGAAATTCTTTCAGG-3'	99
Six3os9	F 5'-GGCTGGATGCAGACAAAAGC-3'	R 5'-TCTGGTGGATCCCACTCTCC-3'	98
Six3	F 5'-GGCCAAGAACAGGCTCCA-3'	R 5'-GTGGACGGTGACTCTGCTG-3'	94
Otx2os1	F 5'-ATCCAGCTTTTGAAAGCATCAG-3'	R 5'-TTCATGACCCTTCGATATTTCC-3'	104
Otx2os2	F 5'-TTTACCTGGAAATATCGAAGATG-3'	R 5'-TTCTGAGTGTCTAGAGGTGATGG-3'	101
Otx2os3	F 5-'AGAAGAAGAGGATTTCAGCTTACG-3'	R 5'-TCATGACCCTTCTGCTTCCTG-3'	96
Otx2	F 5'-GGACTGCAGGGCAGAGAC-3'	R 5'-GAGTGACGGAACTAGGAGCAA-3'	97
Rho	F 5'-GCCACACTTGGAGGTGAAATC-3'	R 5'-AAGCGGAAGTTGCTCATCG-3'	100
Cngal	F 5'-ACTCGTACAAAAGGCGAGGAC-3'	R 5'-CTTTGTTGCTGCTGTTGTTGAC-3'	95
Prph2	F 5'-CGGGACTGGTTCGAGATTC-3'	R 5'-ATCCACGTTGCTCTTGATGC-3'	98
Pde6b	F 5'-TGAAGATGAAGATGTTTTCACG-3'	R 5'-CTCTGCGTGTCTCACAGTTG-3'	93
Hprt	F 5'-AGCTTGCTGGTGAAAAGGAC-3'	R 5'-GTCAAGGGCATATCCAACAAC-3'	94

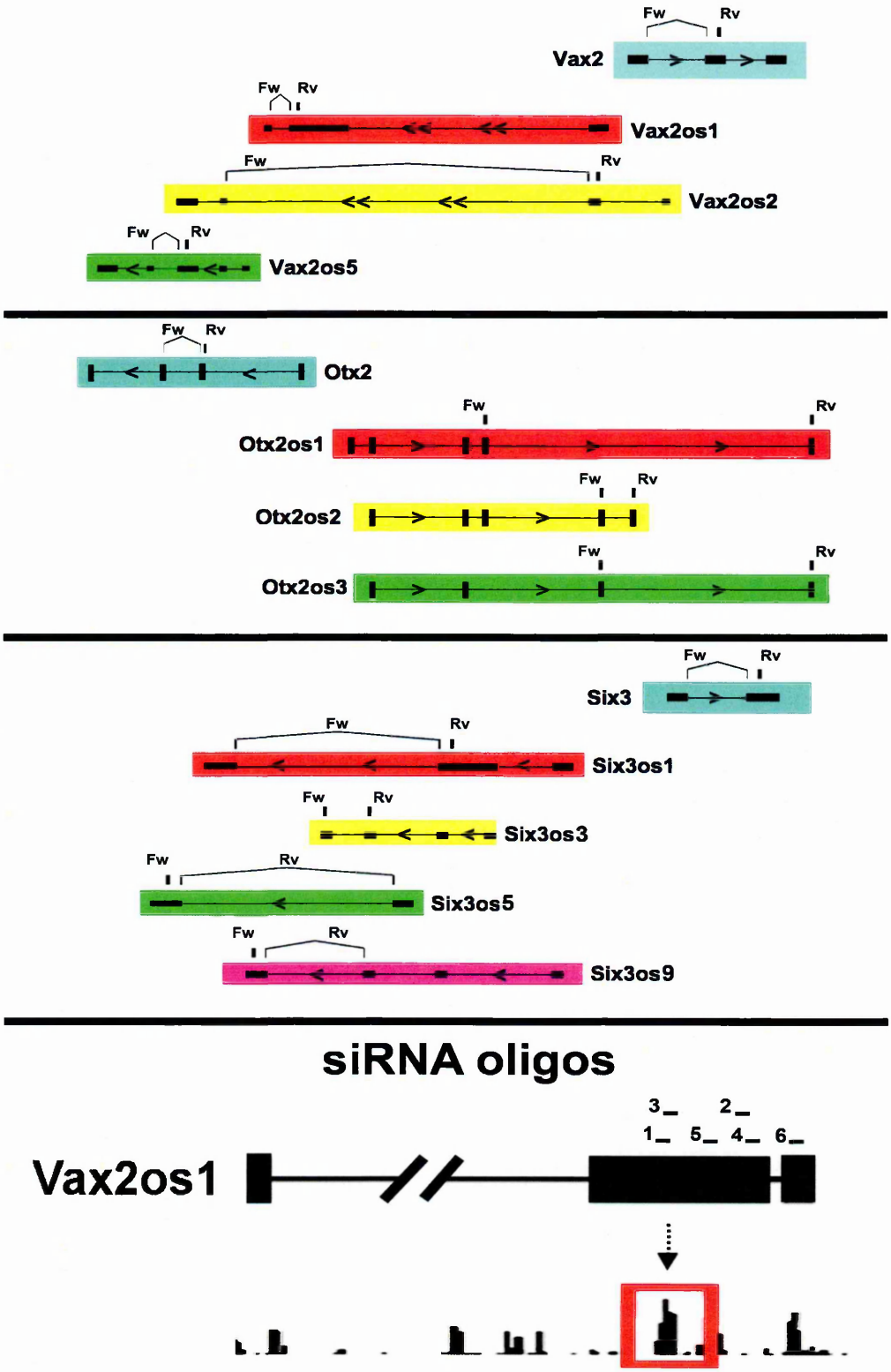

Figure 34. Genomic localization of the primers used fro qPCR and RNA interference studies.

2.3 Synthesis of RNA probes for *in situ* hybrydization

Antisense and sense cDNA templates were obtained by RT-PCR amplification of total RNA from C57/Bl6 mice with the appropriate oligonucleotide primers. These PCR products were then cloned into the Topo TA vector (Invitrogen). This vector contains two different promoter sequences (T7 and Sp6) for the expression of both the sense and antisense strands of the cloned product. The sequences of the primers used to obtain templates are shown in Table 2.

Table 2. List of the sequences of the primers used to obtain templates for RNA in situ hybridization experiments

Primer Name	**5'--> 3' Sequence**
Vax2os1.Fw	GGACAGCCCCGTGGTACAGA
Vax2os1.Rw	TTATTCAAAAAGAAGGATGCG
Vax2os5.Fw	ACCATCGTGACTTCTCCACAG
Vax2os5.Rw	GACTTAACTTCTCCCGGGTTTC
Six3os.Fw	CTCTGAGCGCGACCCTACC
Six3os.Rw	ACTGGGCATCTTGCACTGTAC
Otx2os.Fw	GGAAAAAAGACTTTTCTTTTTTTTC
Otx2os.Rw	CTGCTGCTGCTGCTGCTGGT

2.4 Transformation of E.coli with plasmid DNA

E.coli DH5α cells were prepared for transformation as follows: cells were grown to mid-log phase (A_{600}=0.6) in Luria Broth (LB: 1% bactotryptone, 1% NaCl and 0.5% Bacto-yeast extract) at 37°C with shaking. Cells were harvested by centrifugation at 2000 x g at 4°C, resuspended into 100ml (for each 100ml of culture) of 50% $CaCl_2$. This suspension was then centrifuged at 5000 x g for 15 min at 4°C. The resulting pellet was resuspended into 100ml (for each 100ml of culture) of 50% $CaCl_2$ and centrifuged again. The cells were

resuspended in 3 ml of ice cold 10% glycerol solution, aliquoted and stored at -80°C. For each transformation, DNA was added to 50 µl of competent cells, and incubated in ice for 20 min; then cells were subjected to heat shock at 42°C for 2 min and successively incubated on ice for 10 min. Cells were recovered in 1 ml of LB and incubated for 40 min at 37°C, before plating on LB-agar containing appropriate antibiotics. Plates were incubated at 37°C overnight to allow bacterial colonies to grow (Sambrook and Russell, 2001).

2.5 Isolation of plasmid DNA from E.coli

Mini-preps plasmid DNA preparations were carried out using the QIAGEN MINI prep kits. Procedure is based on the alkaline lysis method (Sambrook and Russell, 2001), but using a support column to purify isolated plasmid DNA. One aliquot of plasmid DNA was diluted in 1:200 in milliQ water, and the concentration was determined according to the following formula: absorbance of one A_{260} unit indicates a DNA concentration of 50 µg/ml.

2.6 Linearization of the plasmids

For the linearization of the plasmid, 10µg of plasmid DNA were digested using 20 units of the appropriate restriction enzyme (New England Biolabs) in 50µl of buffer provided by the manufacturer with the enzyme. The reaction was incubated for 1 hour at 37°C. Enzyme digestion was then controlled by agarose gel analysis. The digested product was confirmed by agarose gel electrophoresis. The product was then purified by extraction with phenol/chlorophorm and precipitated with 70% ethanol. The linearized plasmid was

then resuspended at the concentration of 0.2µg/µl in DEPC-treated H_2O (DEPC, Diethyl pyrocarbonate) to be used as template for the *in vitro* RNA transcription.

2.7 *In vitro* RNA transcription

To synthesise RNA probes the reaction mix was set up as follow:

5 µl of linearized plasmid/PCR product (1µg)

2 µl of 10X transcription buffer (Roche)

2 µl of DIG-labelling mix (Roche)

2 µl of appropriate RNA polymerase (T3, T7, SP6)-40 Units (Roche)

0.5 µl of RNase inhibitor

8.5 µl DEPC H_2O

The reaction mix was incubated for two hours at 37°C, after which 2 µl (20 Units) of DNase-RNase free was added to the reaction mix and incubated for 15 minutes at 37°C to degrade template DNA. 80 µl of H_2O were added to the reaction followed by precipitation with 0.1 volume 4M LiCl and 3x volume absolute ethanol at -20°C for two hours. The probe was then centrifuged at 2000 x g for 30 minutes at 4°C, washed with 70% ethanol, air-dried, dissolved in 40 µl of DEPC H_2O and stored at -20°C.

2.8 RNA *in situ* hybridization on cryostat sections

Sections were thawed after removal from -80°C, fixed with 4% PFA in PBS for 15 minutes at room temperature. The slides were washed twice in PBT (1X PBS+0.1% Tween-20), followed by bleaching with 6% H_2O_2 in PBT for 5 min at room temperature.

The sections were washed 3 times for 5 min in PBT, and the tissue was treated with either 1 µg/ml (mouse tissue) proteinase K for 15 min to permeabilise the tissue. Proteinase K activity was blocked by incubation with 2 mg/ml glycine solution in PBT for 10 min, followed by extensive washes with PBT. Post-fixation was performed with 0.2% glutaraldehyde / 4% PFA solution for 15 min at room temperature.

After 3 washes with PBT for 5 minutes sections were prehybridized with pre warmed hybridization buffer (50% formamide, 5X SSC pH4.5, 50 µg/ml Yeast RNA, 1% SDS, 50 µg/ml Heparin) in humidified chamber (5X SSC, 50% formamide) for at least one hour at the appropriate hybridization temperature. The slides were overlaid with 200 µl of hybridization solution containing 200-400 ng/ml of DIG labelled cRNA probe, heated to 65°C for 10 minutes and then kept on ice to prevent re-naturation. The individual slides were covered with parafilm, placed into a humidified chamber and incubated over night at hybridization temperature as indicated in Table 3.

Post-hybridization washes were performed 3 times for 15 minutes with prewarmed post-hybridization solution 1 (50% formamide, 4X SSC, 1% SDS) at hybridization temperature; 3 times for 15 min with prewarmed post-hybridization solution 2 (50% formamide, 2X SSC) at temperature 5°C lower then the hybridization temperature and finally 3 washes for 10 minutes with TBST (1X TBS, 2mM Levamisole, 0.1% Tween-20) at room temperature. The sections were incubated for 1 hour at room temperature with blocking solution (10% sheep serum in 100mM Maleic acid, 150mM NaCl, 0.1% Tween-20).

Alkaline phosphatase conjugated anti-DIG antibody was diluted 1:2000 in blocking solution and 200 µl were used to overlay each slide. Incubation was performed at 4°C over night in a humidified chamber. The following day sections were washed 4 times for 15

minutes with TBST followed by 3 washes for 10 min with NTMT (100mM NaCl, 100mM TrisCl pH 9.5, 50mM $MgCl_2$, 0.1% Tween-20, 2mM Levamisole).

After extensive washes sections were exposed to the substrate for alkaline phosphatase, nitroblue tetrazolium and 5-bromo-4-chloro-3-indoyl phosphate (NBT-BCIP; Sigma). Reaction was blocked by washes with PBS, pH 5.5, followed by postfixation in 4% PFA for 20 min. Slides were coverslipped with 70% glycerol in PBS or dehydrated and mounted with Eokitt.

2.9 Cell culture

The 661W photoreceptor cell line was a generous gift of Dr. Al-Ubaidi, University of Oklahoma. 661W cells (al-Ubaidi et al., 1992) were grown at 37°C and 5% CO2 in DMEM supplemented with 10% FBS, penicillin (100 U/ml) and streptomycin (50 mg/ml). The cells were cultured overnight and transfected with 0.4 mg of DNA using PolyFect transfection reagent (Qiagen) according to the manufacturer's instructions. The 661W cells were cultured for 1 day after transfection and then treated with 4 mM Na butyrate, 50 mM taurine, 50 ng/ml bFGF and 27.32 mg/ml heparin.

The Y79 cells (HTB-18, ATCC) were maintained as stock cultures in RPMI-1640 medium (GIBCO) supplemented with penicillin, streptomycin and 20% FBS. For the differentiation experiments, the cells were plated in a synthetic medium, which is serum-free MEM containing a N2 supplement (GIBCO) (MEM-N2). They were cultured in poly-L-ornithine/laminin-coated culture 100 mm dishes (SIGMA) and maintained for 3 days. Sodium butyrate (NaBu) was dissolved in MEM at the final concentration of 1mM.

2.10 Immunofluorescence and FACS

For the *in vitro* immunofluorescence experiments, the cells were fixed with 4% paraformaldehyde for 10 min, permeabilized with 0.3% TritonX-100 in PBS for 5 min and blocked with 5% goat serum and 4% BSA in PBS for 30 min.

The primary antibody mixtures were applied overnight at 4°C. For the immunofluorescence analysis on the eye sections, mouse eyes were fixed overnight in 4% paraformaldehyde in PBS at 4°C, incubated 1 h in 20% sucrose/PBS and incubated overnight in 30% sucrose/PBS at 4°C.

The eyes were orientated and flash frozen in O.C.T (Kaltek) using liquid nitrogen steam. The cryopreserved sections were permeabilized with 0.5% TritonX-100 in PBS, blocked with 10% goat serum in PBS/0.2% TritonX-100 for 30 min. For the BrdU and Ki67 staining, sections were boiled, after fixation, in sodium citrate buffer 10mM pH 6.0 for 3 min. An additional denaturation step with cloridric acid 2N for 30 min and neutralization in PBS was carried out for the BrdU detection.

The primary antibodies used are: a monoclonal anti-BrdU (mouse, clone BU-33, Sigma) 1:300 and anti-phospho-Histone-H3 (Ser10, rabbit, Millipore) 1:200 for both the *in vitro* and *in vivo* studies; anti-Ki67 (mouse, clone B56, BD Pharmingen) 1:100 for the *in vitro* studies and monoclonal anti-Ki67 (rat, clone TEC-3, Dako), for the *in vivo* studies; monoclonal anti-Neuronal class III ß-Tubulin (mouse, clone Tuj-1, Covance); anti-Rhodopsin (mouse, clone RET-P1, Sigma) 1:1000; monoclonal anti-acetylated-αTubulin, (mouse, clone 6-11B-1, Sigma) 1:500, anti-Opsin, Blue (sw) and Green/Red (mw) (rabbit, Millipore) 1:200; anti-Chx10 (goat, clone C-17, Santa Cruz Biotechnology) 1:100. ABC kit (Vector Laboratories) and TSA-plus Fluorescein (Perkin Elmer) were used according to the manufacturer's instructions to amplify the signal in Ki67 staining on eye sections.

Slides were incubated with the Alexa Fluor secondary antibodies (Invitrogen) 1:1000. Cells and sections were counterstained with 4.6-diamidino-2-phenylindol, DAPI (Vector Laboratories). Slides were photographed using both Leica DM5000 and Zeiss Axioplan microscopes.

The flow cytometric analysis on GFP positive cells was performed on a FACS ARIA Flow cytometer (BD Biosciences) and the results were analyzed using the DIVA software. Pooled cells from five biological replicates were sorted and permeabilized with ice-cold 70% ethanol for 1 h and then digested with 0.05 mg/ml of RNase A (Roche) for 30 min at 4°C. The cells were then pelleted and resuspended in 2 ml with 0.005 mg/ml Propidium Iodide (P-4170; Sigma) for 1 h at 4°C before being analyzed (FCS-A vs FCS-W plot).

Unless otherwise reported, each of the *in vitro* experiment was performed using three biological replicates with at least 10 fields of view for each replicate.

2.11 RNA interference

RNA oligos for siRNAs were designed by the company Dharmacon while oligos for shRNAs were designed by the company Oligoengine.

RNA interference experiments were conducted using Lipofectamine2000 (Invitrogen). In brief, plate 2-6 x 10^4 cells per well in 100 µl of the appropriate complete growth medium without antibiotics and with serum if cells are normally cultured in the presence of serum.

Dilute the appropriate amount of siRNA in 50 µl of Opti-MEM I Reduced Serum Medium (Invitrogen) without serum (or other medium without serum). Mix Lipofectamine2000 gently before use, then dilute the appropriate amount in 50 µl of Opti-

MEM® I Medium. Mix gently and incubate for 5 minutes at room temperature. After the 5 minute incubation, combine the diluted siRNA with the diluted Lipofectamine™ 2000.

Mix gently and incubate for 20 minutes at room temperature to allow the siRNA:Lipofectamine2000 complexes to form. Add the 100 µl of siRNA:Lipofectamine2000 complexes to each well. Mix gently by rocking the plate back and forth. Incubate the cells at 37°C in a CO2 incubator for 24-72 hours until they are ready to assay for gene knockdown.

Stable clones of 661W cells overexpressing shRNAs against *Vax2os1* were generated by transiently transfecting pSuper vector (Oligoengine) carrying the cassette for shRNA expression and the cassette for antibiotic selection (500 ug/ml of Geneticin, G418).

The sequences of the oligos used for transient and stable RNA interference experiments are described in Table 3.

The genomic localization of the primers is shown in Figure 34.

Table 3. Sequences of oligos for RNAi experiments.

OLIGO NAME	**SEQUENCE 5'---> 3'**
shRNA1 (for stable RNAi)	CAAGTCCGTGCTAGGTCAA
shRNA2 (for stable RNAi)	CGACTTCTCTGGAATGCTT
siRNA3 (for transient RNAi)	GGTCAAGGTCCCTGGCAAA
siRNA4 (for transient RNAi)	GTGGCAAGGAGCTGTGGAA
siRNA5 (for transient RNAi) not shown	GTTGGTGGCCTAAGAACAA
siRNA6 (for transient RNAi) not shown	GGACTGACGGCAAGAAAGT

2.12 Tunel Assay

Apoptotic nuclei were detected by the TdT-mediated dUTP terminal nick-end labeling kit according to the manufacturer's instructions (TUNEL, Roche). Briefly, sections were fixed with paraformaldehyde 4%, for 20 min, then permeabilized with 0.1% Triton X-100 and 0.1% Sodium Citrate for 2 min on ice. After, sections were incubated with tunel reaction mixture, containing the fluorescein-coniugated nucleotides and the terminal transferase enzyme, for 60 min at 37°C.

2.13 AAV virus and BrdU administration

All the procedures on animals were performed under a protocol approved by the Institute of Genetics and Biophysics Ethics Committee, Naples, Italy, and by the Italian Ministry of Health. Wild-type C57BL/6 mice (Charles River) were used. Recombinant AAV2/8 viruses were produced by the TIGEM AAV Injection Core according to protocols described elsewhere (Hildinger et al., 2001).

As DNA templates the same plasmids used for the *in vitro* experiments were used for AAV production. For each viral preparation, physical titers [genome copies per milliliter (GC/ml)] were determined by PCR quantification using Taqman (Gao et al., 2000). Adult animals were sacrificed by neck dislocation.

Postnatal mice at post-natal day 1 (PN1-2) were anesthetized by hypothermia for 2' at 4°C (Venables et al., 2002) and injected subretinally in the dorsal retinal areas with 1 ul of AAV vectors corresponding to $1x10^9$ genome copies (GC). In particular the right eye was always injected with AAVs overexpressing *Vax2os1* and the left eye with one of the two control AAV vectors. The same individual performed all the surgical procedure to minimize variability in injection technique.

The BrdU was administrated intraperitoneally at the concentration of 0.05mg/gr to PN5 mice and sacrificed 24h after in case of short pulse studies or another administration of BrdU was performed the day after in case of long pulse studies.

For the *in vivo* experiments at least n=4 of animals was used for each experiment.

2.14 Statistics

Data are presented as means ± SE or ± SEM where indicated. Two-tailed Student's t test, likelihood ratio test for Negative Binomial (Maxwell and Delaney, 2004), and Pearson's chi-square test were used to determine statistical significance where indicated. $P \leq 0.05$ was considered significant.

3 RESULTS

3.1 GENOMIC ORGANIZATION OF lncRNAS *VAX2OS*, *OTX2OS* AND *SIX3OS*

In the last few years, Dr. Banfi's laboratory has focused its efforts on the identification of non-coding transcripts expressed at high levels in the developing eye. The first result towards this goal was the identification and initial characterization of a set of *cis*-Natural Antisense Transcripts (*cis*-NATs) and Opposite Strand (OS) transcripts associated with eight transcription factor genes known to play a basic role in eye development in vertebrates (Alfano et al., 2005) (see Introduction, section 2.6). All of these transcripts are spliced and polyadenylated like regular messenger RNAs and undergo a significant number of splicing events. Furthermore, these identified OS transcripts are likely to represent non-coding RNA transcripts as they lack open reading frames (ORFs) of any significant length. By using an integrated approach involving bioinformatics as well as experimental procedures, such as RT-PCR and real-time PCR, it was demonstrated that these transcripts are specifically or predominantly expressed in the retina at significant levels (Alfano et al., 2005). Among them, the long non-coding RNAs *Vax2os*, *Otx2os and Six3os* are the object of my PhD thesis. In particular, for all three transcripts I have performed a transcriptional analysis in the mouse retina. Moreover, I have focused my attention on *Vax2os* for functional studies, as detailed below.

The genomic organization of the *Six3os*, *Otx2os* and *Vax2os* transcripts is described in Figure 34. *Six3os* presents a high number of different splicing events producing a heterogeneous population of OS transcripts that consists of 11 splice isoforms. Moreover, all of these nearly identical isoforms are localized upstream of the putative *Six3* regulatory

region and the minimal distance between these two transcriptional units is below 2.5 kb (Figure 34A). The *Otx2os* transcripts are characterized in a similar way, although the number of different splice isoforms is considerably smaller than that of *Six3os* (3 spliced isoforms) (Figure 34B). Three different transcriptional clusters (comprising five spliced isoforms) characterize the genomic organization of the *Vax2os* and one of these begins to be transcribed in the first intron of the ''sense'' gene *Vax2* (isoform 2) (Figure 34C). The remaining isoforms, namely *Vax2os1, 3 and 4*, are transcribed near the first exon of *Vax2* (below 500 bp) while the distance between *Vax2os5* and *Vax2* is below 10 kb (Figure 34C).

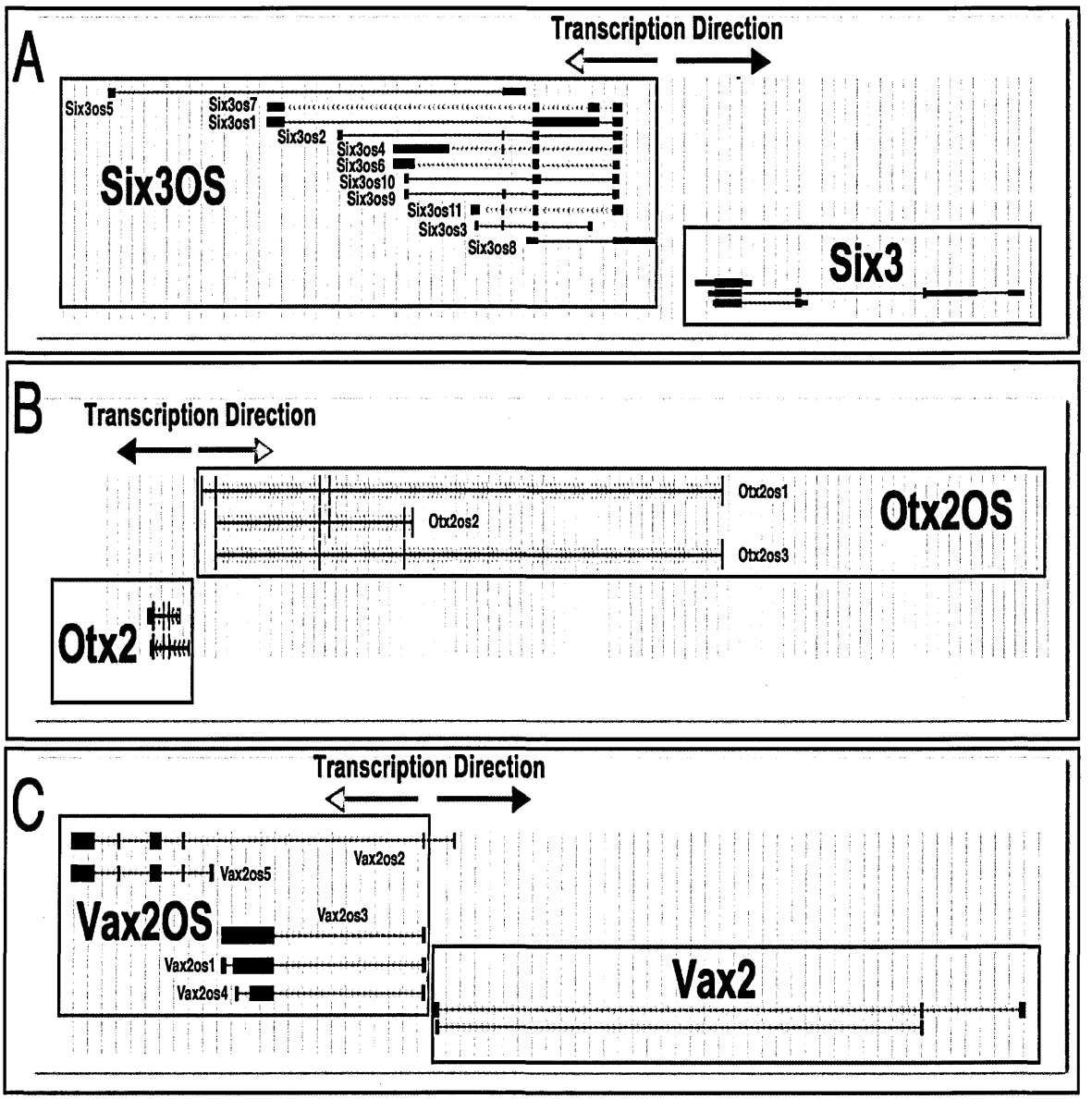

Figure 35. Genomic organization of long non-coding Six3os, Otx2os and Vax2os in mouse.

3.1.1 Expression pattern of lncRNAs Vax2os, Otx2os and Six3os in the mouse retina

My first goal was to assess the expression pattern for all of these OS isoforms in the post-natal stages of mouse retina development. To achieve this aim, I performed qRT-PCR experiments on mice at post-natal days (PN)1, PN4 and PN8 and at adult stages (2–12 months). For these experiments I used isoform-specific primers designed by means of freely available software and I was able to distinguish from each other unambiguously, whenever possible, all tested splice isoforms derived from the same transcriptional unit. The results of this analysis are shown in Figures 35-37.

For *Vax2os*, isoform1 (*Vax2os1*, red bars in Figure 35) is the most highly expressed during mouse retina development in comparison with isoform2 and isoform3 (yellow and green bars, respectively), although at lower levels if compared to the sense gene *Vax2* (light blue bars) expression. In the adult retina, isoform1 seems to be the most expressed isoform. Interestingly, in the adult retina the overall *Vax2os* expression levels seem to be higher than those of the *Vax2* "sense" gene.

Concerning *Otx2os* (Figure 36), isoform3 (green bars) is the most highly expressed isoform during mouse retina development in comparison with isoform1 and isoform2 (red and yellow bars, respectively), but also in this case the expression levels are relatively low when compared to those of the sense gene *Otx2*. Furthermore, in the adult retina, isoform3 shows a decrease of expression levels whereas isoform1 seems to be the most highly expressed isoform at this stage (Figure 36).

Finally, isoform4 (purple bars) of the *Six3os* cluster is always the most highly expressed isoform including at adult stages and its expression levels are very abundant when compared to the expression of *Six3* at the same developmental stages (Figure 37).

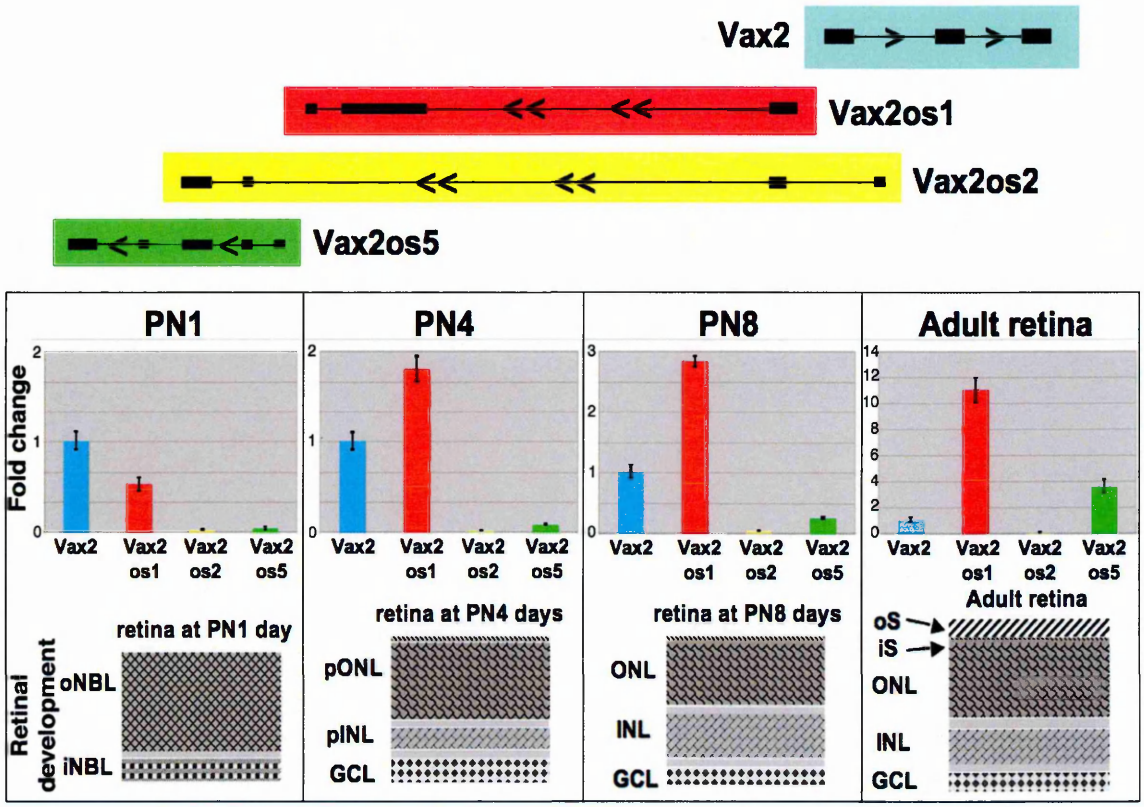

Figure 36. Expression analysis for Vax2os isoforms in post-natal and adult mouse retina by qRT-PCR.

oNBL, outer neuroblastic layer; iNBL, inner neuroblastic layer; ONL, outer nuclear layer; INL, inner nuclear layer; GCL, ganglion cell layer; iS and oS, inner and outer segments of photoreceptors.

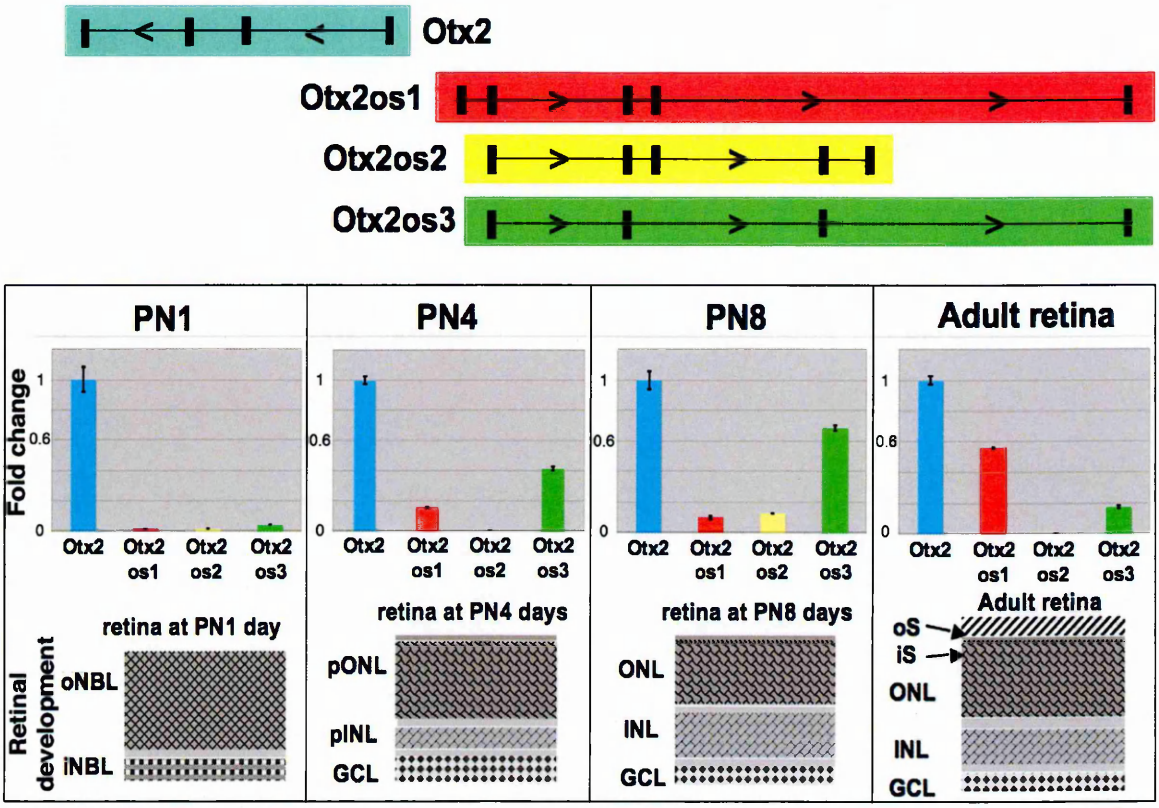

Figure 37. Expression analysis for Otx2os isoforms in post-natal and adult mouse retina by qRT-PCR.

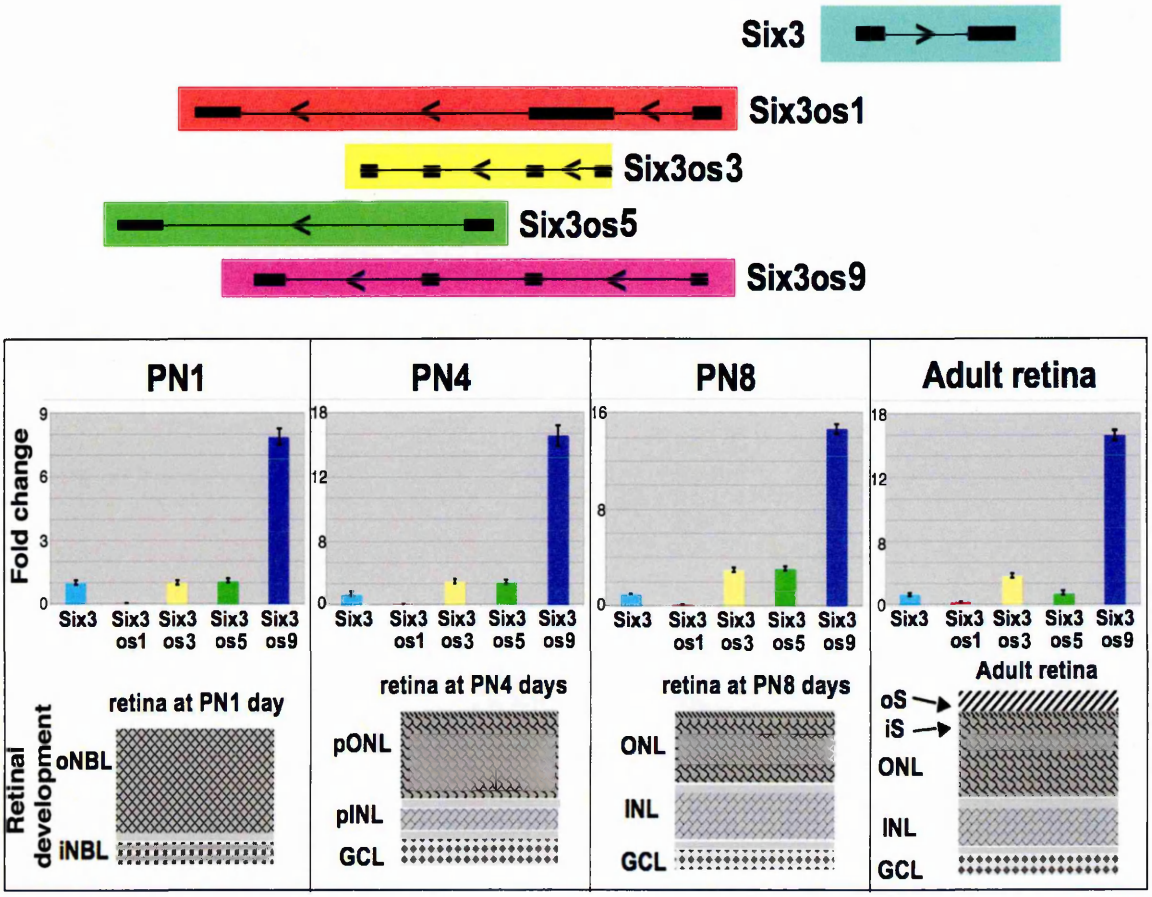

Figure 38. Expression analysis for Six3os isoforms in post-natal and adult mouse retina by qRT-PCR.

These results clarify the expression pattern of these OS isoforms in mouse retina development and also provide us with valuable information about the recognition of the OS isoforms that are expressed with the most significant levels during retinal development. This will be very important for future gain- and loss of function experiments because I will be able to target the most biologically relevant parts of the OS transcripts when performing over-expression and/or inactivation assays.

In conclusion, it is interesting to note that these OS isoforms seem to change their expression activity during retinal development although additional experiments also on embryonic stages are required in order to gain a more detailed picture of the expression pattern of OS transcript isoforms in the developing mouse retina.

After the expression analysis of the OS isoforms by quantitative PCR, I was able to design specific RNA probes to use in RNA *in situ* hybridization experiments. Probes for digoxigenin labelling were designed in order to detect the most highly expressed isoforms described by quantitative PCR, namely *Vax2os1*, *Vax2os5*, *Otx2os3* and *Six3os9*, although the latter two are not specific because they share with the other corresponding isoforms the majority of their sequences. For this reason I will refer to the latter as *Otx2os* and *Six3os* for the *in situ* hybridization analysis.

Vax2os1 expression in the adult retina is restricted to the outer nuclear layer, ONL, where the photoreceptor cell nuclei (rod and cone cells) are distributed (Figure 38). Furthermore, the localization of the *Vax2os1* signal is only visible in the ventral area of the adult mouse retina suggesting the presence of a high ventral-low dorsal gradient of expression. This interesting expression pattern is reminiscent of the expression pattern of the sense gene *Vax2*, previously studied in our lab, although *Vax2* is mostly expressed in the ganglion cell layer (GCL) and inner nuclear layer (INL) in the adult mouse retina

(Alfano et al., 2005). Concerning the *Vax2os3* isoform I did not detect any signal at any time point although this data has to be further confirmed to exclude technical problems. *Otx2os* begins to be expressed at increasing levels from the late post-natal stages of retina maturation until the adult stage. The signal is barely visible in the inner nuclear layer at post-natal day 8, while in the adult retina it is more intense and clearly distributed (Figure 39). In fact, the particular distribution of the signal in the outermost part of the INL may allow us hypothesize a localization in the bipolar cells although until now this observation has not been supported by any immunohystological assay.

Finally, *Six3os* is expressed at high levels in post-natal day 1 retinas, in particular in the outer neuroblastic layer oNBL (Figure 40), where proliferative and differentiative processes are still occurring and will lead to the final maturation of the different retinal cell types, especially the rod and bipolar cells. This result is comparable with the expression profile of the sense gene *Six3*, which is expressed at high levels throughout the retinal layers at the PN1 stage, including also in the inner neuroblastic layer, iNBL. In addition, the expression localization of both transcripts in the adult retina is maintained in the same retinal layers, INL and GCL, although *Six3os* shows a weaker signal in comparison to the expression of *Six3* (Figure 40).

Therefore these pilot *in situ* hybridization experiments elucidate the temporal-spatial expression pattern for three OS transcripts in the late developing and adult mouse retina. Together with the results obtained by studying the isoform-specific expression, I will now be able to plan dedicated experimental strategies including the choice of the spliced OS isoform to analyse, the retinal cell line to target *in vivo* and the cellular background to reproduce as the *in vitro* counterpart.

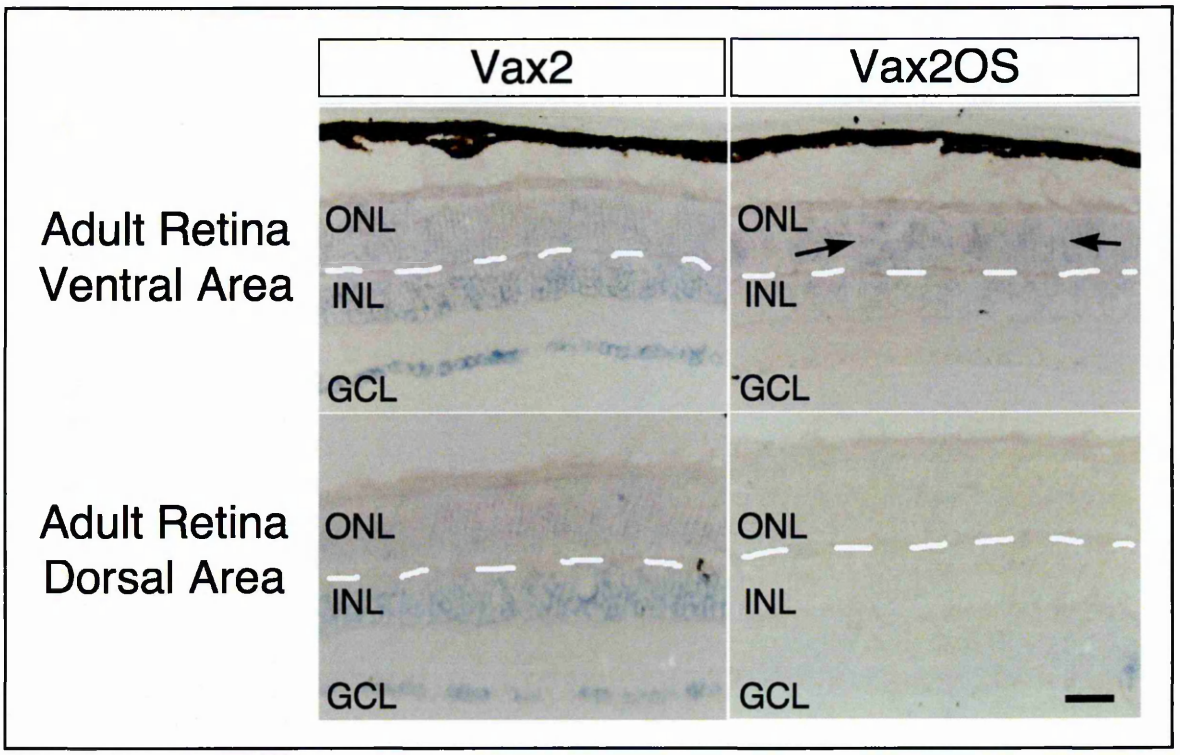

Figure 39. RNA in situ hybridization for Vax2os and Vax2 in the adult mouse retina.

White dotted lines delimit the ONL from the INL. Arrowheads show the expression of Vax2os1 in the ONL of a mouse adult retina. Bar indicates 20 μm.

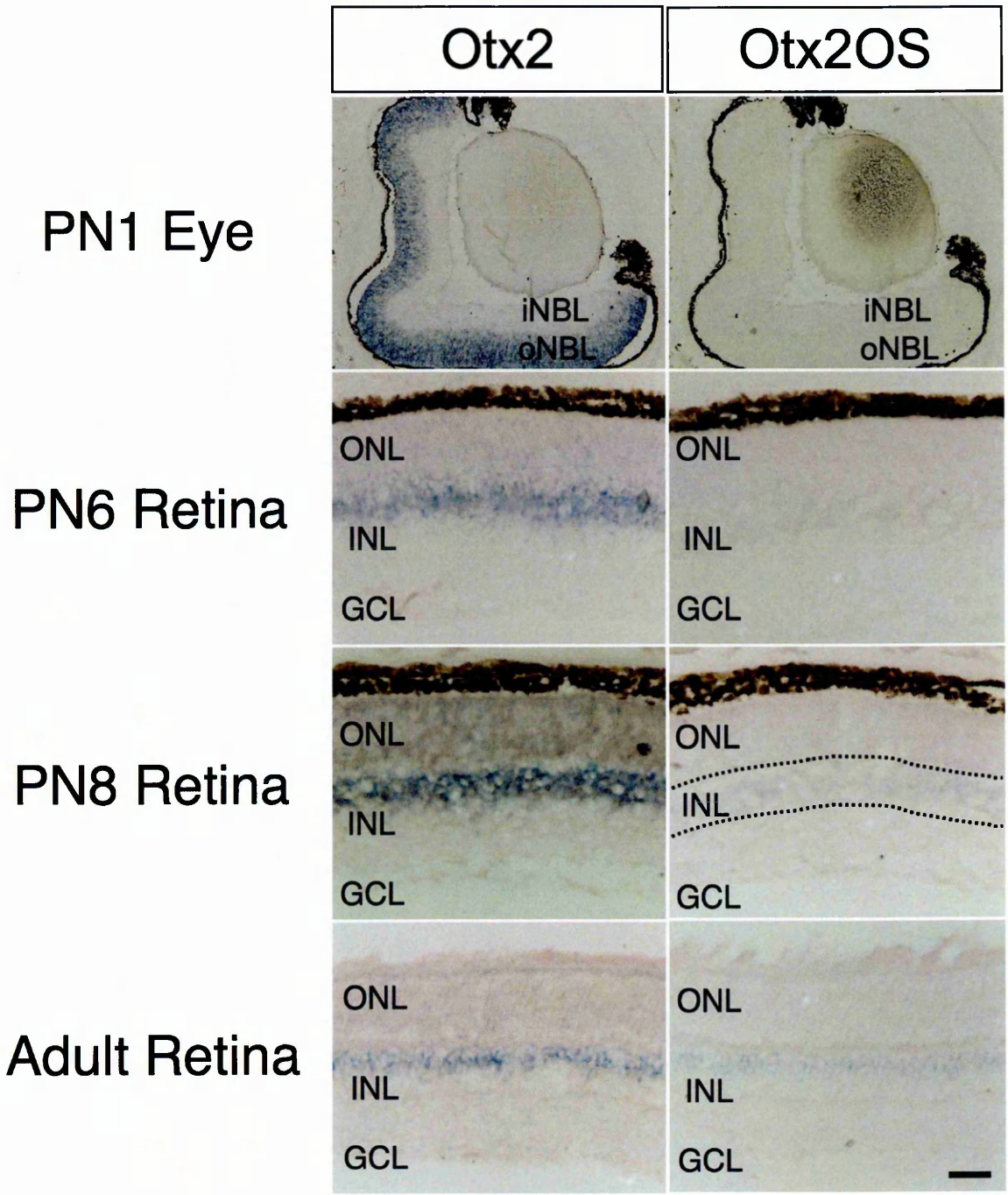

Figure 40. RNA in situ hybridization for Otx2os and Otx2 in the postnatal and adult mouse retinas.

Bar indicates 100μm in the PN1 samples and 20μm in the other samples.

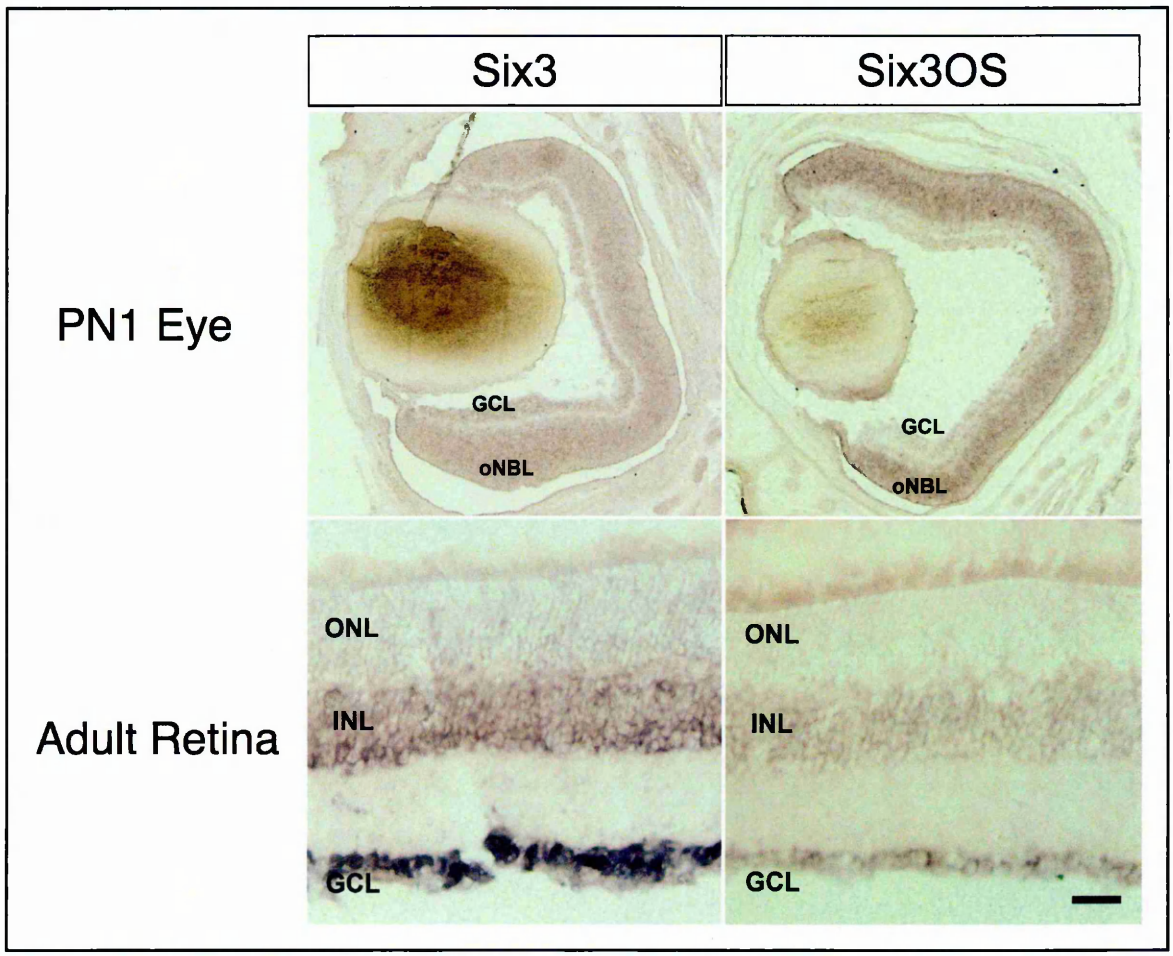

Figure 41. RNA in situ hybridization for Six3os and Six3 in the postnatal and adult mouse retinas.

Bar indicates 100μm in the PN1 samples and 20μm in the adult samples.

3.2 FUNCTIONAL CHARACTERIZATION OF lncRNA *VAX2OS IN VITRO*

The interesting expression pattern of lncRNA *Vax2os,* high ventral - low dorsal in the adult retina (previously described in section 3.1.1 and illustrated in Figure 38), prompted me to select it for a more detailed expression analysis in order to obtain a precise spatio-temporal profile of this transcriptional unit also during retinal development. To achieve this aim, I first performed an analysis of the temporal expression profile of all the *Vax2os* isoforms in embryonic retinal stages by quantitative Reverse Transcriptase-PCR (qRT-PCR) analysis (Figure 41A-B). We found that the *Vax2os1* isoform displayed the highest expression levels also in the embryonic retinal stages. Among the other isoforms, *Vax2os3*, *Vax2os4* and *Vax2os5* displayed lower but yet noticeable expression levels, whereas *Vax2os2* was barely detected at the stages analyzed (Figure 41B). The expression levels of *Vax2os* isoforms in postnatal and adult stages (previously described) were also put together in order to obtain a more complete representation of data (Figure 41B).

Furthermore I performed a more comprehensive RNA ISH analysis of the expression profile of the most relevant *Vax2os* isoforms during all the main stages of retina development. We selected the *Vax2os1* and *Vax2os5* transcripts that showed the highest expression levels by qRT-PCR and were the most representative of all the different isoforms. I detected a reliable signal for the *Vax2os1* isoform while the *Vax2os5* could not be detected at any stage analyzed suggesting that its expression levels may be below the threshold of detection by RNA ISH procedures. I observed that *Vax2os1* expression was limited to the ventral part of the retina at all the embryonic stages analyzed (i.e., E12.5, E14.5 and E16.5) (Figure 42A-C). Of note, this expression domain was prevalent in the outer neuroblastic layer (oNBL) of the retina at E12.5 and E14.5 (Figure 42A-B).

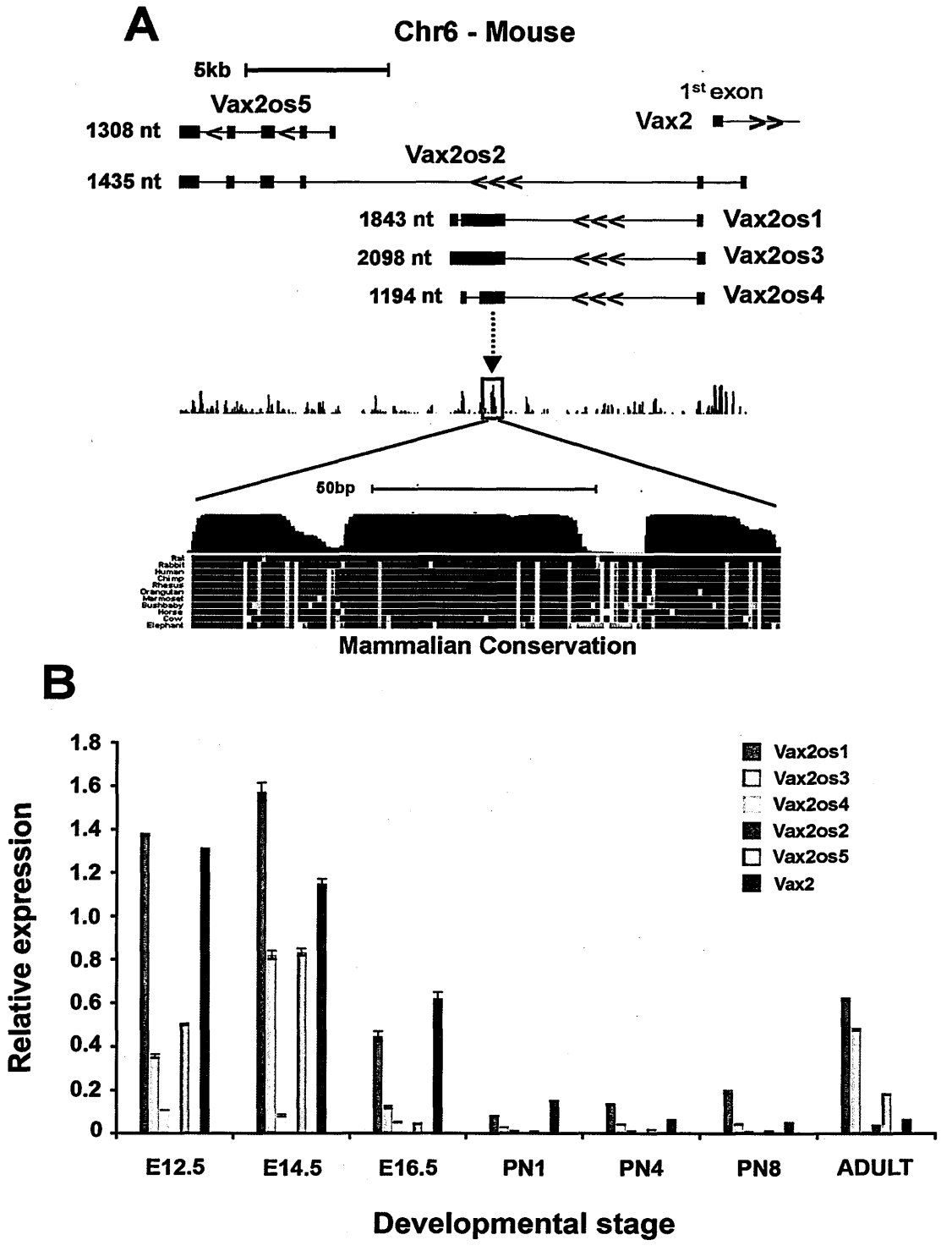

Figure 42. Expression analysis of Vax2os during the mouse retinal development.

(A) Schematic representation of the genomic organization of the Vax2os isoforms. (B) Expression analysis of Vax2os isoforms and Vax2 by qRT-PCR during mouse eye development.

At these stages, the oNBL contains most of the retinal cells that are still proliferating, including the rod photoreceptor progenitor cells. I did not observe any *Vax2os1* expression at the early post-natal stages of retina development, namely PN1, PN4 and PN8 (Figure 42D-F). The localization of *Vax2os1* in the adult retina is shown as control (Figure 42 G-H).

Overall, the above results indicated that *Vax2os1* is the isoform that displays the most significant expression levels during retinal development. Considering also the presence of a conserved sequence domain within its sequence (Figure 41A), I hypothesized that the *Vax2os1* isoform is more likely than the other isoforms to exert a functional role. Therefore, towards the goal of performing a functional characterization of the *Vax2os* lncRNA, I focused my efforts on the *Vax2os1* isoform, as detailed below.

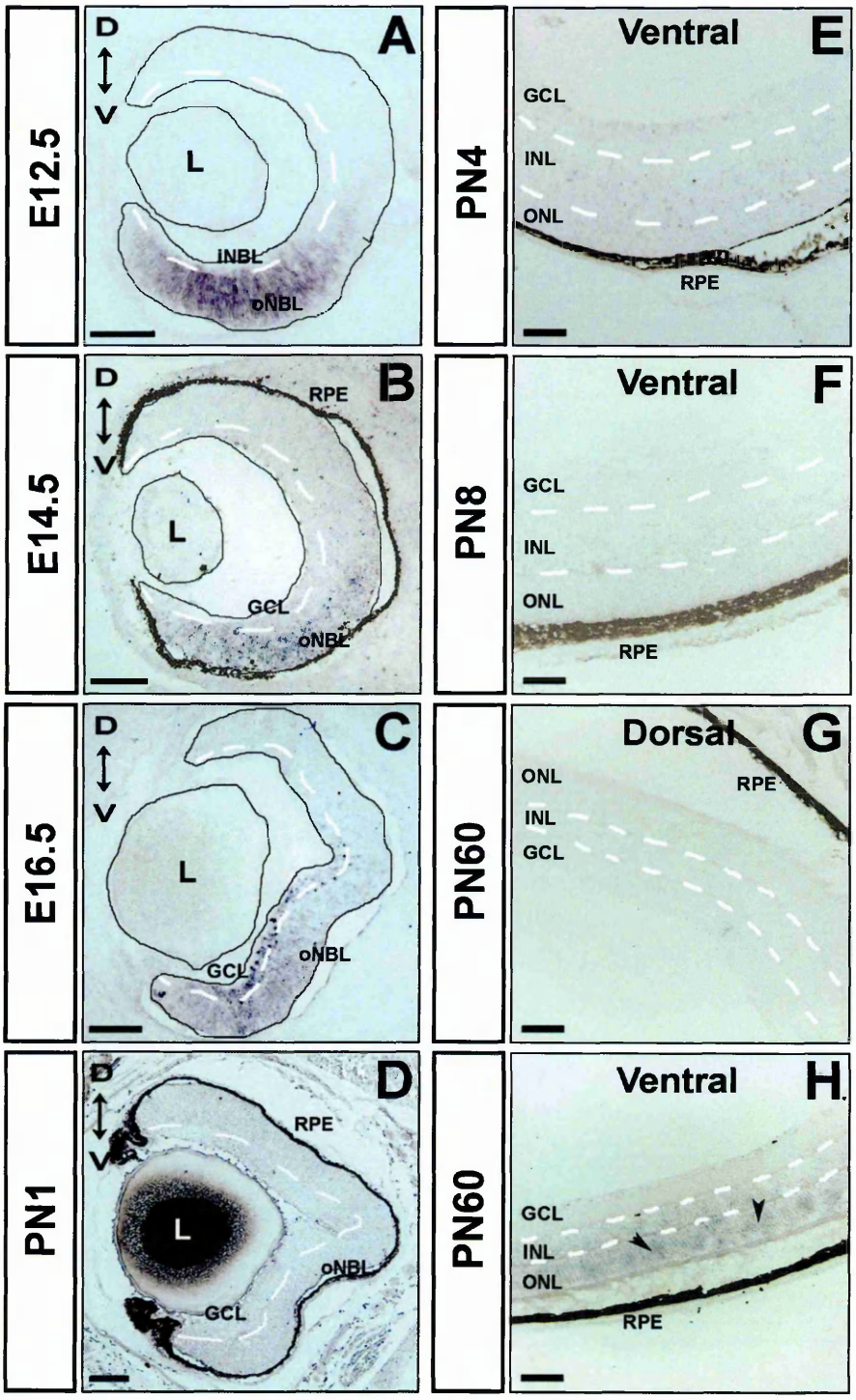

Figure 43. Vax2os1 expression pattern in the embryonic and postnatal mouse retina by RNA in situ hybridization (ISH).

(A-C) Vax2os1 is expressed in the ventral areas of the mouse embryonic retina from stages E12.5 to E16.5. (D-F) In the postnatal stages, Vax2os1 is not detected by RNA ISH while in the adult retina Vax2os1 is expressed only in the outer nuclear layer of the ventral retina (arrowheads) (G,H). Magnifying bars are 100 μm in A-D; 40 μm in E-H.

3.2.1 *In vitro expression studies and identification of a putative VAX2OS human homolog*

Taking into account the expression of *Vax2os1* in the proliferating retinal cells and in the mature photoreceptor cells, we decided to carry out functional analysis of this transcript in an *in vitro* system recapitulating photoreceptor cell types. Towards this goal, we selected the mouse photoreceptor-like 661W cell line (al-Ubaidi et al., 1992). The 661W cells derive from retinal tissues of mice expressing SV40 T antigen under the control of the human IRBP promoter (al-Ubaidi et al., 1992). The expression of T antigen driven by the hIRBP promoter led to the formation of tumors in the brain and retina of mice (al-Ubaidi et al., 1992).

I treated 661W cells for 48 hours with a medium supplemented with sodium butyrate, taurine, heparin and basic Fibroblast Growth Factor (or FGF2) in order to induce cell cycle exit and to promote a further differentiation of cells towards photoreceptors, as previously described (Comitato et al., 2007). I confirmed the validity of this protocol by both assessing the increase in the expression levels of photoreceptor marker genes and by morphological analysis of the cells after treatment (Figure 43A-E). Under these conditions of differentiation, *Vax2os1* was significantly upregulated (Figure 44).

Interestingly, I obtained similar results in the human retinoblastoma Y79 cell line (Reid et al., 1974) when I tested a putative human *VAX2OS* homologous sequence, corresponding to the above described evolutionarily conserved sequence element. In particular, I observed a striking upregulation of the human *VAX2OS* in the Y79 cells treated with sodium butyrate to enhance their differentiation towards a photoreceptor-like fate (Peng and Chen, 2007) (Figure 45A-C).

The above results are not only in agreement with the significant expression of *Vax2os1* in the mature photoreceptor cell layer but strongly suggest the conservation of a functional *VAX2OS* transcript also in the human genome.

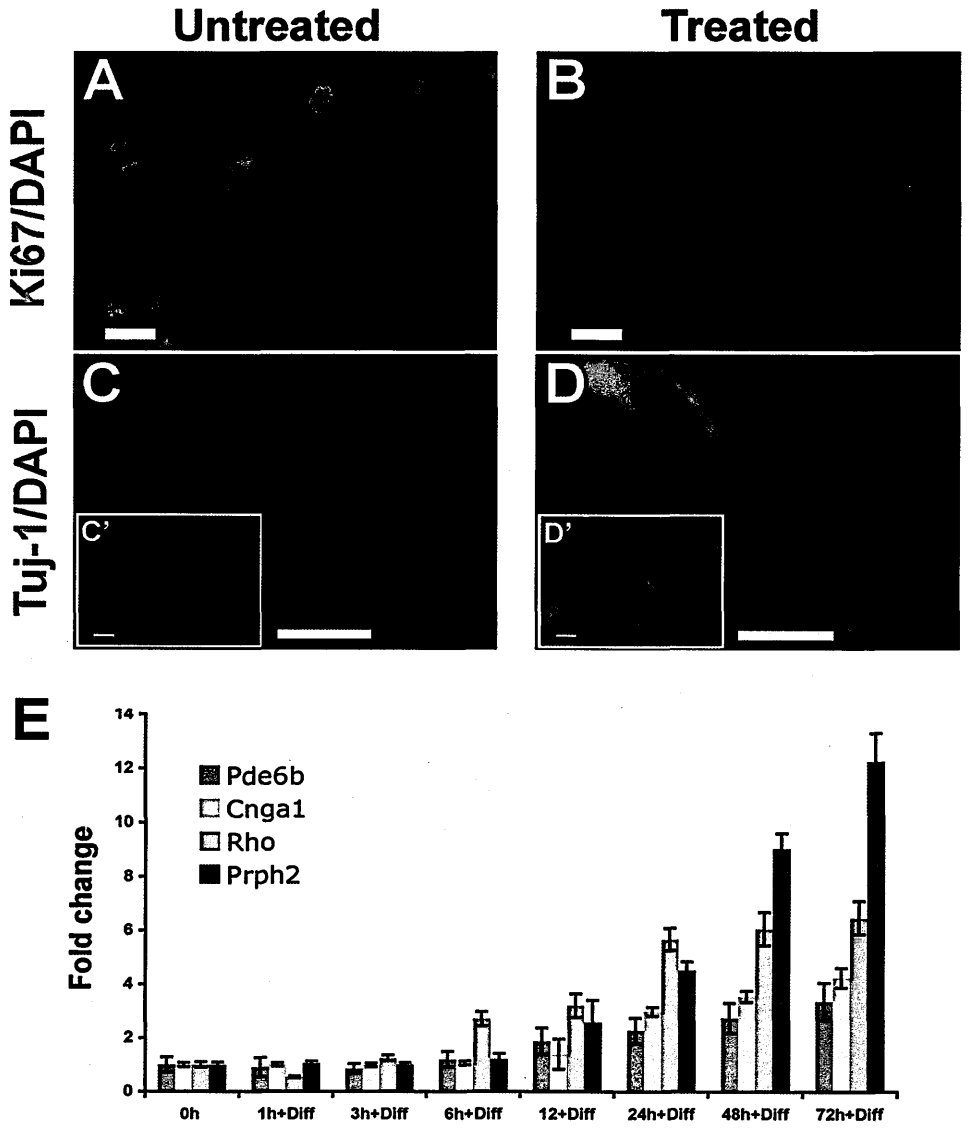

Figure 44. Set-up of a protocol for 661W cell differentiation.

(A-B) Ki67 immunostaining reveals a decrease in the Ki67-positive 661W cells after 48 hours of treatment (see text for details). (C-D) Fluorescence immunostaining experiments reveal the upregulation of Tuj-1 (Neuron-specific class III beta-tubulin) after the differentiation treatment. (E) Expression analysis of four photoreceptor-specific genes by qRT-PCR in the 661W cells at several time intervals during the differentiation protocol. Cnga1, Cyclic nucleotide-gated channel alpha 1; Pde6b, Phosphodiesterase6-beta; Prph2, Peripherin2. Magnifying bars are 20 μm in A-D; 100 μm in C'-D'.

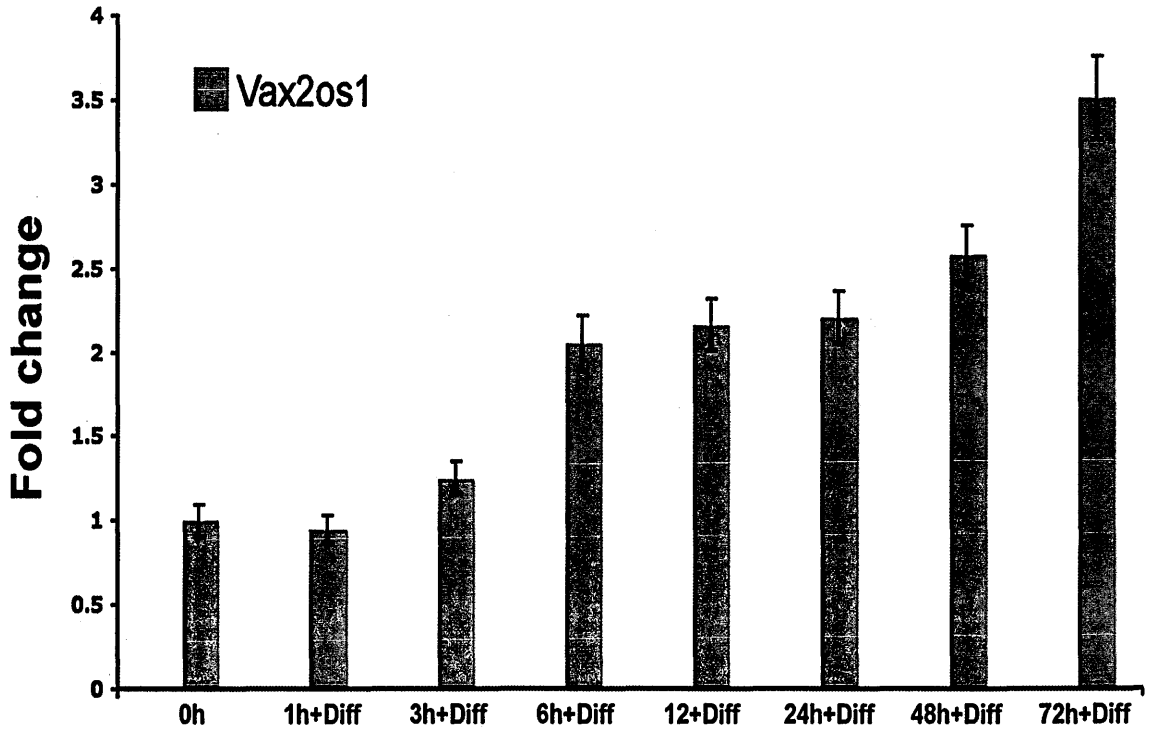

Figure 45. Expression levels of Vax2os1 are increased in the differentiated 661W cells.

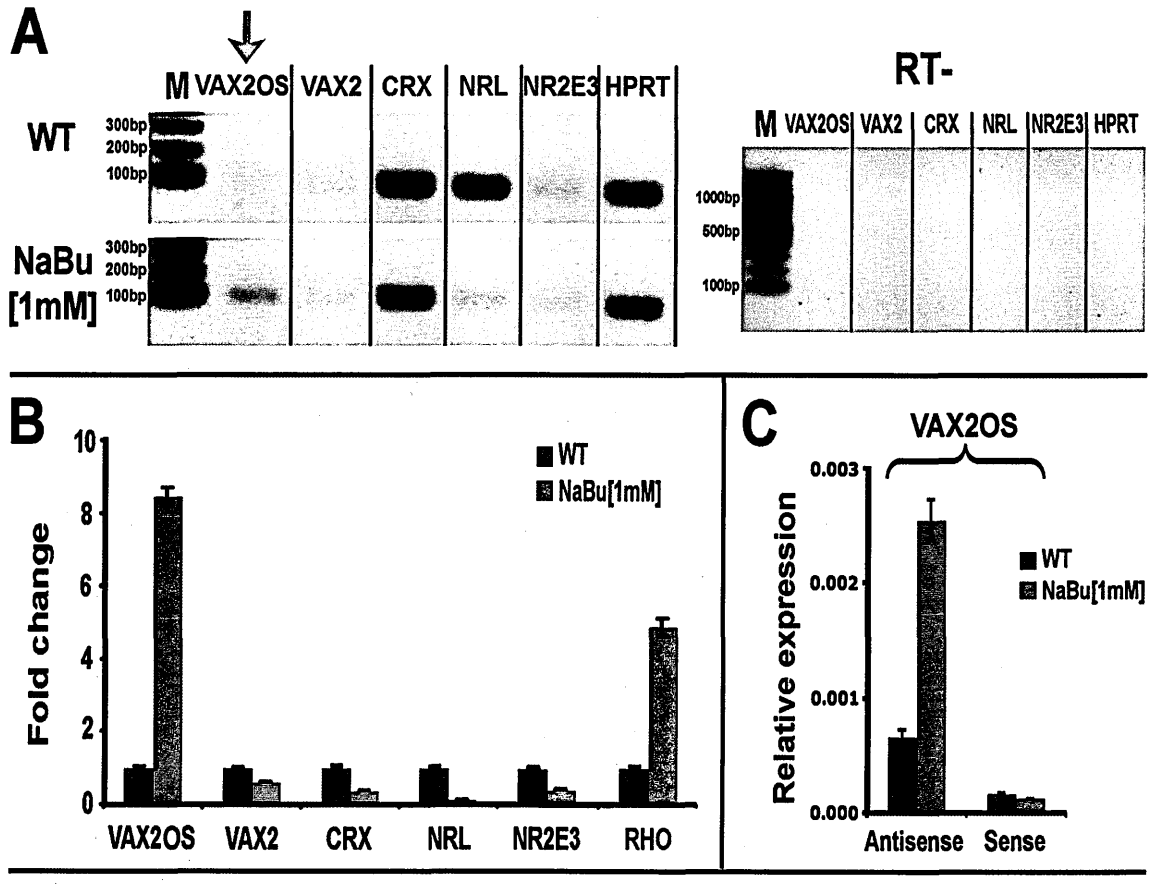

Figure 46. Identification and expression analysis of a putative human VAX2OS transcript.

(A) Semiquantitative RT-PCR for the human VAX2OS (red arrow) and other photoreceptor marker genes in the wild type (top panel) and treated (bottom panel) Y79 cells. Right panel indicate RT minus negative controls. (B) qRT-PCR for human VAX2OS, VAX2 and four photoreceptor genes in the wild type (blue bars) and treated (red bars) Y79 cells. (C) Strand-specific qRT-PCR. Antisense transcription in the human VAX2OS locus is upregulated in Y79 after the differentiation protocol. NaBu, sodium butyrate.

3.2.2 *Vax2os1* overexpression impairs the cell cycle progression of differentiating 661W cells

I decided to carry out inactivation studies of the *Vax2os1* transcript in 661W cells. Towards this goal we designed a strategy based on the use of shRNAs (short harpin RNAs) and siRNAs (small interfering RNAs).

Unfortunately, all attempts to down regulate *Vax2os1* by RNA interference technology performed either in transient conditions using four different siRNA oligos or in stable conditions, by analysing fifteen cell clones, failed to yield acceptable levels of *Vax2os1* repression (Figure 46A-B).

Therefore, I carried out overexpression studies of the *Vax2os1* transcript in 661W cells. To overexpress *Vax2os1* in 661W cells, I transiently transfected 661W cells with *Vax2os1* and applied the differentiation protocol for 48 hours (24 hours after transfection) (Figure 47A). To achieve this aim, I generated a plasmid vector carrying a bidirectional transcriptional cassette that expresses both *Vax2os1* and the Green Fluorescent Protein (GFP) reporter gene under the control of the CMV (cytomegalovirus) and CBA (CMV early enhancer/chicken β actin) promoters, respectively (Figure 47B). As controls, I used a) a similar construct carrying a mutated form of the *Vax2os1* transcript, namely with an internal deletion of about 800 bases, including the above described conserved sequence domain (delOS1) and b) a construct that expressed only the GFP reporter under the control of the CBA promoter (Figure 47B).

I did not detect any apparent change in cell morphology in the 661W cells that overexpressed *Vax2os1* (OS1-OE) compared to the cells transfected with either the GFP reporter only (GFP-OE) or the delOS1 construct (delOS1-OE). However, I observed a

significant perturbation in the cell cycle rate of the OS1-OE cells after 48 hours of differentiation, compared to either the GFP-OE- or delOS1-OE-transfected cells. This was assessed by evaluating the ratio between cells positive to either the cell proliferation marker Ki67 or the mitotic marker phospho-Histone-H3 (pHH3) vs. the total pool of GFP-positive cells (Figure 48A-D). Given the fact that *Vax2os1* is expressed during retinal development and in particular, in the proliferating precursor cells, I went into detail to assess a role for *Vax2os1* in the cell cycle regulation in 661W cells.

In order to obtain more precise information on the cell cycle progression of the OS1-OE cells and to analyze in detail each phase of the cell cycle, I carried out Propidium Iodide (PI) staining experiments. In particular, GFP-labelled OS1-OE cells, control GFP-OE and delOS1-OE cell pools were sorted by Fluorescence Activated Cell Sorting (FACS) methodology following PI staining. This analysis revealed an increased number of OS1-OE 661W cells in the S and G2/M phases after 48 hours of differentiation compared with the GFP-OE and delOS1-OE control cells (Figure 48E-F), which suggests that *Vax2os1* overexpression determines an alteration of the cell cycle rate in 661W cells.

I studied the localization and the expression levels of differentiation markers in the OS1-OE cells and control cells to detect possible alterations in cells following *Vax2os1* overexpression. To achieve this aim, I carried out immunofluorescence stainings with an antibody against Tuj-1, which is a marker for differentiated neuronal cells. The staining revealed fewer OS1-OE cells positive to Tuj-1 compared with the control cells (GFP-OE) (Figure 49A). Furthermore, the expression of rhodopsin, a rod photoreceptor-specific marker, was significantly down regulated in the OS1-OE cells compared to the control cells (Figure 49B). I did not observe any perturbation after *Vax2os1* overexpression in the 661W cells that did not undergo the differentiation protocol (Figure 49C). Interestingly, the

expression of the neighbouring gene, *Vax2*, did not change in OS1-OE compared to GFP-OE cells (Figure 50).

Overall, these *in vitro* data suggest that high levels of *Vax2os1*, during cell differentiation, lead to a perturbation of cell cycle progression in 661W cells.

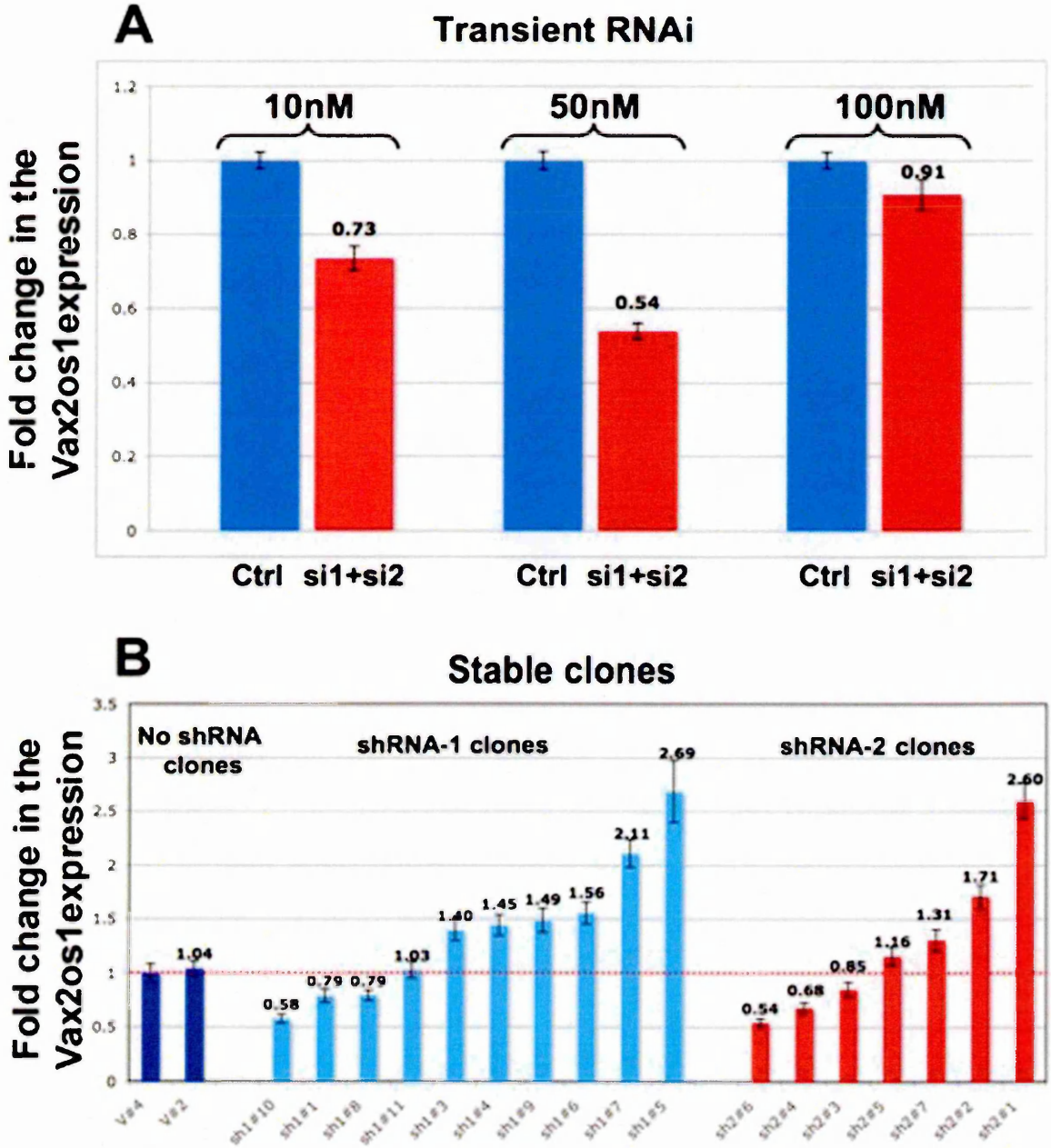

Figure 47. Loss of function studies for Vax2os1 in 661W cells.

(A) Espression levels of Vax2os1 after transient RNA interference experiments using two oligos at three different oligo concentrations. (B) Espression levels of Vax2os1 in 17 cell clones overexpressing two different short-harpin RNAs against Vax2os1. We could not achieve significant levels of Vax2os1 downregulation in the analyzed system. In the x-axis of B, V# represents stable cell clones without the shRNA.

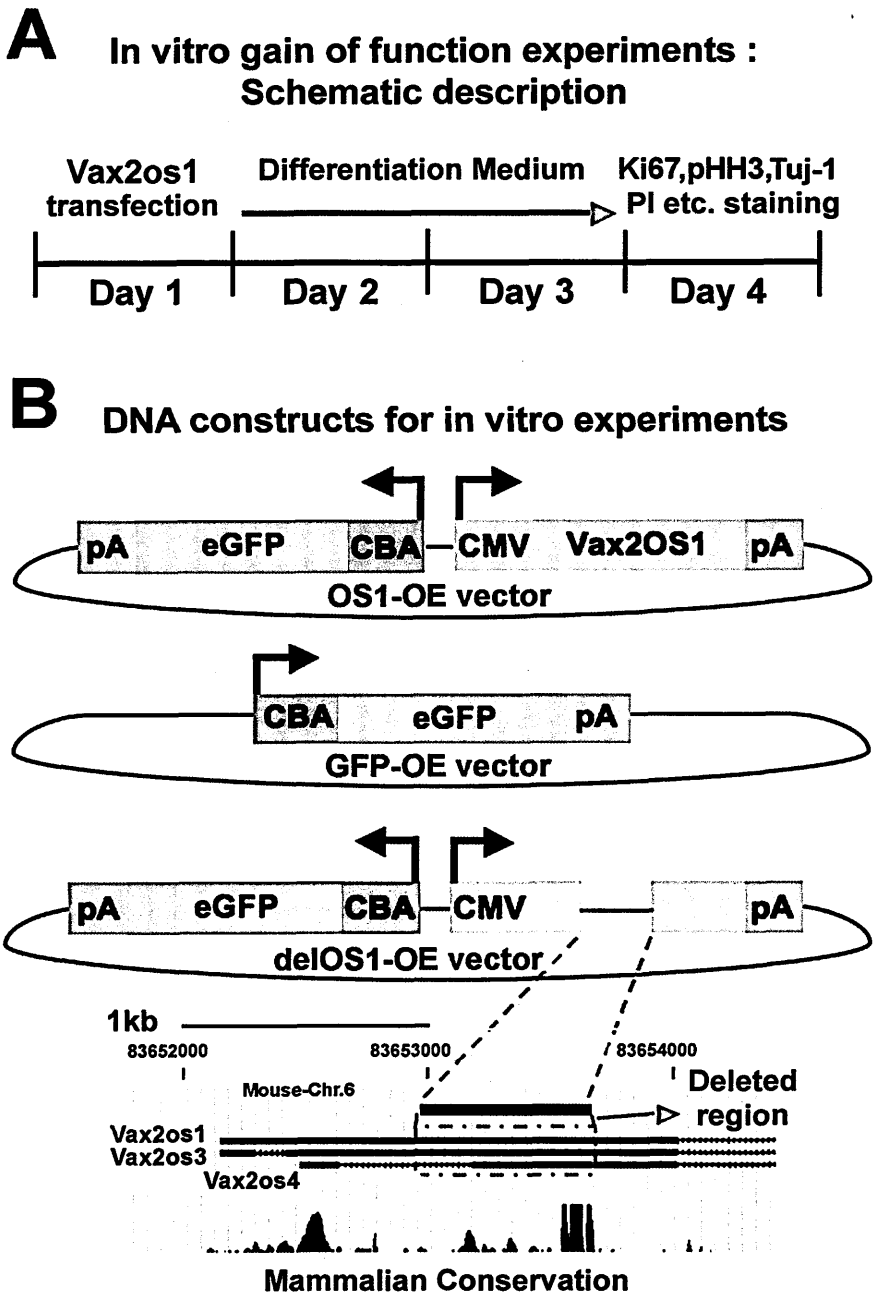

Figure 48. Strategy used for in vitro studies.

(A) Experimental plan for the in vitro overexpression approaches described in the text. (B) Graphical representation of the plasmid constructs used for the in vitro studies. The OS1-OE construct expresses both the Vax2os1 and the GFP genes under the control of two different promoters. The expression cassettes are oriented in the opposite direction as indicated by the arrows. The delOS1-OE construct contains a truncated form of Vax2os1, obtained by ApaI digestion. The deleted region is approximately 800 base pair long and comprises the conserved genomic region (red dotted square).

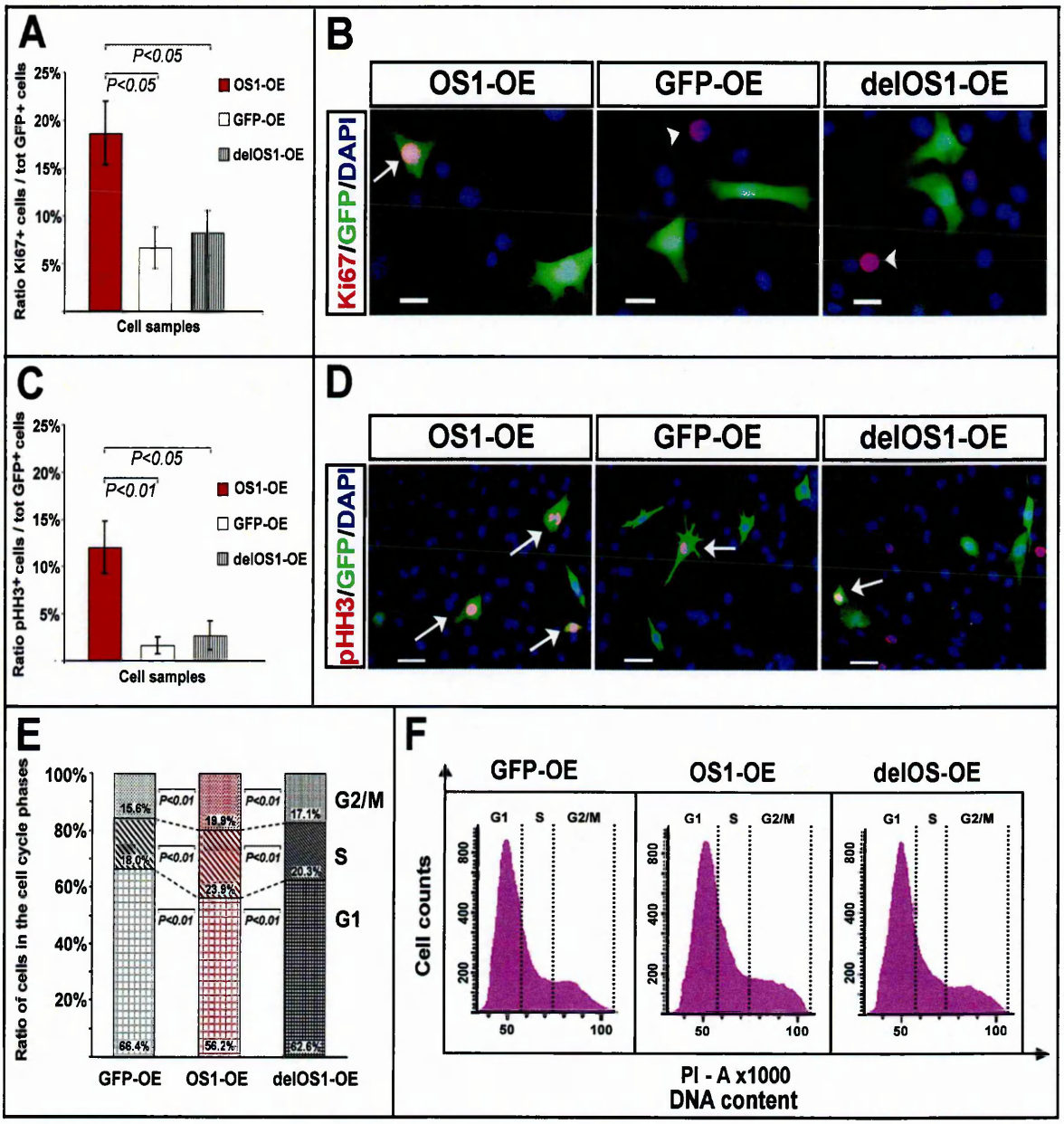

Figure 49. Vax2os1 overexpression impairs the cell cycle of 661W cells.

(A,B) Ki67 fluorescence immunostaining. (C,D) phospho-Histone-H3, pHH3, fluorescence immunostaining. (E,F) Cell cycle analysis with Propidium Iodide (PI). (E) Histograms show the distribution (in percentage) of the single cycle phases for the OS1-OE cells in comparison with the GFP-OE and delOS1-OE control cell pools. (F) Flow cytometric DNA content analysis of the OS1-OE cells and GFP-OE and delOS1-OE control cells stained with PI. Magnifying bars are 20 μm in B; 40 μm in D.

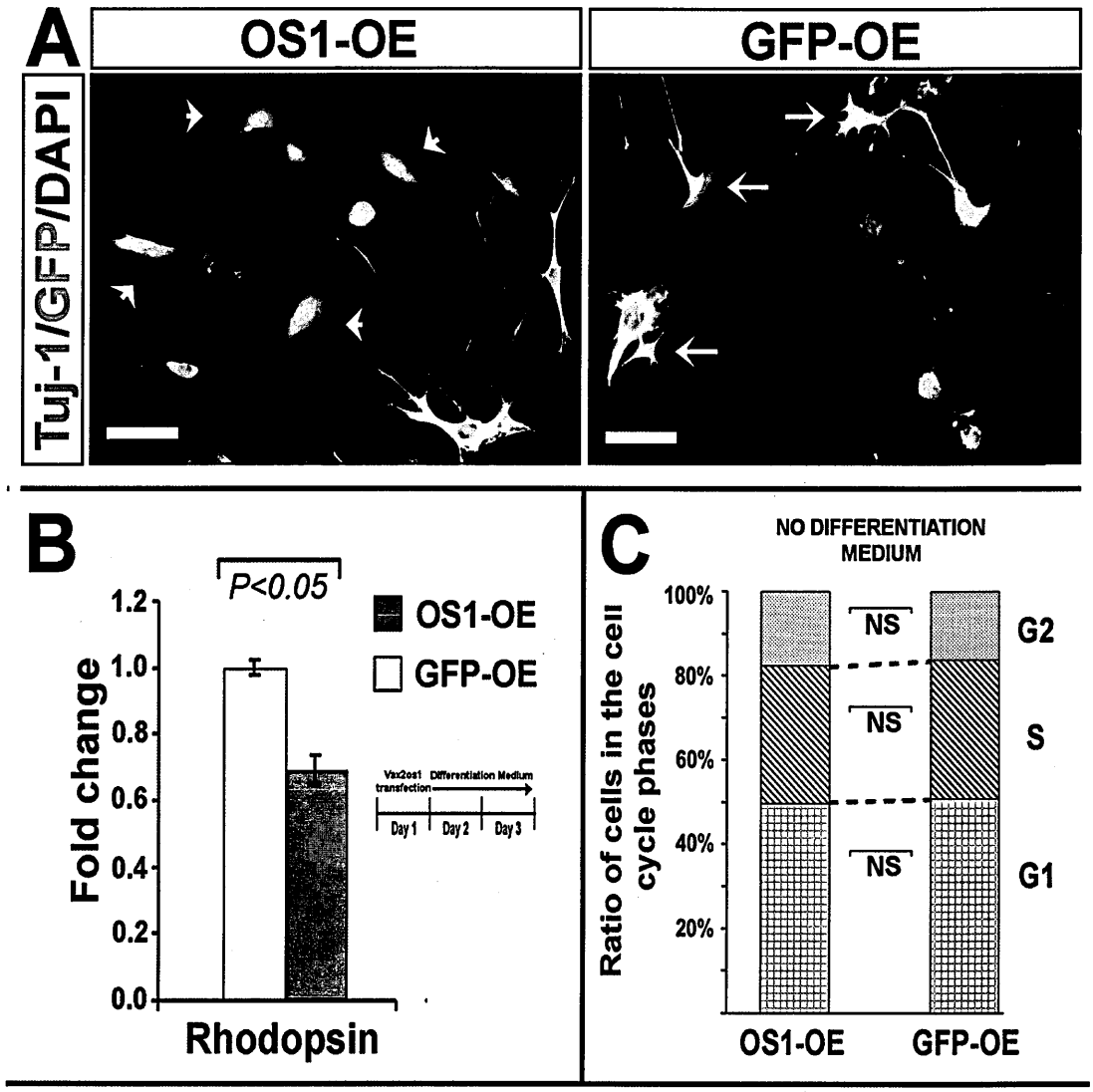

Figure 50. Vax2os1 overexpression impairs the cell cycle and proper differentiation of 661W cells.

(A) Tuj-1 fluorescence immunostaining (in red) reveals a downregulation of this protein in the 661W cells transfected with the Vax2os1 construct (in green) in comparison with control cells, transfected with the control GFP construct. Arrows indicate the localization of Tuj-1 in the control cells expressing GFP, GFP-OE, (yellow, in merge panel) while arrowheads show the expression of Tuj-1 in the OS1-OE. (B) The expression levels of the Rhodopsin gene are downregulated in the OS1-OE cells after 48 hours of differentiation compared with the control GFP-OE cells, as assessed by qRT-PCR. (C) No differences in the analysis of the cell cycle phases are observed between the OS1-OE and GFP-OE cells when no differentiation medium was added. Magnifying bars are 20 μm in A.

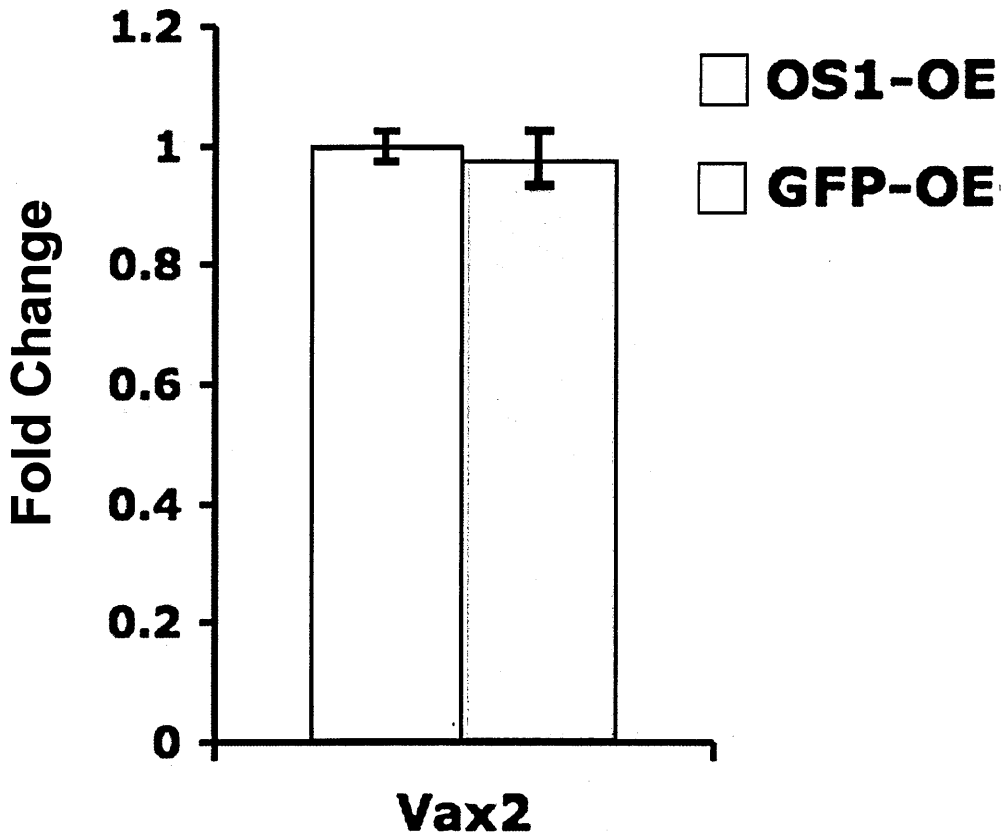

Figure 51. Vax2os1 overexpression in 661W cells does not change the expression of the neighbouring gene Vax2.

Data are presented as means ± SEM (N=5).

3.3 *IN VIVO* STUDIES

3.3.1 Misexpression of Vax2os1 affects retinal progenitor cell proliferation

To determine the role of *Vax2os1 in vivo,* we used Adeno-Associated Virus (AAV)-mediated gene delivery (Allocca et al., 2007) for *Vax2os1* overexpression studies. We took advantage of the same DNA plasmids that were generated for the *in vitro* studies (see section 3.2.2), for the production of AAV constructs that express *Vax2os1* and GFP (AAV-OS1), the deleted form of *Vax2os1* and GFP (AAV-delOS1) and GFP only (AAV-GFP). These constructs were injected in the dorsal retinal areas of post-natal day 1 (PN1) mice to perform a misexpression of *Vax2os1* at both spatial and temporal levels. Indeed, *Vax2os1* is not only prevalently expressed in the ventral retina but, at PN1, this transcript is expressed at very low levels across the entire retina (see sections 1.2 and 2). For each injection experiment, we used the following strategy: the AAV-OS1 construct was injected subretinally in the right eye of a cohort of C57Bl/6 mice whereas the contralateral eye was independently injected with either of the two control constructs. At least four mice, from a minimum of two independent injections, were analysed in each experiment.

I was able to detect GFP expression in the RPE of injected retinal areas, in agreement with the results previously reported for AAV-mediated subretinal delivery at early postnatal stages (Colella and Auricchio, 2010; Surace et al., 2003). In order to evaluate the efficiency of AAV transduction, I performed qRT-PCR at PN5, i.e., four days after injection, and I detected a significant increase of *Vax2os1* expression in the AAV-OS1-injected retinal areas compared with the AAV-GFP-injected eyes (Figure 51).

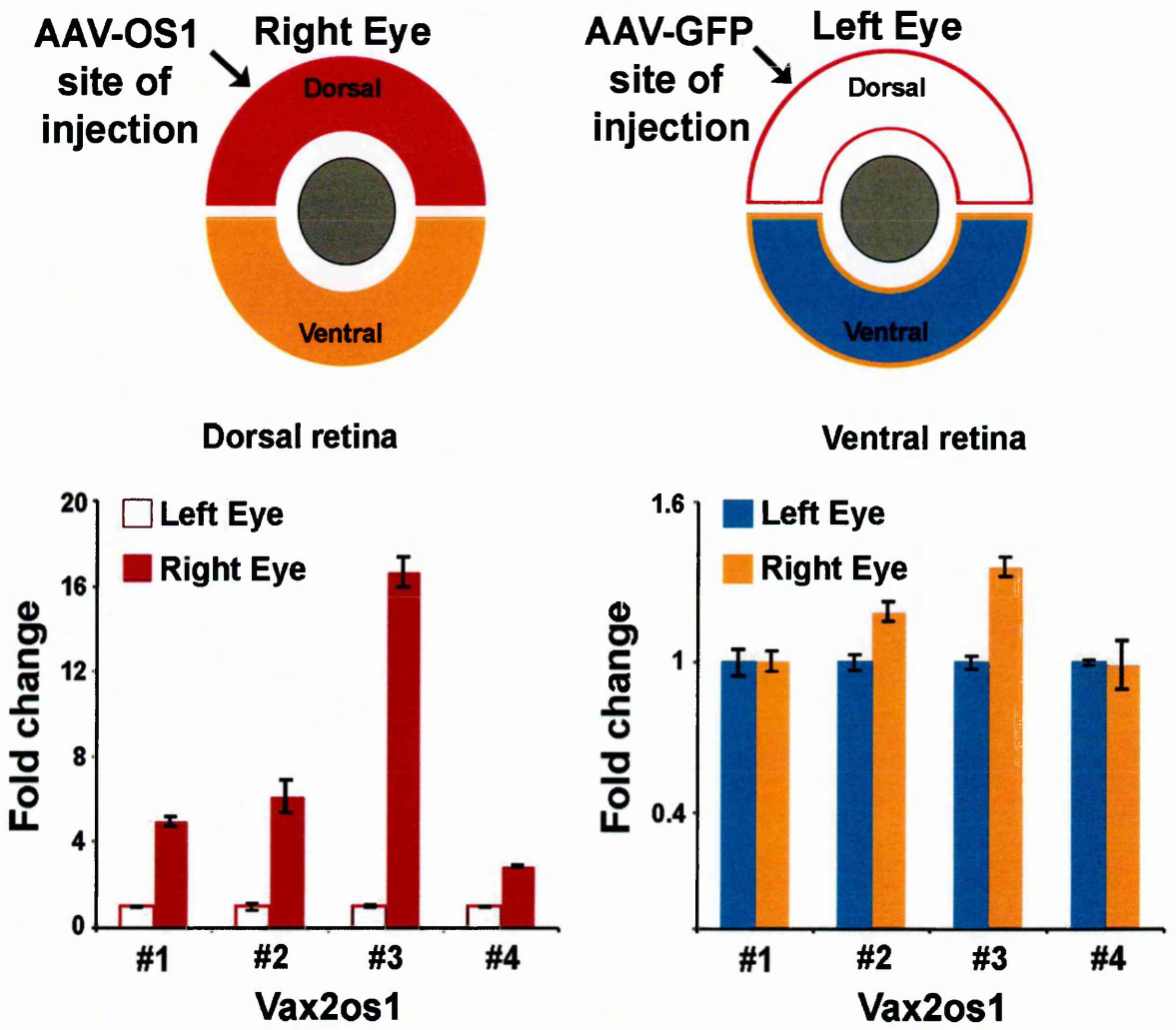

Figure 52. In vivo studies.

Assessment by qRT-PCR of the increased expression levels of Vax2os1 in the AAV-OS1 injected eyes (right eye, red bars) compared to the contralateral eyes that were AAV-GFP-injected (left eyes, white bars). Vax2os1 expression levels from the ventral retinal areas of AAV-OS1-injected (orange bars) and AAV-GFP-injected eyes (blue bars) are also indicated. Data are presented as means ± SEM from two technical replicates.

The animals injected at PN1 were then analyzed at different time points, i.e., PN6, PN12 and PN30. At PN6, the analysis of the AAV-OS1-injected retinas revealed an increased number of proliferating cells particularly in the prospective outer nuclear layer (ONL) as assessed by both Ki67 and pHH3 staining compared with both the AAV-delOS1- and AAV-GFP-injected retinas (control-injected retinas) (Figure 52A-F and 52G-H). Interestingly, this finding was restricted to the dorsal retinal areas, i.e., where the AAV constructs were injected, and only to the ONL (Figure 53A-D). Ki67 is a marker of the entire cell cycle and stains all the cycling cells while pHH3 stains only the late G2 and mitotic cells.

To confirm the above data, I also performed BrdU (5'-Bromo-2'-deoxyUridine) incorporation assay in injected eyes (24 hour-pulses). At PN6, I found an increase of BrdU-positive cells in the prospective outer nuclear layer (ONL) of the dorsal AAV-OS1-injected retinas vs. the control-injected retinal areas (Figure 54A-D). This finding was not observed in the ventral retinal areas (Figure 55A-B). Interestingly, I also detected an increase in the number of cells that were positive to both BrdU and Ki67 staining (BrdU+/Ki67+) in the ONL of the AAV-OS1 injected retinal areas (Figure 54A'-C'). These latter cells represent cycling cells in agreement with the result observed after Ki67 staining. I did not observe any apparent abnormality in the morphology of AAV-OS1-injected retinal areas compared to the control-injected areas (Figures 53 and 54). I could not assess the cellular identity of the increased cycling cells since in the prospective ONL of postnatal mouse retinas at PN6 different types of retinal progenitors are completing their last divisions (Baye and Link, 2008; Yu et al., 2011).

Taken together, these data indicate that the misexpression of *Vax2os1* determines a perturbation in the cell cycle progression of the progenitor cells in the retina at the early stages of postnatal retinal development.

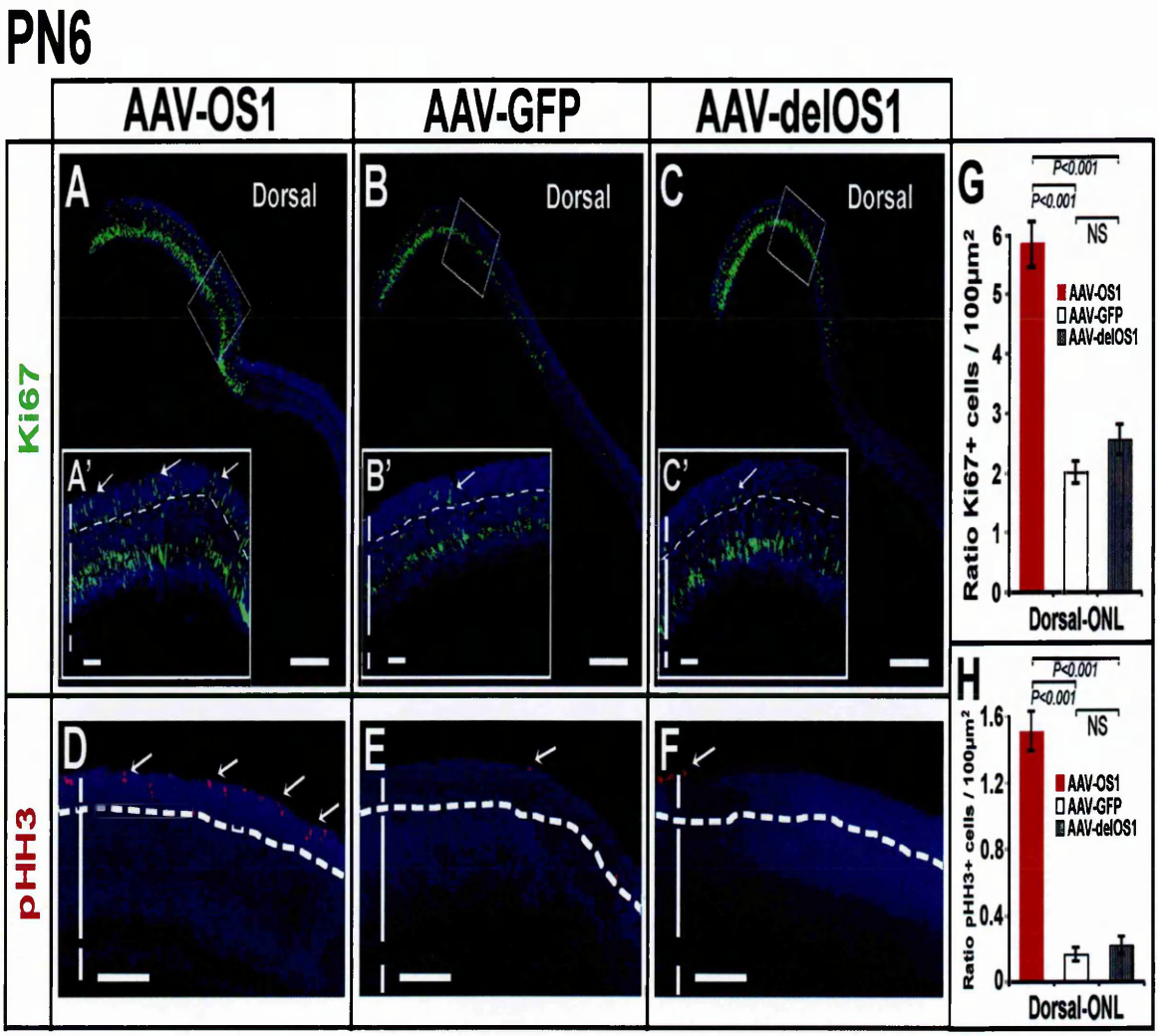

Figure 53. Vax2os1 overexpression in the retinal postnatal stages affects the correct proliferation of retinal progenitor cells.

AAVs overexpressing Vax2os1 and the two control constructs were injected in the dorsal retinal areas of PN1 mice. (A-C) Ki67 fluorescent immunostaining (green signal) observed in the PN6 dorsal retina areas. (A'-C') Higher magnifications of the areas boxed in panels A-C. Arrows indicate Ki67-positive cells in the prospective outer nuclear layer (pONL) of the AAV-OS1 injected retinas and the control construct-injected retinal areas. (D-F) pHH3 fluorescent immunostaining (in red) on the PN6 dorsal retina areas. Arrows show pHH3-positive cells in the pONL of AAV-OS1-injected retinas and the control injected retinal areas. (G-H) Counts of the Ki67 (G), pHH3 (H) -positive cells in the dorsal ONL of the injected retinas at PN6. Areas of 30 µm x 20 µm were used for manual counts. For each animal, multiple retinal areas were analyzed. Magnifying bars are 200 µm in A-C; 40 µm in A'-C'; 100 µm in D-F.

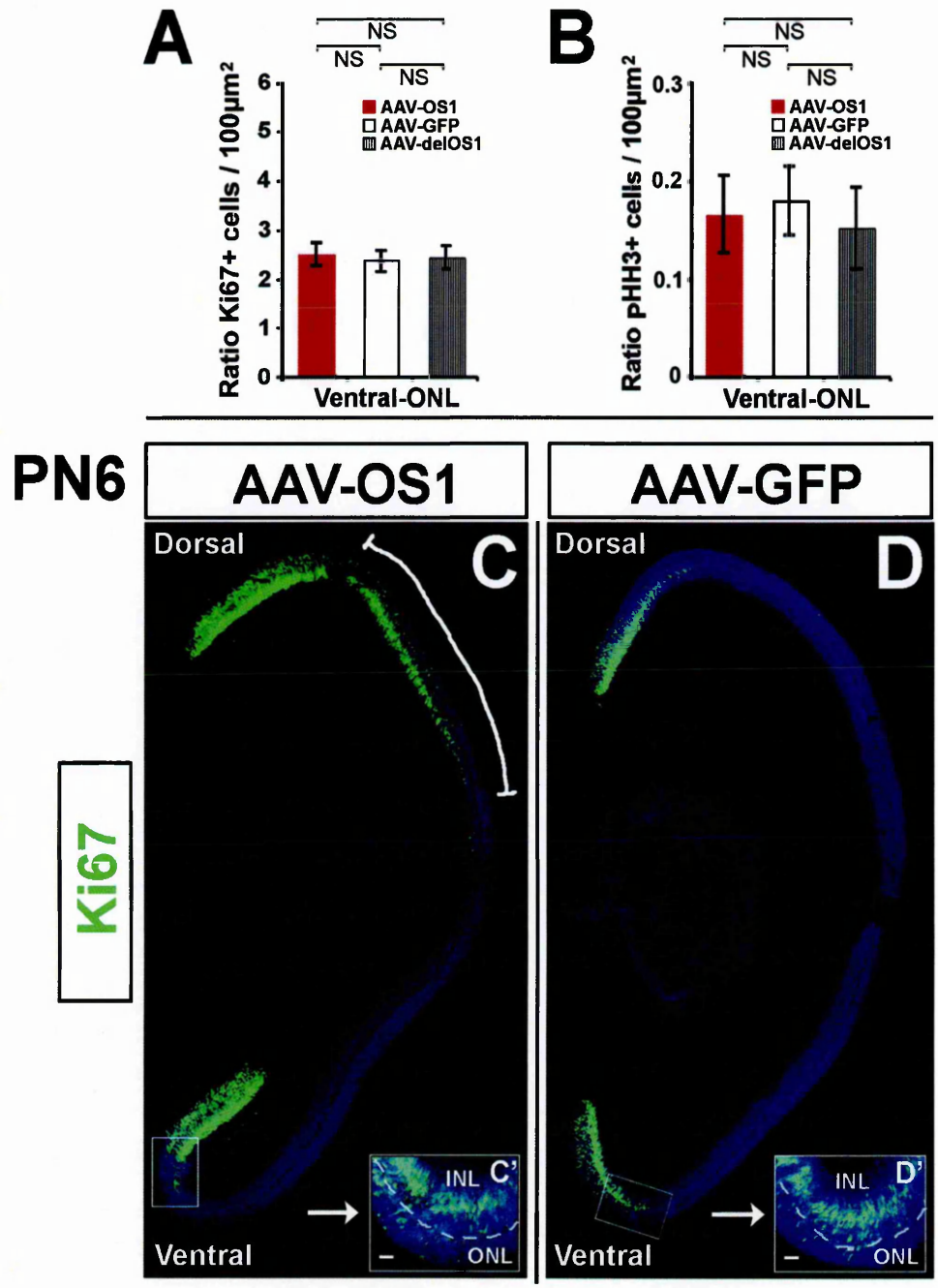

Figure 54. The effects of Vax2os1 overexpression in the retinal progenitor cells are restricted to the areas of injection.

(A-B) Counts of the Ki67 (A) and pHH3 (B) -positive cells in the ventral ONL of injected animals at PN6. (C-D) Ki67 fluorescence immunostaining on the PN6 retinas of the PN1-injected animals reveals no differences in the number of proliferating cells between the ventral area of AAV-OS1- and AAV-GFP-injected eyes. (C'-D') Higher magnifications of the ventral retinal areas boxed in panels C-D. Magnifying bars are 40 µm in C'-D'.

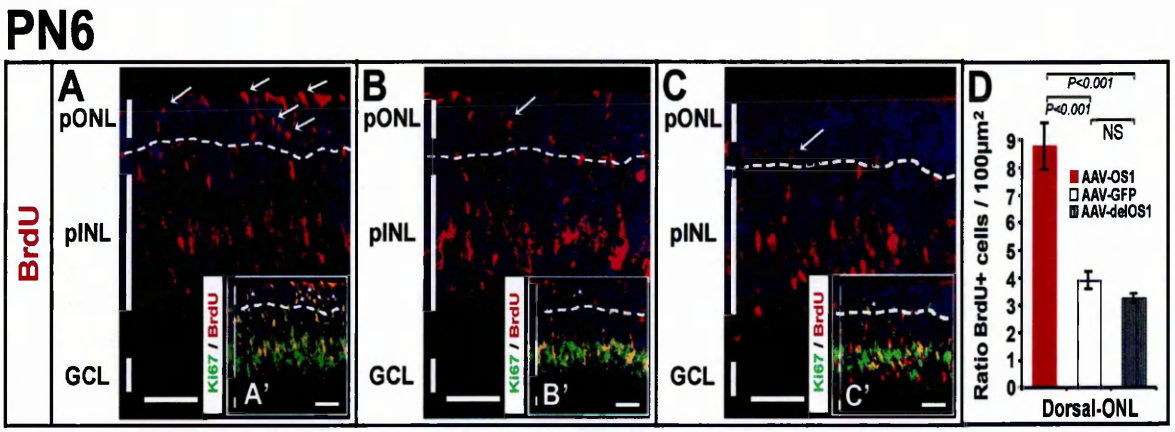

Figure 55. Vax2os1 overexpression in the retinal postnatal stages determines an increase of progenitor cells in the outer nuclear layer.

(A-C) BrdU fluorescent detection in the PN6 dorsal retina areas. The BrdU was administered 24 hours before sacrificing the animals. There is an increase of BrdU-positive cells in the pONL of the AAV-OS1 injected retinas compared to the control-injected retinal areas (arrows). (A'-C') Lower magnifications of panels A-C showing the results of co-immunostaining for BrdU and Ki67. The retinal cells positive to both the markers (in yellow) are present in the pINL and pONL in both the AAV-OS1- and control-injected retinas. However, there is an evident increase in the number of the BrdU/Ki67 positive cells in the pONL of the AAV-OS1 injected retinas compared to the control injected retinal areas (arrowheads). Please note that the lower limit of the pONL is indicated with a dotted line. (D) Counts of the BrdU -positive cells in the dorsal ONL of the injected retinas at PN6. Areas of 30 µm x 20 µm were used for manual counts. Magnifying bars are 20 µm in A-C and A'-C'.

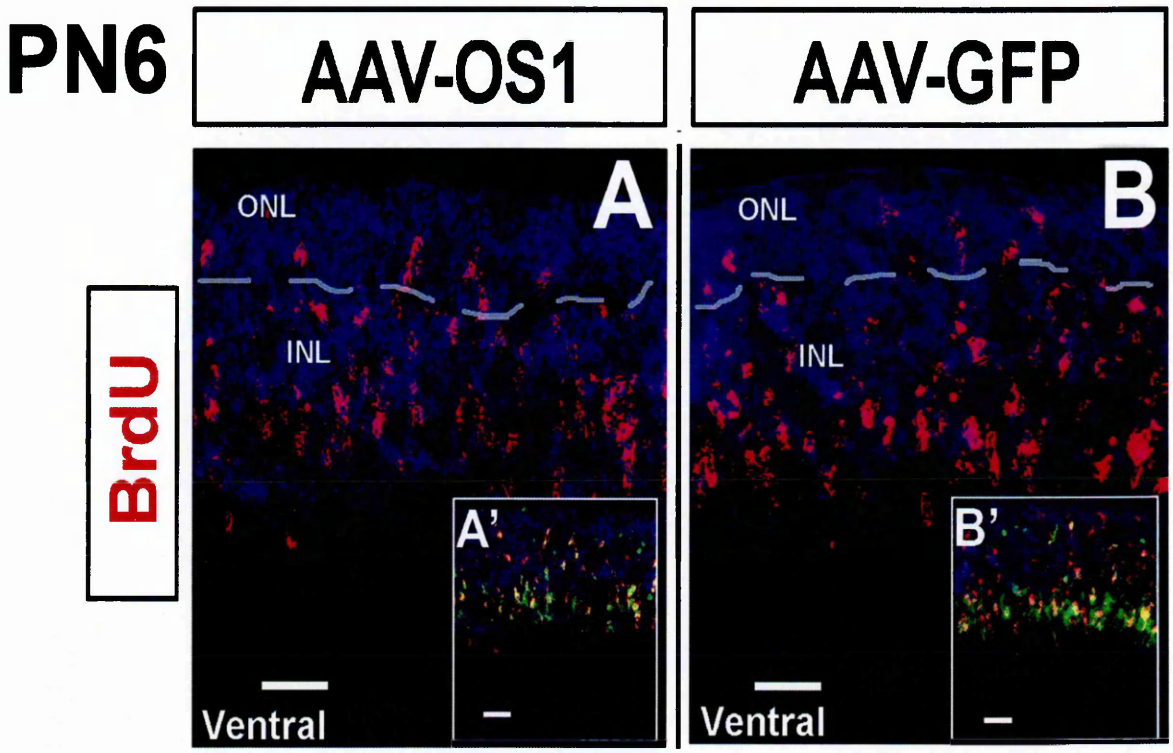

Figure 56. The effect of Vax2os1 overexpression in the increase of retinal progenitor cells is restricted to the areas of injection.

(A-B) BrdU fluorescent detection in the PN6 ventral retina areas. (A'-B') Fluorescence co-immunostaining for BrdU and Ki67 on the same sections shown in A and B, respectively, reveals no difference in the number of the Ki67/BrdU positive cells in the ONL of AAV-OS1 retinas as compared to the AAV-GFP controls. Magnifying bars are 40 μm A-B and A'-B'.

3.3.2 *Vax2os1 plays a role in the cell cycle progression and differentiation of photoreceptor progenitor cells*

At PN12, I still detected an increase of Ki67-positive cells in the dorsal ONL areas of the retinas injected with AAV-OS1 (Figures 56A-A' and 56C), which indicated that these retinal progenitor cells had not yet exited the cell cycle. This is in strong contrast with the result observed in both the AAV-GFP and AAV-delOS1-injected eyes and in the ventral retinal areas (Figure 56B-B') in which there were virtually no Ki67-positive cells suggesting that all the retinal progenitors had exited the cell cycle by this stage (Barton and Levine, 2008). This result indicated that the dorsal retinal progenitor cells that misexpress *Vax2os1* undergo a perturbation in their cell cycle progression.

I hypothesized that this effect could also lead to an impairment of the differentiation processes. To verify this hypothesis, I stained the injected retinas with an antibody against acetylated alpha-Tubulin (acetyl-αTub), which in the outermost region of the peripheral retina at this stage is predominantly expressed in the connecting cilium of the nascent outer photoreceptor segments (nOS) (Arikawa and Williams, 1993; Sung and Chuang, 2010). This experiment revealed a decrease of acetyl-αTub staining in the nOS of the dorsal AAV-OS1-injected retinas compared with similar areas of the control AAV-GFP-injected retinas. This result indicated a possible alteration in the process of ciliogenesis in the nascent photoreceptor axoneme of the AAV-OS1-injected eyes (Figure 57A-E).

I did not find significant differences in acetyl-αTub staining in the ventral areas of the injected retinas (Figure 58A-D). Therefore, this latter finding shows that *Vax2os1* overexpression affects mainly the progression of the photoreceptor progenitor cells toward their final differentiation.

Figure 57. Alteration in the differentiation of photoreceptor cells following Vax2os1 overexpression.

(A,B) Fluorescence co-immunostaining for BrdU and Ki67 in the dorsal areas of PN1-injected retinas at PN12. (A',B') Higher magnifications of the boxed areas in panels A and B, respectively. There is an increase in the number of the cells positive to both BrdU and Ki67 (arrowheads in A') in the outer nuclear layer (ONL) of the AAV-OS1-injected retinas in comparison with the AAV-GFP-injected retinal areas. (C) Counts of the Ki67-positive cells in the dorsal ONL of the injected retinas at PN12. Areas of 160 µm x 40 µm were used for manual counts. Magnifying bars are 200 µm in A,B and 40 µm in A',B'.

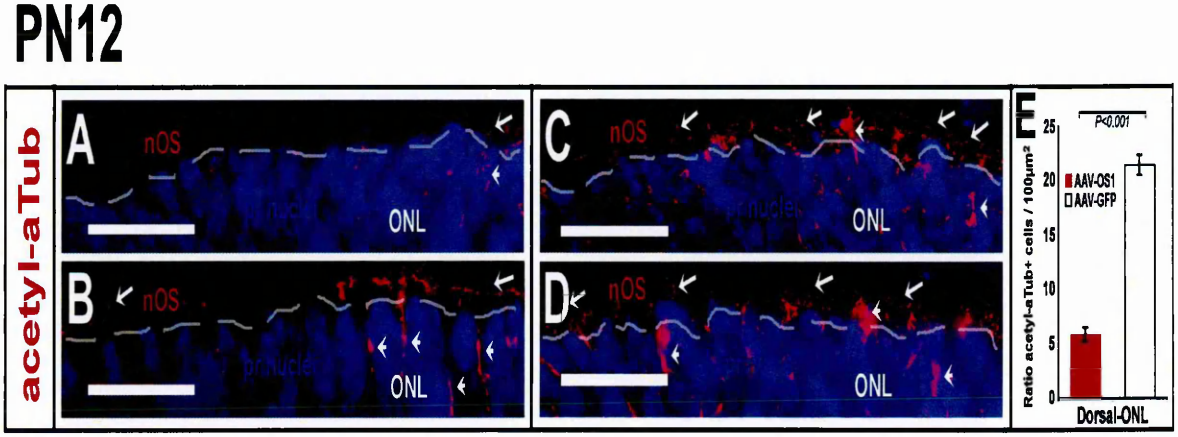

Figure 58. Impaired ciliogenesis in photoreceptors of the AAV-OS1 retinas.

(A-D) Fluorescence immunostaining for acetylated alpha Tubulin (acetyl-αTub) in the dorsal retinal areas of the injected mice at PN12. There is a decrease in the number of the acetyl-αTub-positive photoreceptor cells (arrows) in the AAV-OS1-injected, as compared to the control-injected retinas. The dotted lines delimit the border between the nOS and the ONL. Please note that acetyl-αTub also stains the cytoplasm of Müller glial cells (arrowheads). (E) Counts of the acetyl-αTub-positive photoreceptor outer segments in the dorsal ONL of the injected retinas at PN12. Areas of 80 µm x 5 µm were used for manual counts. Magnifying bars are 20 µm in A-D.

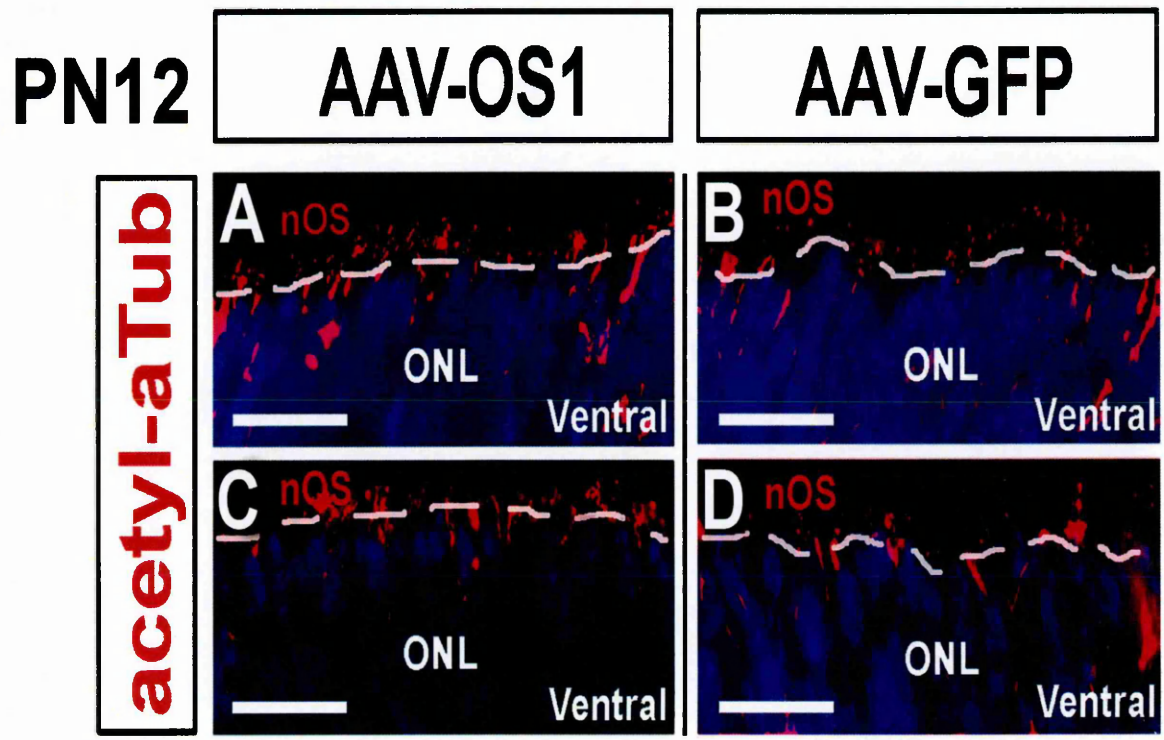

Figure 59. Photoreceptor ciliogenesis is normal in the ventral areas of the injected retinas.

(G-J) Fluorescence immunostaining for acetylated alpha-Tubulin (acetyl-αTub) in the ventral areas of PN12 retinas. No differences were observed in the number of acetyl-αTub-positive cells in the nascent outer segments (nOS) between the AAV-OS1- and AAV-GFP-injected retinas. Magnifying bars are 20 μm in A-D.

In order to verify whether the *Vax2os1*-induced alteration in differentiation observed at PN12 could be linked to an increased cell death of the retinal cells that overexpress *Vax2os1,* I investigated the extent of apoptosis in the injected retinal areas by TUNEL staining. I found a significant increase in the number of apoptotic cells in the photoreceptor layers of the OS1-OE-injected retinas compared with the GFP-injected retinal areas (Figure 59A-E). This effect was specific to the site of injection since I did not observe any increase in cell death in the ventral retinal areas of the injected mice. However, the increase in programmed cell death was restricted to a small number of cells within the injected retinal areas (Figure 59A-D).

I did not observe any difference in the extent of apoptosis at earlier (PN6) or at later stages in the AAV-OS1-injected retinas. Altogether, the above results indicate that the overexpression of *Vax2os1* alters the correct timing of photoreceptor cell proliferation, which leads to an increase in programmed cell death at selected stages of retinal development. At PN30, the dorsal retinal areas of the AAV-OS1-injected animals showed a significant increase of BrdU-positive cells in the ONL compared to the control-injected retinas (Figure 60A-G). This effect was particularly prominent not only in the most peripheral retinal regions, which are known to harbour proliferating cells until the late postnatal stages of retinal development (Figure 60B'-C'), but, even more remarkably, in the adjacent retinal regions, which we termed "near-peripheral" regions (Figure 60A-C'').

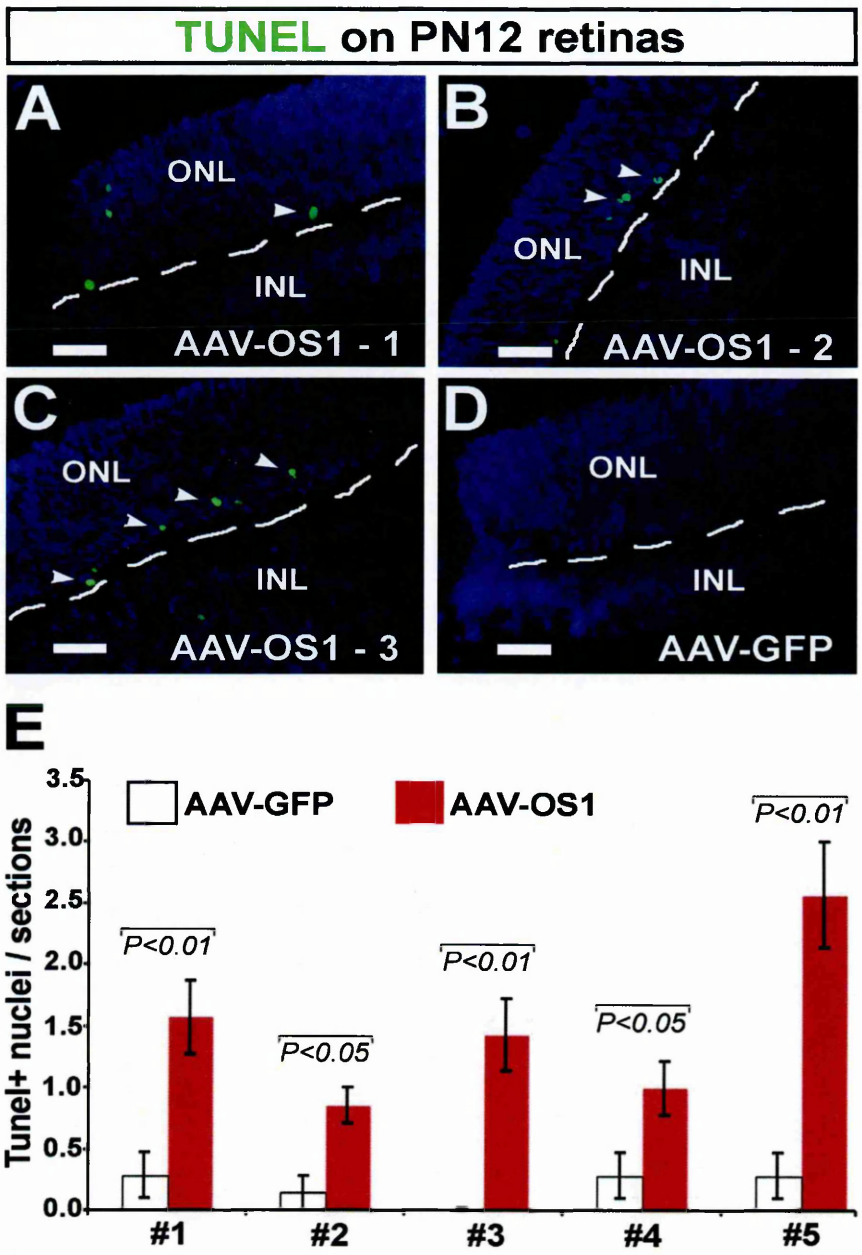

Figure 60. Increase of apoptosis at PN12 in the photoreceptor layer after Vax2os1-overexpression.

(A-D) Detection of programmed cell death by terminal deoxynucleotidyl transferase dUTP nick end labelling method (TUNEL, in green) in the dorsal retinas of the AAV-OS1- (A-C) and AAV-GFP-injected (D) mice. There is an increase in the number of the Tunel-positive cells in the AAV-OS1- vs. control-injected retinas (D). (E) Quantitative assessment/section of the number of Tunel-positive nuclei in the dorsal retinal regions analyzed. A significant increase of the Tunel-positive cells was observed in the AAV-OS1-injected retinas over control-injected retinas in each of the five animals analyzed. Magnifying bars are 20 μm in A-D.

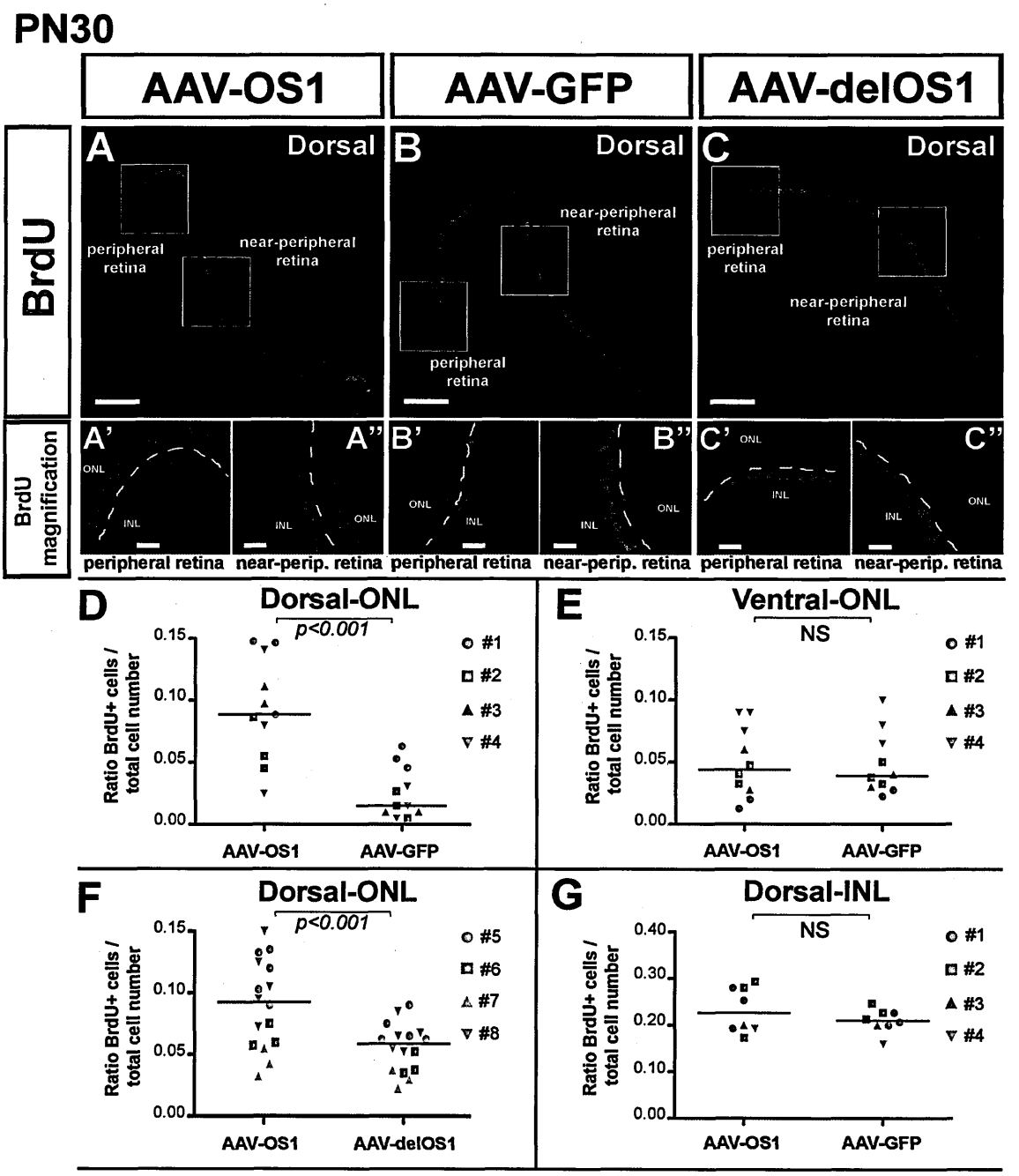

Figure 61. Vax2os1 action is restricted to the photoreceptor cells.

(A-C) The BrdU assay on PN30 dorsal retinal areas of mice injected at PN1. Two pulses of BrdU were performed, at PN5 and PN6, before sacrifice. (A'-C' and A''-C'') Higher magnifications of, respectively, the peripheral and near-peripheral retinal areas boxed in panels A-C. (D-G) Counts of BrdU-positive cells in the near-peripheral retinal areas of injected animals. In each panel, the identity of the animal analyzed is indicated. Areas of 80 μm x 40 μm were used for manual BrdU counts. Magnifying bars are 200 μm in A-C; 40 μm in A'-C''.

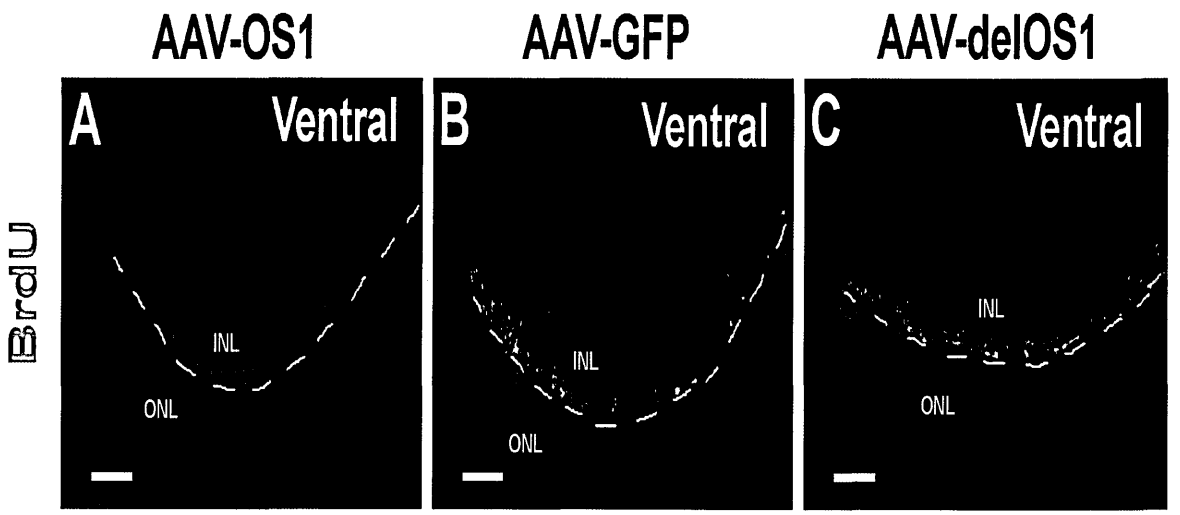

Figure 62. BrdU analysis in the ventral areas of adult retinas injected at PN1.

(C-E) BrdU fluorescence immunostaining revealed no differences in BrdU incorporation in the ventral retinal areas between the AAV-OS1- and AAV-GFP- injected eyes (C-D) or AAV-delOS1-injected eyes. . Magnifying bars are 40 μm in A-C.

No significant differences were observed in the number of BrdU-positive cells either in the INL, nor in more ventral areas of the AAV-OS1- compared with the control-injected retinas (Figures 60D-G and 61A-C). These findings suggest that at the time of the BrdU injections, namely PN5 and PN6, a greater number of photoreceptor progenitors (mainly rod progenitors) were still proliferating in the AAV-OS1 peripheral retina than in the injected control retinas as previously described (see Figure 54).

Regarding the expression of the neighbouring gene, *Vax2*, I did not detect any significant variation in the relative expression levels after *Vax2os1* overexpression in the AAV-OS1 compared to control AAV-GFP retinas at PN30 (Figure 62).

I could not detect any Ki67-positive cells in the mature retinas (PN30) of either the AAV-OS1-injected or control AAV-GFP and AAV-delOS1-injected retinas (Figure 63A-B). Moreover, I did not observe any difference in apoptosis between the AAV-OS1-injected and control-injected retinas.

Finally, immunofluorescence stainings using rod (Rhodopsin), cone (mw- and sw-Opsin) and bipolar cell (Chx10) markers did not reveal any anomalies in retinal cell type identity between the injected areas of the AAV-OS1-injected and control-injected retina samples (Figure 64).

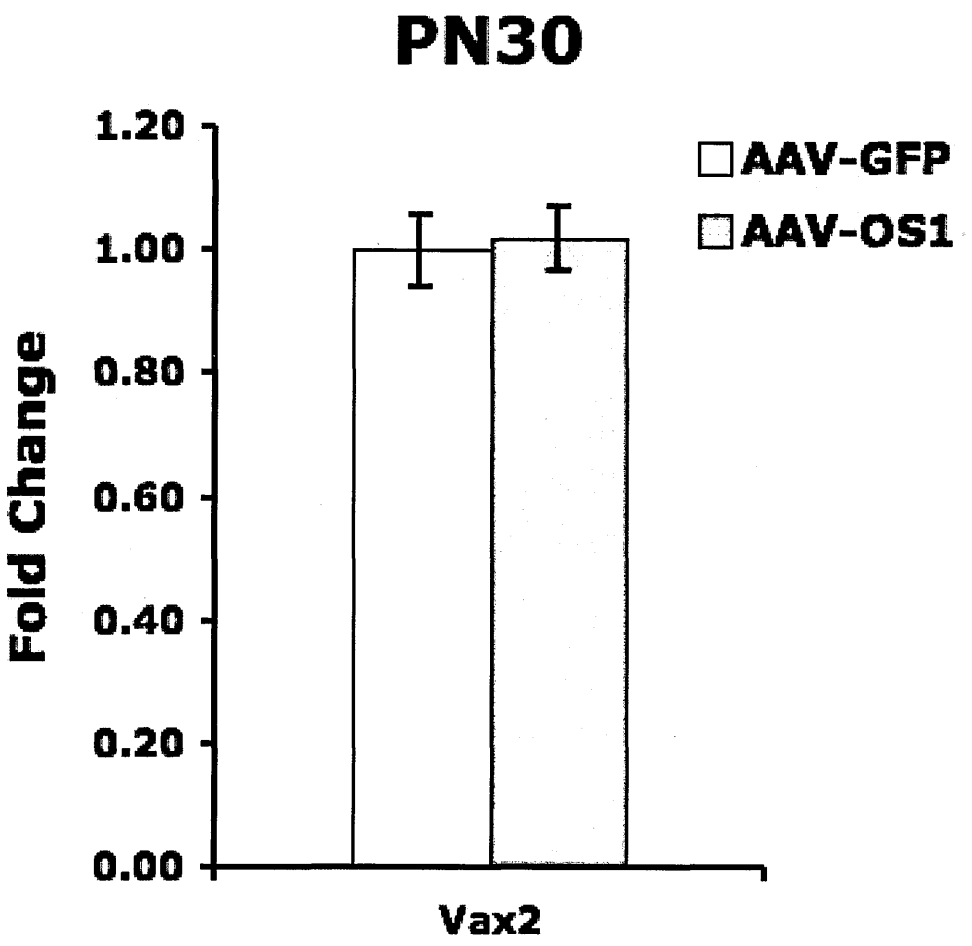

Figure 63. The expression levels of Vax2 do not change in AAV-OS1 retinas.

Data are presented as means ± SEM (N=5).

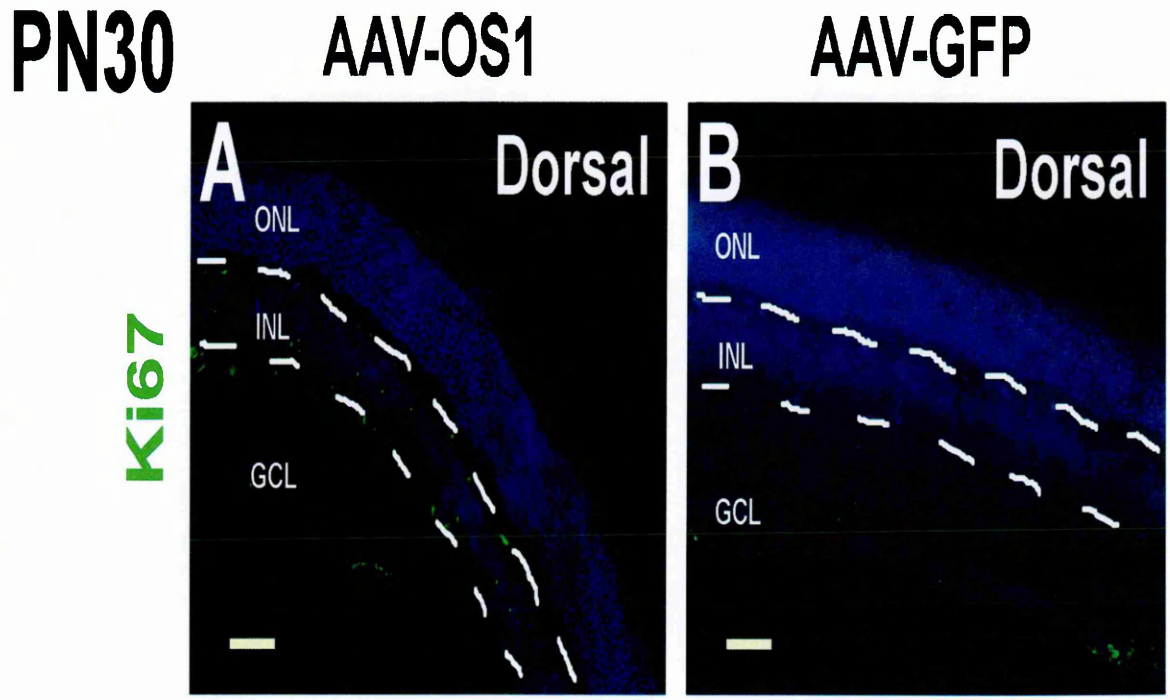

Figure 64. Ki67 analysis at the adult stage of PN1-injected retinas.

(A-B) Ki67 fluorescence immunostaining on the PN30 retinas. No differences were observed in the dorsal areas of AAV-OS1-injected as compared to the AAV-GFP-injected eyes. Magnifying bars are 40 μm in A-B.

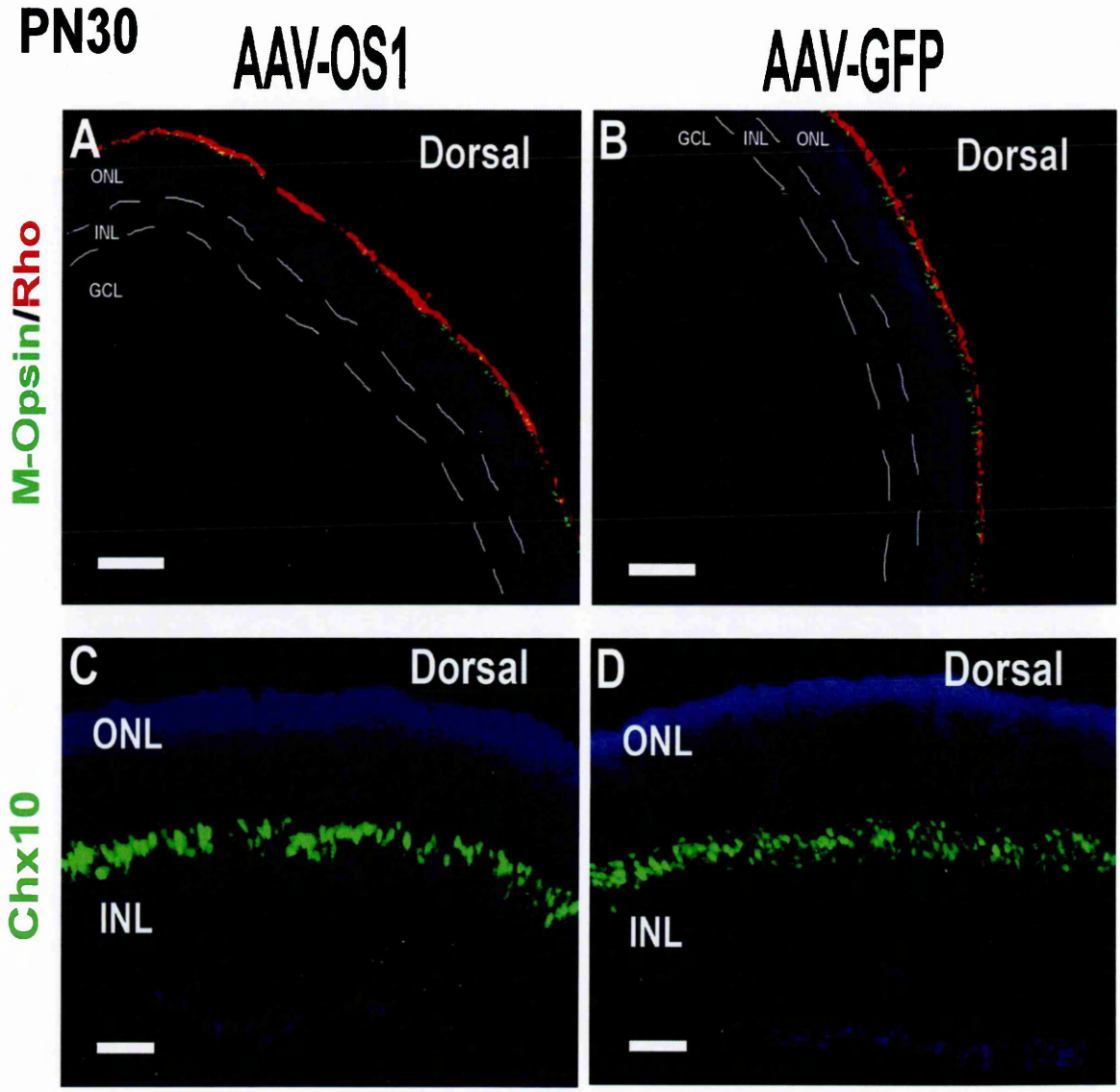

Figure 65. Analysis of rod, cone and bipolar cell markers in the adult retinas.

(A-B) Immunofluorescence staining in the PN30 retina with an anti-Rhodopsin (rod cells, red signal) and with an anti-M-Opsin (cone cells, green signal) antibody of eyes injected at PN1 with the AAV-OS1 and with the AAV-GFP constructs. (C-D) Immunofluorescence staining with an anti-Chx10 (bipolar cells, green signal). Magnifying bars are 40 μm in A-D.

Taken together, all of the above data suggest that *Vax2os1* misexpression at the early postnatal stages of retinal development causes a perturbation in the cell cycle progression of the retinal neuroblasts. This effect leads to a delay in the differentiation of the photoreceptor progenitor cells, which highlights a role of this lncRNA in controlling the proper maturation of photoreceptors.

4 DISCUSSION

4.1 Expression analysis of lncRNAs *Six3os, Otx2os* and *Vax2os* in the mouse retina

Long non-coding RNAs (lncRNAs) are emerging as functional molecules that mediate important cellular processes (Nagano and Fraser, 2011). However, there are only a few reports regarding the functional role of lncRNAs in retinal development (Rapicavoli et al., 2010; Young et al., 2005). In the last few years, in our laboratory, we have focused our attention on the identification of lncRNAs expressed at high levels in the developing retina. The first result that we obtained was the identification of a set of Opposite Strand transcripts associated with transcription factor genes known to play a basic role in eye development in vertebrates (Alfano et al., 2005).

Among these, for my PhD study, I began a preliminary study of expression analysis for the lncRNAs *Vax2os*, *Otx2os* and *Six3os*, related to the *Vax2*, *Otx2* and *Six3* genes, respectively. All of these transcripts are spliced and polyadenylated like "classic" messenger RNAs and undergo a significant number of splicing events. Furthermore, these identified OS transcripts are likely to represent non-coding RNA transcripts as they lack open reading frames (ORF) of any significant length. More particularly, *Six3os* presents a high number of different splicing events producing a heterogeneous population of OS transcripts that consists of more than 10 splice isoforms. Moreover, all of these nearly identical isoforms are localized upstream of the putative *Six3* regulatory region and the minimum distance between these two transcriptional units is below 2.5 kilobases. The *Otx2os* transcripts are characterized in a similar way, although the number of different

splice isoforms is considerably smaller compared to *Six3os* (3 splice isoforms). Three different transcriptional clusters characterize the genomic situation of *Vax2os* genomic organization and one of these begins to be transcribed in the first intron of the ''sense'' gene *Vax2*.

My first goal was to carry out the following tasks: i) the determination of the expression pattern of each selected OS isoform by quantitative PCR during mouse retina development and ii) the determination of the spatiotemporal expression pattern of selected OS transcripts during mouse retina development by RNA *in situ* hybridization analysis.

Therefore, I assessed the expression pattern for all of these OS isoforms in the post-natal stages of mouse retina development. To achieve this aim, I performed quantitative PCR experiments on mice at post-natal days PN1, PN4 and PN8 and at adult stages. In greater detail, whole eyes (without the optic nerve) from the developmental stages of interest or dissected adult retinas were harvested from the sacrificed mice (C57Bl/6 strain) and the total RNA was extracted. Regarding the PCR amplification, I used isoform-specific primers designed on freely available software and I was able to distinguish from each other unambiguously, whenever possible, all tested splice isoform derived from the same transcriptional unit.

For *Vax2os*, isoform 1 (*Vax2os1*) was the most highly expressed during mouse retina development in comparison with isoform 2 (*Vax2os2*) and isoform 3 (*Vax2os3*), although at lower levels if compared to the expression of the sense gene *Vax2*. Interestingly, in the adult retina the overall *Vax2os* expression levels seem to be higher than those of the *Vax2* ''sense'' gene.

Concerning *Otx2os*, isoform 3 (*Otx2os3*) was the most highly expressed isoform during mouse retina development in comparison to isoform 1 (*Otx2os1*) and isoform 2 (*Otx2os2*), but also in this case the expression levels were relatively low when compared to

those of the sense gene *Otx2*. Furthermore, in the adult retina *Otx2os3* showed a decrease of expression levels whereas *Otx2os1* was the most highly expressed isoform at this specific time point. Finally, isoform 9 of the *Six3os* (*Six3os9*) cluster was always the most highly expressed isoform including at adult stages and the expression levels were very abundant when compared to the *Six3* expression at the same developmental stages.

These results clarified the expression pattern of the OS isoforms in the mouse retina development and also provided us with valuable information about the recognition of the OS isoforms expressed at the most significant levels during retinal development. This was a very important finding also in terms of further experimental approaches, e.g., gain- of function experiments. Moreover, it is interesting to note that these OS isoforms seem to change their expression activity during retinal development.

After the expression analysis of the OS isoforms by quantitative PCR, I was interested also in understanding where these transcripts were localized in the developing retina since this retinal tissue is composed of seven different neuronal cell types, distributed in three distinct nuclear layers. To achieve this aim, I performed RNA *in situ* hybridization analysis on the most highly expressed OS transcripts, previously described. I observed that both *Vax2os1* and *Otx2os3* did not seem to be expressed (or were expressed at very low levels, below the threshold of RNA in situ detectability) in the post-natal retinal stages (PN1, PN6 and PN8) whereas their expression in adult retina was readily detectable. *Six3os9* instead was highly expressed in post-natal day 1 retinas also in comparison with the sense gene *Six3* as well as in adult retina although at lower levels.

The *Vax2os1* expression in the adult retina was restricted to the outer nuclear layer, ONL, where the photoreceptor cell nuclei (rod and cone cells) are distributed. Furthermore, the localization of the *Vax2os1* signal was only visible in the ventral area of the adult mouse retina suggesting the presence of a high ventral-low dorsal gradient of expression.

This interesting expression pattern is reminiscent of the expression pattern of the sense gene *Vax2*, previously studied in our lab, although *Vax2* is most highly expressed in the ganglion cell layer (GCL) and inner nuclear layer (INL) in the adult mouse retina.

Otx2os3 began to be expressed at increasing levels from late post-natal stages of retina maturation until the adult stage. The signal was barely visible in the inner nuclear layer at post-natal day 8, while in the adult retina it was more intense and clearly distributed. In fact, the particular distribution of the signal in the outermost part of the INL allows me to hypothesize a localization in the bipolar cells although this observation has not been supported by any immunohystological assay.

Finally, *Six3os9* was expressed at high levels in post-natal day 1 retinas, in particular in the outer neuroblastic layer, ONBL, where proliferative and differentiative processes are still occurring and will lead to the final maturation of the different retinal cell types, especially the rod and bipolar cells. This result is comparable with the expression profile of the sense gene *Six3*, which was expressed at high levels throughout the retinal layers at the PN1 stage, including also in the inner neuroblastic layer, INBL. In addition, the expression localization of both transcripts in the adult retina was maintained in the same retinal layers, the INL and GCL, although *Six3os9* showed a slighter signal in comparison to the expression of *Six3*.

Therefore, these RNA *in situ* experiments show that *Otx2os* and *Six3os* are coexpressed with their corresponding sense genes suggesting that they may be functionally related. However, regarding a possible mechanism of function, it is unlikely that the latter OS transcripts exert their function through the formation of dsRNAs with their corresponding sense genes, as suggested by the fact that the majority of their transcribed spliced isoforms do not seem to overlap the corresponding sense transcripts. *Vax2os*, instead, present a complementary expression pattern with its corresponding sense genes,

Vax2. In fact, I cannot exclude that the expression of *Six3os* and *Otx2os* transcripts, at the single cell level, is mutually exclusive.

The study of OS transcripts associated to transcription factors playing an important role in eye development and function may also have implications in the elucidation of the molecular basis of eye diseases. Mutations in *Six3*, *Otx2 and Vax2* have been related to the pathogenesis of eye developmental anomalies either in human or in mouse (Barbieri et al., 2002; Graw, 2003). The evidence that the NATs associated with these genes may participate in the regulation of their expression and consequently in the processes underlying eye development suggests these antisense transcripts may also play a role in the pathogenesis of eye developmental diseases.

Therefore these pilot experiments elucidate the temporal-spatial expression pattern for three OS transcripts in the late developing and adult mouse retina. Together with the results obtained by studying the isoform-specific expression, I have been able to plan dedicated experimental strategies including the choice of the spliced OS isoform to analyse, the retinal cell line to target *in vivo* and the cellular background to reproduce as the *in vitro* counterpart. In the next section, indeed, I will comment on the results obtained by the gain of function approach for *Vax2os1* both *in vitro* and *in vivo*.

4.2 Functional characterization of lncRNA *Vax2os* in the mouse retina

In this study, we have gained an insight into the functional role of the retinal-specific lncRNA, *Vax2os1*, during retinal photoreceptor progenitor cell cycle progression and differentiation. This transcript displays a peculiar and dynamic expression profile in the mouse retina: it is abundantly expressed in the proliferating areas of the ventral embryonic

retina while it is considerably down regulated in the early postnatal stages of retinal development. In the mature retina, *Vax2os1* expression is up regulated again and is restricted to the ONL of the ventral retina (Fig. 1), presumably more in rod than in cone cells, as suggested in a previous study (Corbo et al., 2007). This particular expression pattern prompted us to test whether Vax2os1 could be implicated in the regulation of photoreceptor cell proliferation and differentiation.

To gain an insight into the Vax2os1 function, we designed loss-of-function and gain-of-function approaches both in vitro and in vivo. However, all attempts to down regulate Vax2os1 by RNA interference technology failed to yield acceptable levels of Vax2os1 repression. We suppose that the secondary structure of this lincRNA may have disturbed the action of small interfering RNA oligos by afflicting their right recognition site or by lowering the thermodynamic stability of the RNA/oligo duplex. Nevertheless, in order to obtain a more complete picture of the physiological role of *Vax2os1* in the retina, it will be essential to study the effects of its inactivation *in vivo*, possibly by means of targeted homologous recombination, or *in vitro* by antigene peptide nucleic acids (agPNAs) that target transcriptional start sites.

Therefore, I generated an *in vivo* mouse model of spatiotemporal misexpression of *Vax2os1*. To this purpose, I chose a stage (PN1) in which the majority of the retinal progenitor cells still have to undergo their final divisions (Barton and Levine, 2008). At this stage, the mouse retina predominantly consists of photoreceptor progenitor cells, which, through asymmetric divisions, gradually generate post-mitotic photoreceptors and new cycling progenitors with a concomitant increasing time of cell cycle length (Alexiades and Cepko, 1996; Li et al., 2000). I observed an impairment in the cell cycle progression of the retinal progenitor cells following *Vax2os1* overexpression at different time-points following injection at PN1 (Figures 2-6). In particular, I showed that this effect is mainly evident in

the photoreceptor progenitor cells as determined after BrdU pulses carried out at early stages and analyzed at PN30, i.e., when all the retinal layers are clearly defined and formed. However, I did not observe any obvious anomaly in the retinal morphology and in the final differentiation of photoreceptors in the mature retina of the *Vax2os1*-injected mice. Based on the above results, I conclude that the misexpression of *Vax2os1* in the dorsal retina determines a cell cycle perturbation in the photoreceptor progenitors, which consists in a pronounced delay in cell cycle exit that, if prolonged during development, might induce some photoreceptor progenitors to undergo apoptosis (Figure 5).

In mammals, the genesis of the mature photoreceptors occurs during a long temporal window either with a long cell proliferation phase (rods) or with a long post-mitotic cell maturation phase (cones). In particular, the rod photoreceptor progenitors are subject to a proliferation phase, which can last for several days in rodents, during which they gradually acquire a restriction of their differentiation competence and undergo progressive cell specification and commitment toward their fate Turner et al., 1990. During the latter phase, the photoreceptor progenitors must be competent to respond to inductive cues and cell fate determinants whose action can influence the rate of progress through the cell cycle of progenitor cells. I hypothesize that *Vax2os1* may represent one of these factors and could prevent photoreceptor progenitor cells from undergoing a premature cell cycle exit at inappropriate times. The observed expression levels of *Vax2os1* (high in the early phase of progenitor proliferation and low in the post-natal retina during the final divisions of progenitor cells) seem to support this hypothesis.

Another intriguing aspect of the *Vax2os1* transcript is represented by its relationship with its neighbouring gene, *Vax2*. Expression studies performed by RNA ISH showed a similar expression pattern in the ventral retina for both transcripts although they profoundly diverge in terms of retinal cell specificity, *Vax2os1* being expressed in the photoreceptors

and *Vax2* in the retinal ganglion cells and interneurons. We previously reported that the inactivation of *Vax2* by targeted recombination was accompanied by a concomitant downregulation of *Vax2os1* (Alfano et al., 2005). However, in the present work, we have not detected any significant variation in the expression levels of *Vax2* after *Vax2os1* overexpression either *in vitro* (661W cells) or *in vivo,* in the mouse retina.

This result suggests either that *Vax2* controls the expression of *Vax2os1* but not vice versa or that the down-regulation of *Vax2os1* observed in the retina of *Vax2* knockout mice is due to the loss of an expression control element located within the genomic fragment targeted by homologous recombination. In any case, this result indicates that the functional role played by *Vax2os1* in photoreceptor cell differentiation is not mediated by changes in the expression levels of *Vax2.*

Finally, our findings suggest a physiological role of *Vax2os1* in ventral mouse retina development and maturation since *Vax2os1* is also expressed in the adult photoreceptors. One of the main differentiation events that occur in an asymmetric fashion across the dorsal-ventral axis of the mammalian eye is represented by cone photoreceptor differentiation with an asymmetric distribution of the mw-Opsin and sw-Opsin along the dorsal-ventral axis of the retina (Cepko, 1996; Hennig et al., 2008; Satoh et al., 2009). Interestingly, we recently found that *Vax2*, the neighbouring gene of *Vax2os1*, plays an important role in controlling cone opsin expression in the vertebrate eye by modulating the retinoic acid (RA) signaling (Alfano et al., 2011). On the other hand, the rod photoreceptor cells do not show any evident asymmetric expression pattern of their main proteins, e.g., Rhodopsin. Nevertheless there is some evidence of the asymmetric properties of the rod photoreceptors along the dorsal-ventral axis in the mammalian retina. For instance, it is known that rod photoreceptor cell death occurs preferentially in the dorsal retina of rats exposed to bright light (Gordon et al., 2002).

For all these reasons, it is tempting to speculate that *Vax2os1* may play an important role in the appropriate specification of the ventral rod photoreceptors by acting as a cell cycle regulator of the retinal progenitors and in the maintenance of the adult photoreceptor cells. Obviously, further studies are required to support the above hypothesis. In particular, it will be of the utmost importance to verify the presence and the identity of possible molecular interactors of *Vax2os1*, either proteins, such as key components of the cell cycle, transcription factors or histone-modifying proteins, as previously described for other lncRNAs (Feng et al., 2006; Khalil et al., 2009; Loewer et al., 2010), or other RNA molecules.

The recognition that *Vax2os1* is endowed with a functional role in the proper development of the mammalian retina further highlights the concept that the contribution of lncRNAs to the regulation of basic biological processes and gene regulatory networks must be taken into consideration. The availability of comprehensive transcriptome datasets generated from different tissues using Next-Generation Sequencing procedures is expected to shed further light on the identification of additional functional lncRNAs and into the initial elucidation of their contribution to physiopathological processes.

IV. REFERENCES

Agathocleous, M., and Harris, W.A. (2009). From progenitors to differentiated cells in the vertebrate retina. Annual review of cell and developmental biology *25*, 45-69.

al-Ubaidi, M.R., Font, R.L., Quiambao, A.B., Keener, M.J., Liou, G.I., Overbeek, P.A., and Baehr, W. (1992). Bilateral retinal and brain tumors in transgenic mice expressing simian virus 40 large T antigen under control of the human interphotoreceptor retinoid-binding protein promoter. The Journal of cell biology *119*, 1681-1687.

Alexiades, M.R., and Cepko, C. (1996). Quantitative analysis of proliferation and cell cycle length during development of the rat retina. Dev Dyn *205*, 293-307.

Alfano, G., Conte, I., Caramico, T., Avellino, R., Arno, B., Pizzo, M.T., Tanimoto, N., Beck, S.C., Huber, G., Dolle, P., *et al.* (2011). Vax2 regulates retinoic acid distribution and cone opsin expression in the vertebrate eye. Development (Cambridge, England) *138*, 261-271.

Alfano, G., Vitiello, C., Caccioppoli, C., Caramico, T., Carola, A., Szego, M.J., McInnes, R.R., Auricchio, A., and Banfi, S. (2005). Natural antisense transcripts associated with genes involved in eye development. Human molecular genetics *14*, 913-923.

Allocca, M., Mussolino, C., Garcia-Hoyos, M., Sanges, D., Iodice, C., Petrillo, M., Vandenberghe, L.H., Wilson, J.M., Marigo, V., Surace, E.M., *et al.* (2007). Novel adeno-associated virus serotypes efficiently transduce murine photoreceptors. Journal of virology *81*, 11372-11380.

Allocca, M., Tessitore, A., Cotugno, G., and Auricchio, A. (2006). AAV-mediated gene transfer for retinal diseases. Expert opinion on biological therapy *6*, 1279-1294.

Altshuler, D., Lo Turco, J.J., Rush, J., and Cepko, C. (1993). Taurine promotes the differentiation of a vertebrate retinal cell type in vitro. Development (Cambridge, England) *119*, 1317-1328.

Amaral, P.P., and Mattick, J.S. (2008). Noncoding RNA in development. Mamm Genome *19*, 454-492.

Arikawa, K., and Williams, D.S. (1993). Acetylated alpha-tubulin in the connecting cilium of developing rat photoreceptors. Investigative ophthalmology & visual science *34*, 2145-2149.

Ashe, H.L., Monks, J., Wijgerde, M., Fraser, P., and Proudfoot, N.J. (1997). Intergenic transcription and transinduction of the human beta-globin locus. Genes & development *11*, 2494-2509.

Auricchio, A., Kobinger, G., Anand, V., Hildinger, M., O'Connor, E., Maguire, A.M., Wilson, J.M., and Bennett, J. (2001). Exchange of surface proteins impacts on viral vector cellular specificity and transduction characteristics: the retina as a model. Human molecular genetics *10*, 3075-3081.

Baker, M. (2011). Long noncoding RNAs: the search for function. Nature methods *8*, 379-383.

Barbieri, A.M., Broccoli, V., Bovolenta, P., Alfano, G., Marchitiello, A., Mocchetti, C., Crippa, L., Bulfone, A., Marigo, V., Ballabio, A., *et al.* (2002). Vax2 inactivation in mouse determines alteration of the eye dorsal-ventral axis, misrouting of the optic fibres and eye coloboma. Development (Cambridge, England) *129*, 805-813.

Barbieri, A.M., Lupo, G., Bulfone, A., Andreazzoli, M., Mariani, M., Fougerousse, F., Consalez, G.G., Borsani, G., Beckmann, J.S., Barsacchi, G., *et al.* (1999). A homeobox gene, vax2, controls the patterning of the eye dorsoventral axis. Proceedings of the National Academy of Sciences of the United States of America *96*, 10729-10734.

Bartel, D.P. (2009). MicroRNAs: target recognition and regulatory functions. Cell *136*, 215-233.

Barton, K.M., and Levine, E.M. (2008). Expression patterns and cell cycle profiles of PCNA, MCM6, cyclin D1, cyclin A2, cyclin B1, and phosphorylated histone H3 in the developing mouse retina. Dev Dyn *237*, 672-682.

Baye, L.M., and Link, B.A. (2008). Nuclear migration during retinal development. Brain research *1192*, 29-36.

Belecky-Adams, T., Cook, B., and Adler, R. (1996). Correlations between terminal mitosis and differentiated fate of retinal precursor cells in vivo and in vitro: analysis with the "window-labeling" technique. Developmental biology *178*, 304-315.

Bernstein, S.L., Kutty, G., Wiggert, B., Albert, D.M., and Nickerson, J.M. (1994). Expression of retina-specific genes by mouse retinoblastoma cells. Investigative ophthalmology & visual science *35*, 3931-3937.

Bertone, P., Stolc, V., Royce, T.E., Rozowsky, J.S., Urban, A.E., Zhu, X., Rinn, J.L., Tongprasit, W., Samanta, M., Weissman, S., *et al.* (2004). Global identification of human transcribed sequences with genome tiling arrays. Science (New York, NY *306*, 2242-2246.

Bhatia, B., Singhal, S., Lawrence, J.M., Khaw, P.T., and Limb, G.A. (2009). Distribution of Muller stem cells within the neural retina: evidence for the existence of a ciliary margin-like zone in the adult human eye. Experimental eye research *89*, 373-382.

Biehlmaier, O., Neuhauss, S.C., and Kohler, K. (2001). Onset and time course of apoptosis in the developing zebrafish retina. Cell and tissue research *306*, 199-207.

Blackshaw, S., Harpavat, S., Trimarchi, J., Cai, L., Huang, H., Kuo, W.P., Weber, G., Lee, K., Fraioli, R.E., Cho, S.H., *et al.* (2004). Genomic analysis of mouse retinal development. PLoS biology *2*, E247.

Bringmann, A., Iandiev, I., Pannicke, T., Wurm, A., Hollborn, M., Wiedemann, P., Osborne, N.N., and Reichenbach, A. (2009). Cellular signaling and factors involved in Muller cell gliosis: neuroprotective and detrimental effects. Progress in retinal and eye research *28*, 423-451.

Carmichael, G.G. (2003). Antisense starts making more sense. Nature biotechnology *21*, 371-372.

Carninci, P., Kasukawa, T., Katayama, S., Gough, J., Frith, M.C., Maeda, N., Oyama, R., Ravasi, T., Lenhard, B., Wells, C., *et al.* (2005). The transcriptional landscape of the mammalian genome. Science (New York, NY *309*, 1559-1563.

Carter-Dawson, L.D., and LaVail, M.M. (1979). Rods and cones in the mouse retina. II. Autoradiographic analysis of cell generation using tritiated thymidine. The Journal of comparative neurology *188*, 263-272.

Cawley, S., Bekiranov, S., Ng, H.H., Kapranov, P., Sekinger, E.A., Kampa, D., Piccolboni, A., Sementchenko, V., Cheng, J., Williams, A.J., *et al.* (2004). Unbiased mapping of transcription factor binding sites along human chromosomes 21 and 22 points to widespread regulation of noncoding RNAs. Cell *116*, 499-509.

Cepko, C.L. (1996). The patterning and onset of opsin expression in vertebrate retinae. Current opinion in neurobiology *6*, 542-546.

Cepko, C.L. (1999). The roles of intrinsic and extrinsic cues and bHLH genes in the determination of retinal cell fates. Current opinion in neurobiology *9*, 37-46.

Chen, J., Sun, M., Hurst, L.D., Carmichael, G.G., and Rowley, J.D. (2005). Genome-wide analysis of coordinate expression and evolution of human cis-encoded sense-antisense transcripts. Trends Genet *21*, 326-329.

Chen, L.L., and Carmichael, G.G. (2010). Decoding the function of nuclear long non-coding RNAs. Current opinion in cell biology *22*, 357-364.

Chen, S., Wang, Q.L., Nie, Z., Sun, H., Lennon, G., Copeland, N.G., Gilbert, D.J., Jenkins, N.A., and Zack, D.J. (1997). Crx, a novel Otx-like paired-homeodomain protein, binds to and transactivates photoreceptor cell-specific genes. Neuron *19*, 1017-1030.

Cheng, H., Khanna, H., Oh, E.C., Hicks, D., Mitton, K.P., and Swaroop, A. (2004). Photoreceptor-specific nuclear receptor NR2E3 functions as a transcriptional activator in rod photoreceptors. Human molecular genetics *13*, 1563-1575.

Chuang, J.Z., Chou, S.Y., and Sung, C.H. (2010). Chloride intracellular channel 4 is critical for the epithelial morphogenesis of RPE cells and retinal attachment. Molecular biology of the cell *21*, 3017-3028.

Colella, P., and Auricchio, A. (2010). AAV-mediated gene supply for treatment of degenerative and neovascular retinal diseases. Current gene therapy *10*, 371-380.

Colella, P., Cotugno, G., and Auricchio, A. (2009). Ocular gene therapy: current progress and future prospects. Trends in molecular medicine *15*, 23-31.

Comitato, A., Spampanato, C., Chakarova, C., Sanges, D., Bhattacharya, S.S., and Marigo, V. (2007). Mutations in splicing factor PRPF3, causing retinal degeneration, form detrimental aggregates in photoreceptor cells. Human molecular genetics *16*, 1699-1707.

Connell, G., Bascom, R., Molday, L., Reid, D., McInnes, R.R., and Molday, R.S. (1991). Photoreceptor peripherin is the normal product of the gene responsible for retinal degeneration in the rds mouse. Proceedings of the National Academy of Sciences of the United States of America *88*, 723-726.

Corbo, J.C., Myers, C.A., Lawrence, K.A., Jadhav, A.P., and Cepko, C.L. (2007). A typology of photoreceptor gene expression patterns in the mouse. Proceedings of the National Academy of Sciences of the United States of America *104*, 12069-12074.

Cornish, E.E., Hendrickson, A.E., and Provis, J.M. (2004). Distribution of short-wavelength-sensitive cones in human fetal and postnatal retina: early development of spatial order and density profiles. Vision research *44*, 2019-2026.

Cuadros, M.A., and Rios, A. (1988). Spatial and temporal correlation between early nerve fiber growth and neuroepithelial cell death in the chick embryo retina. Anatomy and embryology *178*, 543-551.

Das, A.V., Mallya, K.B., Zhao, X., Ahmad, F., Bhattacharya, S., Thoreson, W.B., Hegde, G.V., and Ahmad, I. (2006). Neural stem cell properties of Muller glia in the mammalian retina: regulation by Notch and Wnt signaling. Developmental biology *299*, 283-302.

De Santa, F., Barozzi, I., Mietton, F., Ghisletti, S., Polletti, S., Tusi, B.K., Muller, H., Ragoussis, J., Wei, C.L., and Natoli, G. (2010). A large fraction of extragenic RNA pol II transcription sites overlap enhancers. PLoS biology *8*, e1000384.

del Cerro, M., Seigel, G.M., Lazar, E., Grover, D., del Cerro, C., Brooks, D.H., DiLoreto, D., Jr., and Chader, G. (1993). Transplantation of Y79 cells into rat eyes: an in vivo model of human retinoblastomas. Investigative ophthalmology & visual science *34*, 3336-3346.

den Hollander, A.I., Roepman, R., Koenekoop, R.K., and Cremers, F.P. (2008). Leber congenital amaurosis: genes, proteins and disease mechanisms. Progress in retinal and eye research *27*, 391-419.

Denoeud, F., Kapranov, P., Ucla, C., Frankish, A., Castelo, R., Drenkow, J., Lagarde, J., Alioto, T., Manzano, C., Chrast, J., *et al.* (2007). Prominent use of distal 5' transcription start sites and discovery of a large number of additional exons in ENCODE regions. Genome research *17*, 746-759.

Dinger, M.E., Pang, K.C., Mercer, T.R., Crowe, M.L., Grimmond, S.M., and Mattick, J.S. (2009). NRED: a database of long noncoding RNA expression. Nucleic acids research *37*, D122-126.

Dinger, M.E., Pang, K.C., Mercer, T.R., and Mattick, J.S. (2008). Differentiating protein-coding and noncoding RNA: challenges and ambiguities. PLoS computational biology *4*, e1000176.

Dorsky, R.I., Rapaport, D.H., and Harris, W.A. (1995). Xotch inhibits cell differentiation in the Xenopus retina. Neuron *14*, 487-496.

Dowling, J.E. (1987). The retina: an approachable part of the brain (Cambridge, Mass., Belknap Press of Harvard University Press).

Dyer, M.A., and Cepko, C.L. (2000). Control of Muller glial cell proliferation and activation following retinal injury. Nature neuroscience *3*, 873-880.

Feng, J., Bi, C., Clark, B.S., Mady, R., Shah, P., and Kohtz, J.D. (2006). The Evf-2 noncoding RNA is transcribed from the Dlx-5/6 ultraconserved region and functions as a Dlx-2 transcriptional coactivator. Genes & development *20*, 1470-1484.

Fischer, A.J., and Reh, T.A. (2000). Identification of a proliferating marginal zone of retinal progenitors in postnatal chickens. Developmental biology *220*, 197-210.

Fischer, A.J., and Reh, T.A. (2001). Muller glia are a potential source of neural regeneration in the postnatal chicken retina. Nature neuroscience *4*, 247-252.

Frade, J.M., Rodriguez-Tebar, A., and Barde, Y.A. (1996). Induction of cell death by endogenous nerve growth factor through its p75 receptor. Nature *383*, 166-168.

Fu, Y., and Yau, K.W. (2007). Phototransduction in mouse rods and cones. Pflugers Arch *454*, 805-819.

Fuhrmann, S. (2010). Eye morphogenesis and patterning of the optic vesicle. Current topics in developmental biology *93*, 61-84.

Furukawa, T., Morrow, E.M., Li, T., Davis, F.C., and Cepko, C.L. (1999). Retinopathy and attenuated circadian entrainment in Crx-deficient mice. Nature genetics *23*, 466-470.

Furukawa, T., Mukherjee, S., Bao, Z.Z., Morrow, E.M., and Cepko, C.L. (2000). rax, Hes1, and notch1 promote the formation of Muller glia by postnatal retinal progenitor cells. Neuron *26*, 383-394.

Gao, G., Qu, G., Burnham, M.S., Huang, J., Chirmule, N., Joshi, B., Yu, Q.C., Marsh, J.A., Conceicao, C.M., and Wilson, J.M. (2000). Purification of recombinant adeno-associated virus vectors by column chromatography and its performance in vivo. Human gene therapy *11*, 2079-2091.

Garcia-Porrero, J.A., and Ojeda, J.L. (1979). Cell death and phagocytosis in the neuroepithelium of the developing retina. A TEM and SEM study. Experientia *35*, 375-376.

Geng, X., Lavado, A., Lagutin, O.V., Liu, W., and Oliver, G. (2007). Expression of Six3 Opposite Strand (Six3OS) during mouse embryonic development. Gene Expr Patterns *7*, 252-257.

Gordon, W.C., Casey, D.M., Lukiw, W.J., and Bazan, N.G. (2002). DNA damage and repair in light-induced photoreceptor degeneration. Investigative ophthalmology & visual science *43*, 3511-3521.

Graw, J. (2003). The genetic and molecular basis of congenital eye defects. Nature reviews *4*, 876-888.

Hamel, C.P. (2007). Cone rod dystrophies. Orphanet journal of rare diseases *2*, 7.

Hartong, D.T., Berson, E.L., and Dryja, T.P. (2006). Retinitis pigmentosa. Lancet *368*, 1795-1809.

Hashimoto, T., Zhang, X.M., Chen, B.Y., and Yang, X.J. (2006). VEGF activates divergent intracellular signaling components to regulate retinal progenitor cell proliferation and neuronal differentiation. Development (Cambridge, England) *133*, 2201-2210.

He, Y., Vogelstein, B., Velculescu, V.E., Papadopoulos, N., and Kinzler, K.W. (2008). The antisense transcriptomes of human cells. Science (New York, NY *322*, 1855-1857.

Hendrickson, A., Bumsted-O'Brien, K., Natoli, R., Ramamurthy, V., Possin, D., and Provis, J. (2008). Rod photoreceptor differentiation in fetal and infant human retina. Experimental eye research *87*, 415-426.

Hennig, A.K., Peng, G.H., and Chen, S. (2008). Regulation of photoreceptor gene expression by Crx-associated transcription factor network. Brain research *1192*, 114-133.

Hildinger, M., Auricchio, A., Gao, G., Wang, L., Chirmule, N., and Wilson, J.M. (2001). Hybrid vectors based on adeno-associated virus serotypes 2 and 5 for muscle-directed gene transfer. Journal of virology *75*, 6199-6203.

Hims, M.M., Diager, S.P., and Inglehearn, C.F. (2003). Retinitis pigmentosa: genes, proteins and prospects. Developments in ophthalmology *37*, 109-125.

Hoke, K.L., and Fernald, R.D. (1998). Cell death precedes rod neurogenesis in embryonic teleost retinal development. Brain Res Dev Brain Res *111*, 143-146.

Holt, C.E., Bertsch, T.W., Ellis, H.M., and Harris, W.A. (1988). Cellular determination in the Xenopus retina is independent of lineage and birth date. Neuron *1*, 15-26.

Hsiau, T.H., Diaconu, C., Myers, C.A., Lee, J., Cepko, C.L., and Corbo, J.C. (2007). The cis-regulatory logic of the mammalian photoreceptor transcriptional network. PloS one *2*, e643.

Huarte, M., Guttman, M., Feldser, D., Garber, M., Koziol, M.J., Kenzelmann-Broz, D., Khalil, A.M., Zuk, O., Amit, I., Rabani, M., *et al.* (2010). A large intergenic noncoding

RNA induced by p53 mediates global gene repression in the p53 response. Cell *142*, 409-419.

Hughes, FW., and La Velle, A. (1975). The effects of early tectal lesions on development in the retinal gonglion cell layer of chick embryos. The Journal of comparative neurology *163*, 265-283.

Hughes, W.F., and McLoon, S.C. (1979). Ganglion cell death during normal retinal development in the chick: comparisons with cell death induced by early target field destruction. Experimental neurology *66*, 587-601.

Hyatt, G.A., Schmitt, E.A., Fadool, J.M., and Dowling, J.E. (1996). Retinoic acid alters photoreceptor development in vivo. Proceedings of the National Academy of Sciences of the United States of America *93*, 13298-13303.

Inglehearn, C.F. (1998). Molecular genetics of human retinal dystrophies. Eye (London, England) *12 (Pt 3b)*, 571-579.

Inoue, T., Hojo, M., Bessho, Y., Tano, Y., Lee, J.E., and Kageyama, R. (2002). Math3 and NeuroD regulate amacrine cell fate specification in the retina. Development (Cambridge, England) *129*, 831-842.

Jacquier, A. (2009). The complex eukaryotic transcriptome: unexpected pervasive transcription and novel small RNAs. Nature reviews *10*, 833-844.

Kaikkonen, M.U., Lam, M.T., and Glass, C.K. (2011). Non-coding RNAs as regulators of gene expression and epigenetics. Cardiovascular research *90*, 430-440.

Kapranov, P., Cheng, J., Dike, S., Nix, D.A., Duttagupta, R., Willingham, A.T., Stadler, P.F., Hertel, J., Hackermuller, J., Hofacker, I.L., *et al.* (2007). RNA maps reveal new RNA classes and a possible function for pervasive transcription. Science (New York, NY *316*, 1484-1488.

Kapranov, P., Drenkow, J., Cheng, J., Long, J., Helt, G., Dike, S., and Gingeras, T.R. (2005). Examples of the complex architecture of the human transcriptome revealed by RACE and high-density tiling arrays. Genome research *15*, 987-997.

Karl, M.O., Hayes, S., Nelson, B.R., Tan, K., Buckingham, B., and Reh, T.A. (2008). Stimulation of neural regeneration in the mouse retina. Proceedings of the National Academy of Sciences of the United States of America *105*, 19508-19513.

Karl, M.O., and Reh, T.A. (2010). Regenerative medicine for retinal diseases: activating endogenous repair mechanisms. Trends in molecular medicine *16*, 193-202.

Khalil, A.M., Guttman, M., Huarte, M., Garber, M., Raj, A., Rivea Morales, D., Thomas, K., Presser, A., Bernstein, B.E., van Oudenaarden, A., *et al.* (2009). Many human large intergenic noncoding RNAs associate with chromatin-modifying complexes and affect gene expression. Proceedings of the National Academy of Sciences of the United States of America *106*, 11667-11672.

Kim, T.K., Hemberg, M., Gray, J.M., Costa, A.M., Bear, D.M., Wu, J., Harmin, D.A., Laptewicz, M., Barbara-Haley, K., Kuersten, S., *et al.* (2010). Widespread transcription at neuronal activity-regulated enhancers. Nature *465*, 182-187.

Kolb, H. (1991). Anatomical pathways for color vision in the human retina. Visual neuroscience *7*, 61-74.

Kolb, H., Fernandez, E., Nelson, R., and editors. (2011). Webvision: The Organization of the Retina and Visual System [Internet].

Kubota, R., Hokoc, J.N., Moshiri, A., McGuire, C., and Reh, T.A. (2002). A comparative study of neurogenesis in the retinal ciliary marginal zone of homeothermic vertebrates. Brain Res Dev Brain Res *134*, 31-41.

Kumar-Singh, R. (2008). Barriers for retinal gene therapy: separating fact from fiction. Vision research *48*, 1671-1680.

Kyritsis, A.P., Tsokos, M., Triche, T.J., and Chader, G.J. (1984). Retinoblastoma--origin from a primitive neuroectodermal cell? Nature *307*, 471-473.

Kyritsis, A.P., Wiggert, B., Lee, L., and Chader, G.J. (1985). Butyrate enhances the synthesis of interphotoreceptor retinoid-binding protein (IRBP) by Y-79 human retinoblastoma cells. Journal of cellular physiology *124*, 233-239.

Lamba, D., Karl, M., and Reh, T. (2008). Neural regeneration and cell replacement: a view from the eye. Cell stem cell *2*, 538-549.

Lapidot, M., and Pilpel, Y. (2006). Genome-wide natural antisense transcription: coupling its regulation to its different regulatory mechanisms. EMBO reports *7*, 1216-1222.

Lavorgna, G., Dahary, D., Lehner, B., Sorek, R., Sanderson, C.M., and Casari, G. (2004). In search of antisense. Trends in biochemical sciences *29*, 88-94.

Lee, E.S., Burnside, B., and Flannery, J.G. (2006). Characterization of peripherin/rds and rom-1 transport in rod photoreceptors of transgenic and knockout animals. Investigative ophthalmology & visual science *47*, 2150-2160.

Lee, W.H., Bookstein, R., Hong, F., Young, L.J., Shew, J.Y., and Lee, E.Y. (1987). Human retinoblastoma susceptibility gene: cloning, identification, and sequence. Science (New York, NY *235*, 1394-1399.

Li, Z., Hu, M., Ochocinska, M.J., Joseph, N.M., and Easter, S.S., Jr. (2000). Modulation of cell proliferation in the embryonic retina of zebrafish (Danio rerio). Dev Dyn *219*, 391-401.

Livesey, F.J., and Cepko, C.L. (2001). Vertebrate neural cell-fate determination: lessons from the retina. Nat Rev Neurosci *2*, 109-118.

Loewer, S., Cabili, M.N., Guttman, M., Loh, Y.H., Thomas, K., Park, I.H., Garber, M., Curran, M., Onder, T., Agarwal, S., *et al.* (2010). Large intergenic non-coding RNA-RoR

modulates reprogramming of human induced pluripotent stem cells. Nature genetics *42*, 1113-1117.

Louro, R., El-Jundi, T., Nakaya, H.I., Reis, E.M., and Verjovski-Almeida, S. (2008). Conserved tissue expression signatures of intronic noncoding RNAs transcribed from human and mouse loci. Genomics *92*, 18-25.

Mao, Y.S., Sunwoo, H., Zhang, B., and Spector, D.L. (2011). Direct visualization of the co-transcriptional assembly of a nuclear body by noncoding RNAs. Nature cell biology *13*, 95-101.

Mariner, P.D., Walters, R.D., Espinoza, C.A., Drullinger, L.F., Wagner, S.D., Kugel, J.F., and Goodrich, J.A. (2008). Human Alu RNA is a modular transacting repressor of mRNA transcription during heat shock. Molecular cell *29*, 499-509.

Mattick, J.S. (2007). A new paradigm for developmental biology. The Journal of experimental biology *210*, 1526-1547.

Mattick, J.S., and Gagen, M.J. (2001). The evolution of controlled multitasked gene networks: the role of introns and other noncoding RNAs in the development of complex organisms. Molecular biology and evolution *18*, 1611-1630.

Maxwell, S.E., and Delaney, H.D. (2004). Designing experiments and analyzing data : a model comparison perspective, 2nd edn (Mahwah, N.J. ; London, Lawrence Erlbaum Associates).

Mayordomo, R., Valenciano, A.I., de la Rosa, E.J., and Hallbook, F. (2003). Generation of retinal ganglion cells is modulated by caspase-dependent programmed cell death. The European journal of neuroscience *18*, 1744-1750.

McFall, R.C., Sery, T.W., and Makadon, M. (1977). Characterization of a new continuous cell line derived from a human retinoblastoma. Cancer research *37*, 1003-1010.

McFarlane, S., Zuber, M.E., and Holt, C.E. (1998). A role for the fibroblast growth factor receptor in cell fate decisions in the developing vertebrate retina. Development (Cambridge, England) *125*, 3967-3975.

Mears, A.J., Kondo, M., Swain, P.K., Takada, Y., Bush, R.A., Saunders, T.L., Sieving, P.A., and Swaroop, A. (2001). Nrl is required for rod photoreceptor development. Nature genetics *29*, 447-452.

Mercer, T.R., Dinger, M.E., and Mattick, J.S. (2009). Long non-coding RNAs: insights into functions. Nature reviews *10*, 155-159.

Mercer, T.R., Dinger, M.E., Sunkin, S.M., Mehler, M.F., and Mattick, J.S. (2008). Specific expression of long noncoding RNAs in the mouse brain. Proceedings of the National Academy of Sciences of the United States of America *105*, 716-721.

Mustafi, D., and Palczewski, K. (2009). Topology of class A G protein-coupled receptors: insights gained from crystal structures of rhodopsins, adrenergic and adenosine receptors. Molecular pharmacology *75*, 1-12.

Nagano, T., and Fraser, P. (2011). No-Nonsense Functions for Long Noncoding RNAs. Cell *145*, 178-181.

Nagano, T., Mitchell, J.A., Sanz, L.A., Pauler, F.M., Ferguson-Smith, A.C., Feil, R., and Fraser, P. (2008). The Air noncoding RNA epigenetically silences transcription by targeting G9a to chromatin. Science (New York, NY *322*, 1717-1720.

Naik, R., Mukhopadhyay, A., and Ganguli, M. (2009). Gene delivery to the retina: focus on non-viral approaches. Drug discovery today *14*, 306-315.

Ng, J.H., and Ng, H.H. (2010). LincRNAs join the pluripotency alliance. Nature genetics *42*, 1035-1036.

Nishida, A., Furukawa, A., Koike, C., Tano, Y., Aizawa, S., Matsuo, I., and Furukawa, T. (2003). Otx2 homeobox gene controls retinal photoreceptor cell fate and pineal gland development. Nature neuroscience *6*, 1255-1263.

Nishida, T., Mukai, N., Solish, S.P., and Pomeroy, M. (1982). Effects of cyclic AMP on growth and differentiation of rat retinoblastoma-like tumor cells in vitro. Investigative ophthalmology & visual science *22*, 145-156.

Ogawa, Y., Sun, B.K., and Lee, J.T. (2008). Intersection of the RNA interference and X-inactivation pathways. Science (New York, NY *320*, 1336-1341.

Ohno, M., Fukagawa, T., Lee, J.S., and Ikemura, T. (2002). Triplex-forming DNAs in the human interphase nucleus visualized in situ by polypurine/polypyrimidine DNA probes and antitriplex antibodies. Chromosoma *111*, 201-213.

Ohsaki, K., Morimitsu, T., Ishida, Y., Kominami, R., and Takahashi, N. (1999). Expression of the Vax family homeobox genes suggests multiple roles in eye development. Genes Cells *4*, 267-276.

Ohsawa, R., and Kageyama, R. (2008). Regulation of retinal cell fate specification by multiple transcription factors. Brain research *1192*, 90-98.

Okazaki, Y., Furuno, M., Kasukawa, T., Adachi, J., Bono, H., Kondo, S., Nikaido, I., Osato, N., Saito, R., Suzuki, H., *et al.* (2002). Analysis of the mouse transcriptome based on functional annotation of 60,770 full-length cDNAs. Nature *420*, 563-573.

Orom, U.A., Derrien, T., Beringer, M., Gumireddy, K., Gardini, A., Bussotti, G., Lai, F., Zytnicki, M., Notredame, C., Huang, Q., *et al.* (2010). Long noncoding RNAs with enhancer-like function in human cells. Cell *143*, 46-58.

Pandey, R.R., Mondal, T., Mohammad, F., Enroth, S., Redrup, L., Komorowski, J., Nagano, T., Mancini-Dinardo, D., and Kanduri, C. (2008). Kcnq1ot1 antisense noncoding

RNA mediates lineage-specific transcriptional silencing through chromatin-level regulation. Molecular cell *32*, 232-246.

Pazour, G.J., Baker, S.A., Deane, J.A., Cole, D.G., Dickert, B.L., Rosenbaum, J.L., Witman, G.B., and Besharse, J.C. (2002). The intraflagellar transport protein, IFT88, is essential for vertebrate photoreceptor assembly and maintenance. The Journal of cell biology *157*, 103-113.

Peng, G.H., Ahmad, O., Ahmad, F., Liu, J., and Chen, S. (2005). The photoreceptor-specific nuclear receptor Nr2e3 interacts with Crx and exerts opposing effects on the transcription of rod versus cone genes. Human molecular genetics *14*, 747-764.

Peng, G.H., and Chen, S. (2007). Crx activates opsin transcription by recruiting HAT-containing co-activators and promoting histone acetylation. Human molecular genetics *16*, 2433-2452.

Perron, M., and Harris, W.A. (2000). Determination of vertebrate retinal progenitor cell fate by the Notch pathway and basic helix-loop-helix transcription factors. Cell Mol Life Sci *57*, 215-223.

Peters, J., and Robson, J.E. (2008). Imprinted noncoding RNAs. Mamm Genome *19*, 493-502.

Pollard, K.S., Salama, S.R., Lambert, N., Lambot, M.A., Coppens, S., Pedersen, J.S., Katzman, S., King, B., Onodera, C., Siepel, A., *et al.* (2006). An RNA gene expressed during cortical development evolved rapidly in humans. Nature *443*, 167-172.

Ponting, C.P. (2008). The functional repertoires of metazoan genomes. Nature reviews *9*, 689-698.

Rapaport, D.H., Wong, L.L., Wood, E.D., Yasumura, D., and LaVail, M.M. (2004). Timing and topography of cell genesis in the rat retina. The Journal of comparative neurology *474*, 304-324.

Rapicavoli, N.A., Poth, E.M., and Blackshaw, S. (2010). The long noncoding RNA RNCR2 directs mouse retinal cell specification. BMC developmental biology *10*, 49.

Ravasi, T., Suzuki, H., Pang, K.C., Katayama, S., Furuno, M., Okunishi, R., Fukuda, S., Ru, K., Frith, M.C., Gongora, M.M., *et al.* (2006). Experimental validation of the regulated expression of large numbers of non-coding RNAs from the mouse genome. Genome research *16*, 11-19.

Redrup, L., Branco, M.R., Perdeaux, E.R., Krueger, C., Lewis, A., Santos, F., Nagano, T., Cobb, B.S., Fraser, P., and Reik, W. (2009). The long noncoding RNA Kcnq1ot1 organises a lineage-specific nuclear domain for epigenetic gene silencing. Development (Cambridge, England) *136*, 525-530.

Reh, T.A., Nagy, T., and Gretton, H. (1987). Retinal pigmented epithelial cells induced to transdifferentiate to neurons by laminin. Nature *330*, 68-71.

Reid, T.W., Albert, D.M., Rabson, A.S., Russell, P., Craft, J., Chu, E.W., Tralka, T.S., and Wilcox, J.L. (1974). Characteristics of an established cell line of retinoblastoma. Journal of the National Cancer Institute *53*, 347-360.

Ren, B. (2010). Transcription: Enhancers make non-coding RNA. Nature *465*, 173-174.

Reynolds, J.D., and Olitsky, S.E. (2011). Pediatric retina (Heidelberg, Springer).

Rinn, J.L., Kertesz, M., Wang, J.K., Squazzo, S.L., Xu, X., Brugmann, S.A., Goodnough, L.H., Helms, J.A., Farnham, P.J., Segal, E., *et al.* (2007). Functional demarcation of active and silent chromatin domains in human HOX loci by noncoding RNAs. Cell *129*, 1311-1323.

Rodriguez-Campos, A., and Azorin, F. (2007). RNA is an integral component of chromatin that contributes to its structural organization. PloS one *2*, e1182.

Roque, R.S., Rosales, A.A., Jingjing, L., Agarwal, N., and Al-Ubaidi, M.R. (1999). Retina-derived microglial cells induce photoreceptor cell death in vitro. Brain research *836*, 110-119.

Sambrook, J., and Russell, D.W. (2001). Molecular cloning : a laboratory manual, 3rd edn (Cold Spring Harbor, N.Y., Cold Spring Harbor Laboratory Press).

Satoh, S., Tang, K., Iida, A., Inoue, M., Kodama, T., Tsai, S.Y., Tsai, M.J., Furuta, Y., and Watanabe, S. (2009). The spatial patterning of mouse cone opsin expression is regulated by bone morphogenetic protein signaling through downstream effector COUP-TF nuclear receptors. J Neurosci *29*, 12401-12411.

Seidl, C.I., Stricker, S.H., and Barlow, D.P. (2006). The imprinted Air ncRNA is an atypical RNAPII transcript that evades splicing and escapes nuclear export. The EMBO journal *25*, 3565-3575.

Seigel, G.M. (1999). The golden age of retinal cell culture. Molecular vision *5*, 4.

Sernagor, E. (2006). Retinal development (Cambridge, Cambridge University Press).

Sery, T.W., Lee, E.Y., Lee, W.H., Bookstein, R., Wong, V., Shields, J.A., Augsburger, J.J., and Donoso, L.A. (1990). Characteristics of two new retinoblastoma cell lines: WERI-Rb24 and WERI-Rb27. Journal of pediatric ophthalmology and strabismus *27*, 212-217.

Sheedlo, H.J., Bartosh, T.J., Wang, Z., Srinivasan, B., Brun-Zinkernagel, A.M., and Roque, R.S. (2007). RPE-derived factors modulate photoreceptor differentiation: a possible role in the retinal stem cell niche. In vitro cellular & developmental biology *43*, 361-370.

Shevtsov, S.P., and Dundr, M. (2011). Nucleation of nuclear bodies by RNA. Nature cell biology *13*, 167-173.

Sone, M., Hayashi, T., Tarui, H., Agata, K., Takeichi, M., and Nakagawa, S. (2007). The mRNA-like noncoding RNA Gomafu constitutes a novel nuclear domain in a subset of neurons. Journal of cell science *120*, 2498-2506.

Sung, C.H., and Chuang, J.Z. (2010). The cell biology of vision. The Journal of cell biology *190*, 953-963.

Surace, E.M., and Auricchio, A. (2008). Versatility of AAV vectors for retinal gene transfer. Vision research *48*, 353-359.

Surace, E.M., Auricchio, A., Reich, S.J., Rex, T., Glover, E., Pineles, S., Tang, W., O'Connor, E., Lyubarsky, A., Savchenko, A., *et al.* (2003). Delivery of adeno-associated virus vectors to the fetal retina: impact of viral capsid proteins on retinal neuronal progenitor transduction. Journal of virology *77*, 7957-7963.

Swaroop, A., Kim, D., and Forrest, D. (2010). Transcriptional regulation of photoreceptor development and homeostasis in the mammalian retina. Nat Rev Neurosci *11*, 563-576.

Tan, E., Ding, X.Q., Saadi, A., Agarwal, N., Naash, M.I., and Al-Ubaidi, M.R. (2004). Expression of cone-photoreceptor-specific antigens in a cell line derived from retinal tumors in transgenic mice. Investigative ophthalmology & visual science *45*, 764-768.

Terranova, R., Yokobayashi, S., Stadler, M.B., Otte, A.P., van Lohuizen, M., Orkin, S.H., and Peters, A.H. (2008). Polycomb group proteins Ezh2 and Rnf2 direct genomic contraction and imprinted repression in early mouse embryos. Developmental cell *15*, 668-679.

Torarinsson, E., Yao, Z., Wiklund, E.D., Bramsen, J.B., Hansen, C., Kjems, J., Tommerup, N., Ruzzo, W.L., and Gorodkin, J. (2008). Comparative genomics beyond sequence-based alignments: RNA structures in the ENCODE regions. Genome research *18*, 242-251.

Townes-Anderson, E., Dacheux, R.F., and Raviola, E. (1988). Rod photoreceptors dissociated from the adult rabbit retina. J Neurosci *8*, 320-331.

Travis, G.H. (1998). Mechanisms of cell death in the inherited retinal degenerations. American journal of human genetics *62*, 503-508.

Tropepe, V., Coles, B.L., Chiasson, B.J., Horsford, D.J., Elia, A.J., McInnes, R.R., and van der Kooy, D. (2000). Retinal stem cells in the adult mammalian eye. Science (New York, NY *287*, 2032-2036.

Tsokos, M., Kyritsis, A.P., Chader, G.J., and Triche, T.J. (1986). Differentiation of human retinoblastoma in vitro into cell types with characteristics observed in embryonal or mature retina. The American journal of pathology *123*, 542-552.

Turner, D.L., Snyder, E.Y., and Cepko, C.L. (1990). Lineage-independent determination of cell type in the embryonic mouse retina. Neuron *4*, 833-845.

Vecino, E., Hernandez, M., and Garcia, M. (2004). Cell death in the developing vertebrate retina. The International journal of developmental biology *48*, 965-974.

Venables, W.N., Ripley, B.D., and Venables, W.N. (2002). Modern applied statistics with S, 4th edn (New York, Springer).

Wan, J., Zheng, H., Xiao, H.L., She, Z.J., and Zhou, G.M. (2007). Sonic hedgehog promotes stem-cell potential of Muller glia in the mammalian retina. Biochemical and biophysical research communications *363*, 347-354.

Wang, X., Arai, S., Song, X., Reichart, D., Du, K., Pascual, G., Tempst, P., Rosenfeld, M.G., Glass, C.K., and Kurokawa, R. (2008). Induced ncRNAs allosterically modify RNA-binding proteins in cis to inhibit transcription. Nature *454*, 126-130.

Wetts, R., and Fraser, S.E. (1988). Multipotent precursors can give rise to all major cell types of the frog retina. Science (New York, NY *239*, 1142-1145.

Willingham, A.T., Orth, A.P., Batalov, S., Peters, E.C., Wen, B.G., Aza-Blanc, P., Hogenesch, J.B., and Schultz, P.G. (2005). A strategy for probing the function of noncoding RNAs finds a repressor of NFAT. Science (New York, NY *309*, 1570-1573.

Wilson, M.D., Barbosa-Morais, N.L., Schmidt, D., Conboy, C.M., Vanes, L., Tybulewicz, V.L., Fisher, E.M., Tavare, S., and Odom, D.T. (2008). Species-specific transcription in mice carrying human chromosome 21. Science (New York, NY *322*, 434-438.

Wright, A.F., Chakarova, C.F., Abd El-Aziz, M.M., and Bhattacharya, S.S. (2010). Photoreceptor degeneration: genetic and mechanistic dissection of a complex trait. Nature reviews *11*, 273-284.

Yao, H., Brick, K., Evrard, Y., Xiao, T., Camerini-Otero, R.D., and Felsenfeld, G. (2010). Mediation of CTCF transcriptional insulation by DEAD-box RNA-binding protein p68 and steroid receptor RNA activator SRA. Genes & development *24*, 2543-2555.

Young, R.W. (1984). Cell death during differentiation of the retina in the mouse. The Journal of comparative neurology *229*, 362-373.

Young, R.W. (1985). Cell differentiation in the retina of the mouse. The Anatomical record *212*, 199-205.

Young, T.L., Matsuda, T., and Cepko, C.L. (2005). The noncoding RNA taurine upregulated gene 1 is required for differentiation of the murine retina. Curr Biol *15*, 501-512.

Yu, J., Lei, K., Zhou, M., Craft, C.M., Xu, G., Xu, T., Zhuang, Y., Xu, R., and Han, M. (2011). KASH protein Syne-2/Nesprin-2 and SUN proteins SUN1/2 mediate nuclear migration during mammalian retinal development. Human molecular genetics *20*, 1061-1073.

Zhao, J., Ohsumi, T.K., Kung, J.T., Ogawa, Y., Grau, D.J., Sarma, K., Song, J.J., Kingston, R.E., Borowsky, M., and Lee, J.T. (2010). Genome-wide identification of polycomb-associated RNAs by RIP-seq. Molecular cell *40*, 939-953.

Zhao, J., Sun, B.K., Erwin, J.A., Song, J.J., and Lee, J.T. (2008). Polycomb proteins targeted by a short repeat RNA to the mouse X chromosome. Science (New York, NY *322*, 750-756.

V. Acknowledgements

First of all I would like to thank my internal supervisor Sandro Banfi for his incredible support and helpful discussions during the course of these investigations, and for his help in writing this thesis.

I would like to thank also my external supervisor Veronica van Heyningen for all the suggestions she gave to me and for her continuous encouragement in the scientific carreer.

Special thanks are for the Director of TIGEM, Andrea Ballabio, for his kind interest on my work and Brunella Franco for her corrections to the thesis.

I thank all the people of Banfi's laboratory and TIGEM for their technical support and friendship.
In particular I sincerely thank Mariateresa Pizzo for her special contribution to my thesis.

I would like to thank my extraordinary parents, Pietro and Marialina, and brothers, Fabrizio and Gianmarco, my grandmother, Teresa, and all the family for their entusiasm that pushed me always further.

My final thanks go to Lina for her LOVE. *To known her is to love her!!!*